F. W. KLAIBER
K. F. DUNKER
W. W. SANDERS, Jr.
JUNE 1981

FINAL REPORT

Feasibility Study of Strengthening Existing Single Span Steel Beam Concrete Deck Bridges

HR-214
ISU-ERI-Ames 81251
ERI Project 1460

ENGINEERING
RESEARCH
ENGINEERING
RESEARCH
ENGINEERING
RESEARCH
ENGINEERING
RESEARCH
ENGINEERING
RESEARCH

FINAL REPORT

Feasibility Study of Strengthening Existing Single Span Steel Beam Concrete Deck Bridges

F. W. Klaiber
K. F. Dunker
W. W. Sanders, Jr.

June 1981

TABLE OF CONTENTS

LIST OF FIGURES

LIST OF TABLES

1. INTRODUCTION

1.1. General

Iowa has the same problem that confronts most states in the United States: many bridges constructed more than 20 years ago either have deteriorated to the point that they are inadequate for original design loads or have been rendered inadequate by changes in design/maintenance standards or design loads. Inadequate bridges require either strengthening or posting for reduced loads.

A sizeable number of single span, composite concrete deck - steel I beam bridges in Iowa currently cannot be rated to carry today's design loads. Various methods for strengthening the unsafe bridges have been proposed and some methods have been tried. No method appears to be as economical and promising as strengthening by post-tensioning of the steel beams.

At the time this research study was begun, the feasibility of post-tensioning existing composite bridges was unknown. As one would expect, the design of a bridge-strengthening scheme utilizing post-tensioning is quite complex. The design involves composite construction stressed in an abnormal manner (possible tension in the deck slab), consideration of different sizes of exterior and interior beams, cover-plated beams already designed for maximum moment at midspan and at plate cut-off points, complex live load distribution, and distribution of post-tensioning forces and moments among the bridge beams. Although information is available on many of these topics, there is miminal information on several of them and no information available on the total design problem.

This study, therefore, is an effort to gather some of the missing information, primarily through testing a half-size bridge model and thus determining the feasibility of strengthening composite bridges by post-tensioning. Based on the results of this study, the authors anticipate that a second phase of the study will be undertaken and directed toward strengthening of one or more prototype bridges in Iowa.

1.2. Objectives

Highway bridges in the United States are designed and rated according to specifications adopted by the American Association of State Highway and Transportation Officials (AASHTO) [37,44]. These specifications are based on rational structural analysis, experimental investigation and engineering judgment. On a regular schedule, the AASHTO standards are revised to incorporate new information as it becomes available.

As a result of changes in the AASHTO design and rating specifications and changes in Iowa design loads and deterioration, many Iowa bridges either must be posted at reduced load limits or must be strengthened. A large number of the Iowa state and county bridges that require posting or strengthening fall into the category of single-span, composite steel I-beam/concrete deck bridges constructed between 1940 and 1960. These bridges generally are of short to medium span, 30 to 80 feet, with four to six beams and one to four diaphragms. The overall objective of this research study is to explore the feasibility of strengthening this type of bridge.

Bridge spans can be strengthened by various techniques such as reducing dead load, strengthening critical members, adding supplemental members or modifying the structural system [29]. As a result of evaluating initial data and reviewing the literature, this study was aimed primarily toward post-tensioning of the composite steel - concrete bridge beams. The post-tensioning schemes employed in the experimental work are, in effect, means of strengthening critical members and modifying the structural system of the bridge.

In line with the overall objective of this study, secondary objectives were established:

- Determine load distribution before and after post-tensioning,
- Determine the effects of curbs and diaphragms,
- Develop and test appropriate post-tensioning schemes,
- Develop and test connection brackets for post-tensioning.

In order to verify experimental results, as well as to develop preliminary design methodology, experimental results were checked against predictions from orthotropic plate theory.

Several items that need to be developed for a bridge-strengthening design but that were beyond the scope of this particular study are:

- Check of the shear capacity of a post-tensioned bridge,
- Study of the effects of fatigue on a bridge strengthened by post-tensioning,
- Strategy for corrosion protection of the post-tensioning system,
- Detailed requirements for field application of post-tensioning,
- Study of long-term effects such as creep and deck deterioration/ cracking on post-tensioning.

1.3. Literature Review

The literature review which follows has been organized into four
areas: prestressed steel structures, prestressed composite structures,
bridge strengthening, and bridge deck analysis. Most experimental and
theoretical work in prestressed steel and prestressed composite struc-
tures has dealt with building or bridge structures that were prestressed
during construction, before any composite action could take place.

In most cases where bridges were strengthened by post-tensioning,
the bridges were noncomposite and not nearly as complex in terms of
load distribution and post-tensioning distribution as the Iowa bridges
to which this study is directed. The authors found no references re-
garding distribution of post-tensioning and no material directed to
post-tensioning brackets of the type tested in this study.

1.3.1. Prestressed Steel Structures

Prestressed metal structures have been proposed since 1837, when
Squire Whipple in the United States learned to compensate for the poor
tensile capacity of cast-iron members through prestressing [53]. Whipple
placed ties in such a way as to precompress truss tension members,
thereby protecting the cast-iron members from tension stress and poten-
tial brittle fracture.

In the late 19th and early 20th centuries many U.S. bridges were
constructed with trussed floor beams [6]. The king post or queen post
truss arrangement induced upward forces on floor beams in order to
counteract downward forces due to dead and live loads. The upward
forces were controlled by tightening turnbuckles in the tension rods

and could be adjusted after construction to induce the desired amount
of prestress.

Dischinger in Germany, beginning in 1935 [21], began to conceive
much wider applications for prestressed steel. His proposals included
highway and railway bridges utilizing prestressed plate girders, box
girders, trusses and other structural forms [17].

In 1950, Magnel reported experimental results from a steel truss
prestressed by post-tensioning of the tension chord [36]. Strands were
placed inside the hollow chord and tensioned against anchorages at the
ends of the chord. A later article (1954) [35] described one of Magnel's
projects, a prestressed long span roof truss for a Belgian aircraft
hangar. Magnel stated that prestress loss was only 9% (which is rela-
tively low compared to losses for prestressed concrete).

As a result of the European work in prestressed steel, Coff in the
United States proposed a 250-foot span prestressed steel plate girder
bridge [14]. Coff later patented a prestressed composite system.
Another U.S. patent was granted to Naillon in 1961 for prestressing of
a steel beam by cables [46].

Barnett, in 1957, returned to the queen post truss concept in sug-
gesting the use of prestressed steel "truss beams" [7]. For economy,
Barnett recommended that the tension rod be placed below the beam,
thereby increasing the depth of the structure. He claimed weight sav-
ings of as much as 30% for his method.

A rather extensive testing program for a 90 foot span prestressed
steel truss was reported by Finn and Needham in England in 1964 [20].

During testing, prestressing bars failed several times, apparently as a result of faulty materials.

Subcommittee 3 of the Joint ASCE-AASHTO Committee on Steel Flexural Members reviewed the state of the art in prestressed steel in 1968 [18]. In addition to prestressing by means of high strength steel wires or bars, the subcommittee outlined developments in "prestressing by stressing components of hybrid beams" and "predeflected beam, precompressed concrete composite with steel tension flange." The hybrid beam and predeflected beam methods, although valid means for prestressing new structures, do not appear to be useful in strengthening existing structures.

For prestressing with steel wires or bars, Subcommittee 3 noted that combined secondary P-Δ and Δ-T (increase in force in prestressing due to application of load) effects can be as large as 20%. The Subcommittee estimated loss of prestress due to steel relaxation to be less than 5%. For symmetrical I sections, the subcommittee suggested that prestressing of new structures would not be economical, unless the prestressing cables or bars were placed below the I section. Several potential problems noted include corrosion, deflection and lateral stability.

During the early 1970s, Ferjencik [19] and Tochacek and Amrhein [49] described progress in prestressed steel design in Czechoslovakia. Research was begun in 1960, and actual design specifications were adopted as a result of that research. Ferjencik described a rather extensive catalog of applications of prestressing including applying it to girders and trusses. Tochacek and colleagues [49,50] pointed out that the safety factor for the portions of prestressed steel structures subjected to a

range of both tension and compression can be reduced by up to 20% under

a working stress design. In order to give an adequate and consistent

factor of safety, he suggested use of load factor design.

1.3.2. Prestressed Composite Structures

Apparently as a result of the European work in the late 1940s and

early 1950s and as a result of his own interest in prestressed steel

[14], Coff extended the concept of prestressing to composite structures.

He obtained a U.S. patent for a composite concrete slab - steel beam

system [46]. The system was prestressed by cables attached to the ends

of the slabs and draped along the steel beams, with pin attachments to

the steel beams.

Szilard, proposed a similar composite system in 1959, but with

tendons anchored to the steel beam rather than to the slab [47]. The

concrete slab was to be placed after prestressing of the steel beam and

was attached to the steel beam with ordinary headed stud shear connec-

tors.

In 1963, Hoadley analyzed the behavior of composite slab - steel

beam members, including the Δ-T effect in the prestressing tendon and

the performance of the members up to and including ultimate load [27].

The Δ-T analysis neglected P-Δ secondary effects since those effects

were estimated to be 5 to 10%. Hoadley's analysis showed an increase

in ultimate load capacity for efficient use of prestressing.

Stras reported several tests to ultimate load of prestressed com-

posite beams in 1964 [46], and the tests later were correlated with an

incremental strain analysis by Reagan [41]. After analyzing a series

of highway and bridge beams, Reagan concluded that failure generally

occurred by crushing of the concrete rather than by fracture of the tendon. Reagan also noted that prestressing does not affect the resistance of the section to deflection, since the prestressing tendons do not significantly affect the moment of inertia.

Several U.S. bridges constructed during the early 1960s utilized prestressed composite beams and trusses. Hadley designed two such bridges in Washington state. The first was a 99-ft span composite, precast concrete slab placed on steel trusses with prestressed lower chords [23]. The second bridge was a 150-ft span composite slab - post-tensioned delta girder bridge [24]. A skewed bridge with prestressed steel wide flange beams [15] was also constructed in Pennsylvania. The prestressing tendons were placed the full length of the bridge above the bottom flanges of the beams. Headed shear connectors welded to the top flanges of the beams provided the connection between beams and slab. All three bridges were constructed so that the bridge deck was made composte only after prestressing.

1.3.3. Bridge Strengthening

Since the early 1950s there have been many reports of bridges strengthened by post-tensioning. In 1952, Lee reported the strengthening of British steel highway and railway bridges by post tensioning [34]. Both beam and truss bridges were strengthened. Berridge and Lee [10] described strengthening of a steel truss bridge in 1956, and Knee [32] mentioned strengthening of British steel railway bridges by post-tensioning as if it were a fairly common practice.

Sterian described Rumanian practice in strengthening bridges by various methods, including post-tensioning by cables or rods prior to

1969 [45]. Although Sterian described several methods of strengthening, including addition of cover plates, he viewed post-tensioning as having the most potential. It is interesting to note that a research and model-testing program was completed in Rumania before any bridges were actually post-tensioned.

A proposal by Kandall in 1969 for strengthening steel structures by post-tensioning was unique because he recommended adding material to the compression regions of members [31]. The additional material had to be carefully fitted through or around cross members, making for a relatively complicated strengthening operation.

Vernigora et al. [51] described the successful strengthening of a five-span reinforced concrete bridge in Ontario, Canada. The five spans were post-tensioned by means of draped cables so as to make the repaired bridge continuous rather than simple span.

Belenya and Gorovskii [8] of the Soviet Union presented a rather complete analysis of steel beams strengthened by post-tensioning. According to their analysis, prestressing can add up to 90% capacity to an unprestressed steel beam. They recommended a tie rod length of 0.5 to 0.7 of the span length and recommended considering P-Δ effects only when the depth/span ratio is less than 1/20.

During the past ten years, several Minnesota bridges have been strengthened by post-tensioning. A prestressed concrete bridge damaged by vehicle impact was repaired using post-tensioning [40]. It appears that at least two Minnesota steel beam bridges have been repaired temporarily using post-tensioning [29]. In one case, salvage cable and

timbers were utilized for repair [9]. The repair was checked by means of instrumentation and an actual truck load.

During the 1970s T. Y. Lin International strengthened a multiple-span steel plate girder bridge in Puerto Rico by post-tensioning [30]. The post-tensioning scheme removed approximately 6 in. of dead load deflection at midspan.

From the literature search it appears that others have also recognized the potential of strengthening bridges by post-tensioning as opposed to addition of cover plates and other methods. The authors found no specific information on post-tensioning of existing composite structures, post-tensioning of cover-plated beams, or distribution of prestressing forces and moments to composite bridge decks.

1.3.4. Bridge Deck Analysis

As background for analysis of the experimental results, the authors investigated sources relating to bridge deck analysis, primarily by orthotropic plate theory; load distribution and the effect of diaphragms; and the effective slab width for composite beam stress computations.

A variety of bridge deck analysis methods are available including grillage analysis [16,22,25], orthotropic plate theory [1,4,5,16,22,43], finite differences [16], folded plate theory [16,25], finite elements [16,25], finite strips [16] and others. Because of the accuracy of orthotropic plate theory and the availability of computer programs for orthotropic plate theory from previous ISU bridge load distribution studies [1,22,43], those programs were modified and used for correlation of experimental results. Orthotropic plate theory utilizes two basic parameters: θ, the flexural parameter and α, the torsional parameter.

According to Bakht et al. [3] the composite bridges included in this study should fall into the following $\alpha-\theta$ space: $\alpha = 0.06$ to 0.20 and $\theta = 0.5$ to 2.1. Both model and actual bridge do fall into that $\alpha-\theta$ space as is shown in Table 1. Computation of bridge parameters for bridges with beams of unequal stiffness may be accomplished by use of an effective width as noted by Sanders and Elleby [43].

Many researchers have studied the load distribution within bridge decks [3,12,16,25,42,43]. It is generally agreed that diaphragms play a relatively minor role in load distribution at service loads [2,33]. Midspan diaphragms appear to play the greatest role in live load distribution [52], especially for the interior beams [33]. Kostem concluded, however, that quarter-point diaphragms were more important for load distribution for exterior beams. Diaphragms have a relatively minor effect in orthotropic plate theory since the diaphragm stiffness typically is spread over a considerable width [43]. Diaphrams are considered to have beneficial effect for overloads [33,48].

Effective slab width for composite beam design computations normally follows AASHTO Standards [44]. For correlation of experimental results, however, the authors sought further information. A finite strip analysis [13] found the AASHTO rules to be conservative. However, recent research relating to load factor design [11,26] has determined that, although the exterior girder slab widths are conservative, the interior girder slab widths are unconservative and that, beyond service load levels, both widths should be reduced.

Experimental studies generally have located the neutral axis for a beam by measuring boundary strains on top and bottom flanges [12,38] as

Table 1. Comparison of properties: prototype vs. model.

	Appanoose County 50' × 30' I-Beam Bridge		ISU Structures Laboratory 25' × 15' Model Bridge	
Span (Centerline to Centerline of Bearings)	51.25 ft		25.63 ft	
Deck Slab Width	31.38 ft		15.70 ft	
Deck Slab Thickness	8.25 in. maximum		4.02 in. average	
Interior Diaphragms	W16 × 36		W8 × 10	
Modular Ratio, n	10		8.86 deck, 5.89 curbs	
Orthotropic Plate Theory Flexural Parameter, θ	0.712		0.709	
Orthotropic Plate Theory Torsional Parameter, α	0.106		0.111	
	Exterior Beam	Interior Beam	Exterior Beam	Interior Beam
Steel Beam	W27 × 94	W30 × 116	W14 × 22	W16 × 26
Cover Plate	9 in. × 7/16 in.	9 in. × 1-1/4 in.	4 in. × 1/4 in.	4-1/2 in. × 5/8 in.
Composite Transformed Area, A*	90.72 in.^{2}	122.18 in.^{2}	25.80 in.^{2}	32.27 in.^{2}
Composite Transformed S*	518 in.^{3}	805 in.^{3}	66.7 in.^{3}	99.9 in.^{3}
Composite Transformed I*	12,965 in.^{4}	21,044 in.^{4}	900 in.^{4}	1403 in.^{4}

*Composite section properties are transformed to equivalent steel section properties.

a means of computing effective slab width and moment of inertia. One experimental study [28] showed that the moment of inertia decreased with shrinkage in the concrete slab and that the neutral axis and section properties varied considerably with position of live load.

1.4. General Test Program

On the basis of the literature review [1,3] and the field inspection (Section 2.1), the testing program was planned around a half-scale model of a 50 ft by 30 ft four-beam bridge. The model was instrumented with electrical resistance strain gages and deflection dial gages. During four constructional stages the model was loaded and its performance recorded: steel beam and diaphragm frame, composite deck and steel frame, composite bridge with curbs, and composite bridge with curbs but with diaphragms removed.

Two types of static loading were utilized for testing: 5-kip and 10-kip weights, as individual concentrated loads placed at points on the center line or quarter-point line, and an eccentric three axle truck load simulated by means of hydraulic jacks. During the composite stages, post-tensioning was applied in various sequences either to the exterior beams only or to all of the beams.

In addition to testing of the model bridge, both half scale and full-scale post-tensioning brackets were tested to failure. Brackets were designed for placement above as well as below the bottom flanges on beams.

Strain gage data were collected through a data acquisition system, punched on paper tape and then organized and corrected by means of FORTRAN computer programs.

2. TEST BRIDGE

2.1. Field Inspection

At the beginning of the research study, John Harkin of the Iowa DOT Bridge Department identified 25 to 30 bridges in need of strengthening and provided the authors with plans of approximately 15 of the bridges. The authors reviewed all plans and inspected several of the bridges in Appanoose, Boone, Greene, Polk and Webster counties.

The typical design load for the bridges was an H-20 truck. Most of the bridges were placed at right angles to abutments rather than at skewed angles; many of the bridges were built from standard plans. Exterior beams usually were of shallower depth than interior beams with smaller cover plates over shorter lengths. Intermediate diaphragms generally were of steel and were placed at the one-third points of the beam span. Some diaphragms were close enough to the bottom beam flange to obstruct post-tensioning tendons. Concrete decks were approximately 8 inches thick and had a 3- to 4-inch crown, established by the change in depth from exterior to interior beams. Most bridges had integral reinforced concrete curbs approximately 10 inches in height and steel post and channel rails. Abutments were of varying types: steel, concrete or timber.

The field inspection revealed varying states of repair among the bridges. Some had newly painted steel frames, while on others the frame was badly corroded. Most concrete decks were cracked and some showed considerable efflorescence underneath. Some abutments appeared to be sound and in excellent condition whereas others contained badly

deteriorated concrete. Some abutments had been undercut as the elevation of the stream bed dropped.

It appeared in some cases that strengthening the bridges would require extensive abutment repair as well as sandblasting and repainting of the steel. In most cases, decks would require an overlay after post-tensioning in order to seal cracking from post-tensioning and protect deck reinforcing. The post-tensioning operation generally cannot be performed by crews standing under the bridges but requires scaffolding from below or platforms suspended from above. In some cases portions of diaphragms would have to be removed to accommodate the post-tensioning system.

After considering the range of bridges, facilities and funding available for testing, the authors selected a nominal 50 ft by 30 ft two-lane bridge in Appanoose County as the prototype for the model constructed in the Iowa State University Structures Laboratory. The entire bridge is shown in Fig. 1(a), and some of the deterioration of the concrete portion of an abutment is shown in Fig. 1(b). Several bridges in Greene and Webster Counties were built from plans essentially the same as those of the Appanoose bridge. One of the interior beams from a Webster County bridge with cover plates and diaphragms is illustrated in Fig. 1(c). For that particular bridge, steel did not meet specifications, and second cover plates were added to the interior beams. The rail and curb for the Webster County bridge in Fig. 1(d) are the same as those for the Appanoose County prototype.

17
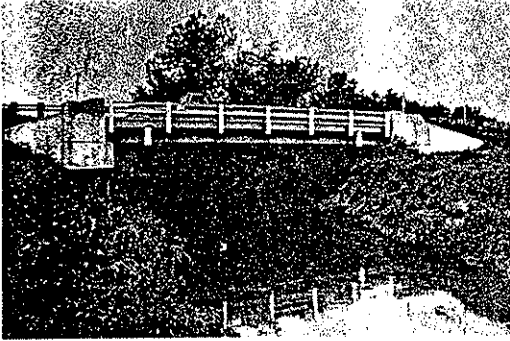
(a) OVERALL VIEW, APPANOOSE
    COUNTY BRIDGE

(b) CONCRETE DETERIORATION AT
    ABUTMENT, APPANOOSE COUNTY
    BRIDGE
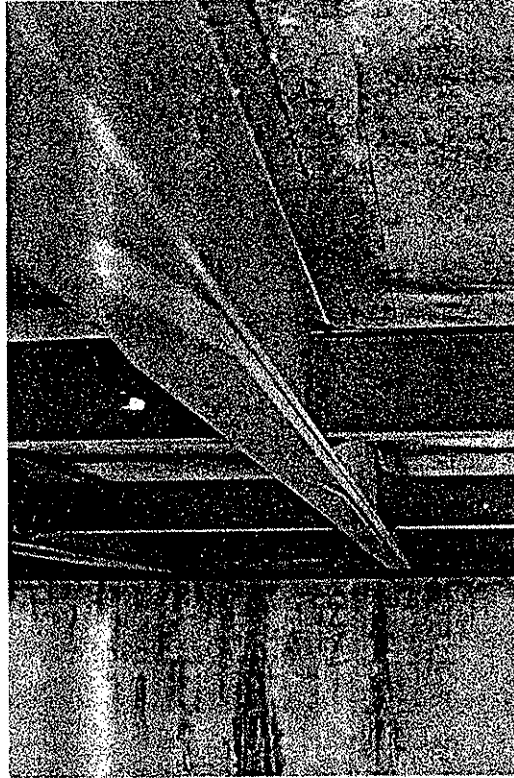
(c) INTERIOR BEAM WITH DOUBLE COVER
    PLATE AND DIAPHRAGMS, WEBSTER
    COUNTY BRIDGE
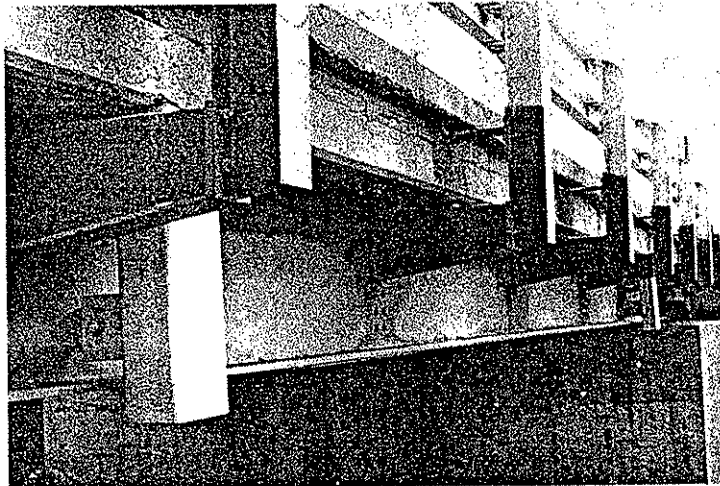
(d) EXTERIOR BEAM WITH CONCRETE CURB STEEL
     RAIL AND DRAINS, WEBSTER COUNTY BRIDGE

Fig. 1. Photographs of prototype bridges.

2.2. Bridge Description

The bridge model (Figs. 2 and 3) was constructed to be, as near as possible, a half-scale replica of the prototype bridge in Appanoose County. Framing and structural steel details may be found in the Appendix. The abutments, since they do not significantly affect the performance of the composite bridge deck under normal circumstances, were designed and constructed for convenience of the laboratory testing program. The model abutments basically were stub reinforced concrete walls, 2 ft 8 in. in height, with armored extensions above beam bearings to contain any unexpected post-tensioning failures. The abutments were positioned on the testing floor to facilitate the jacking arrangement for the simulated truck load. Bearing plates placed on the abutments accurately located bearing points but did not prevent uplift (a problem encountered in the steel frame testing and early composite stage testing).

Since material properties for the prototype bridge were unknown, model material properties were matched as closely as possible to properties typical for bridges constructed in the 1940s. Deck concrete strength was probably in the 2000-3000 psi range; reinforcing steel had a yield stress of about 40,000 psi and A7 structural steel had a minimum yield point of 33 ksi. Model material properties, as reported in Section 2.4, were similar to but somewhat greater than the values above.

All plan dimensions, deck thickness and curb depth were set at half scale. The curb cross section in the model was modified to 5 in. by 5 in. for ease of forming. Reinforcing bar diameters in the model were
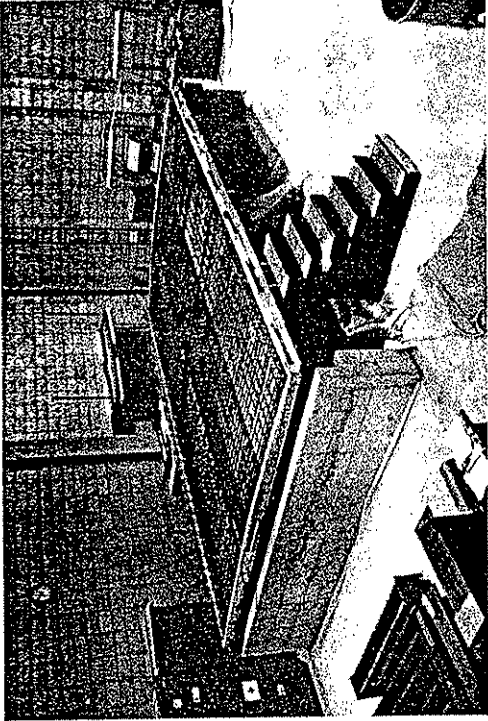
(a) STEEL FRAME
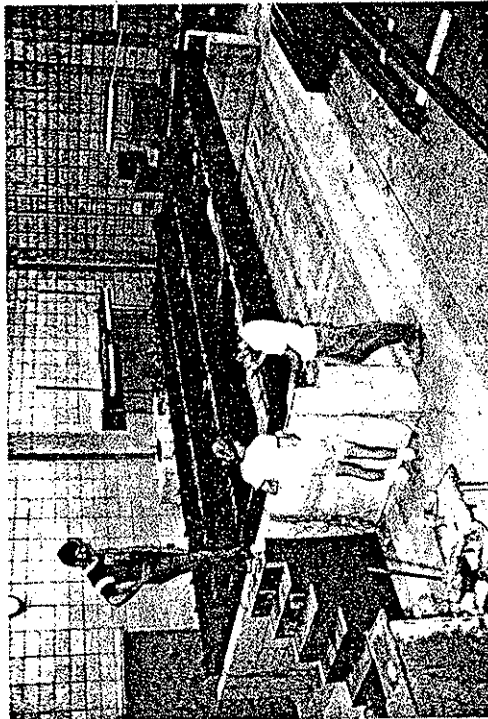
(b) DECK FORMWORK AND REINFORCING

(c) COMPOSITE BRIDGE WITHOUT CURBS
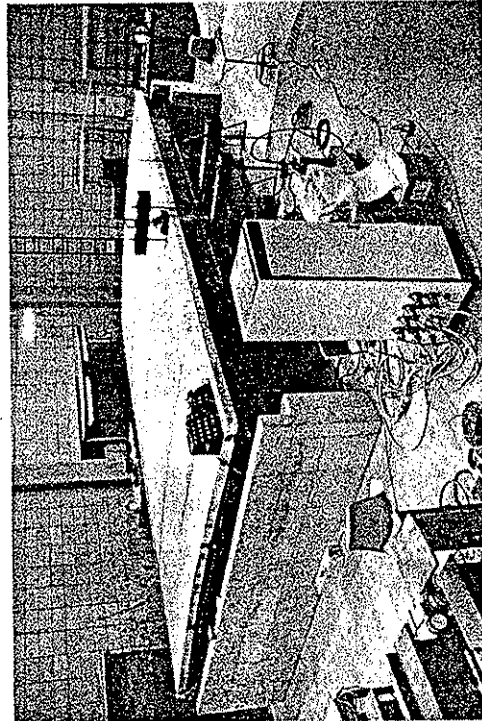
(d) COMPOSITE BRIDGE WITHOUT CURBS, WITH SANDBAG DEAD LOAD AND MIDSPAN CONCENTRATED LOAD

Fig. 2. Photographs of model bridge.

20
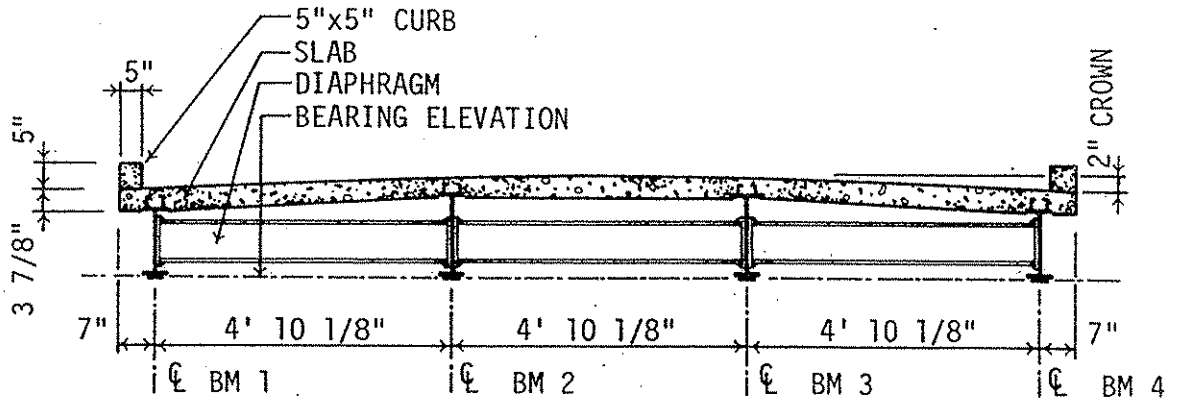
(a) CROSS SECTION AT MIDSPAN
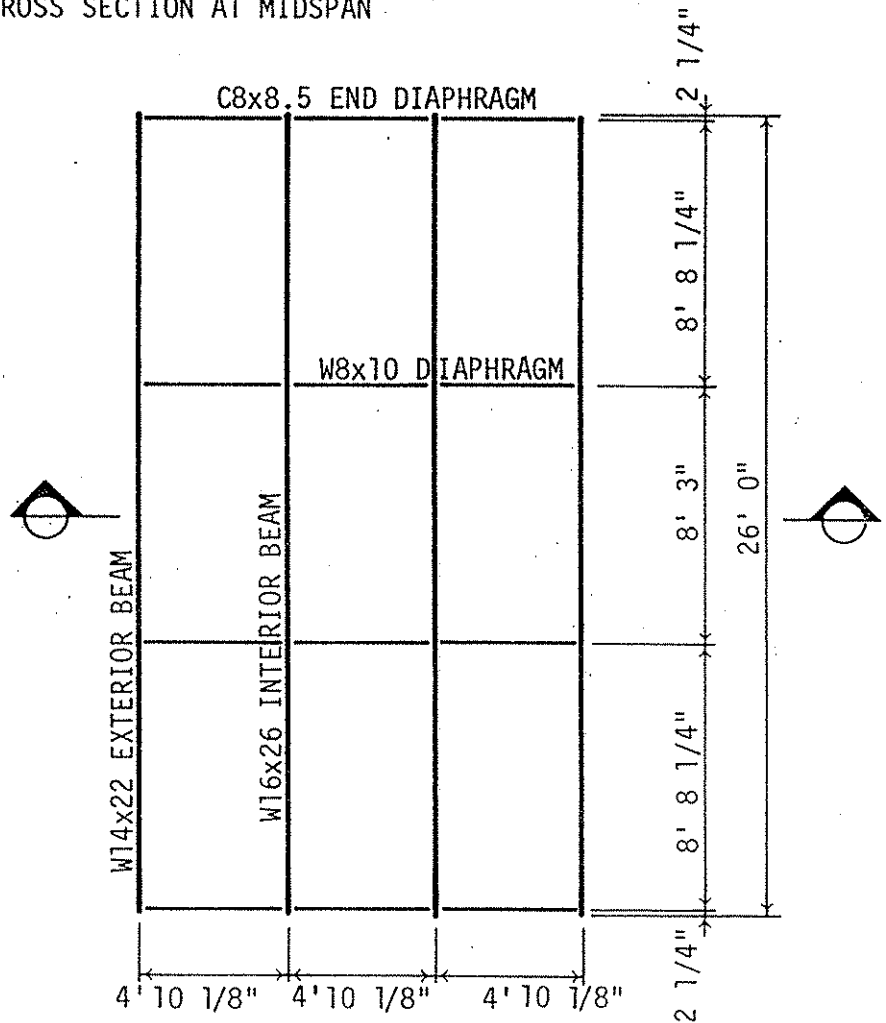
(b) FRAMING PLAN

Fig. 3. Model bridge.

established as half those of the prototype. Bars were placed at spacings varying from about 2-1/2 to 20 in., exactly half the spacings given on the Appanoose County bridge plans.

Because the choice of steel sections was limited to currently available shapes, model beam and diaphragm sections were selected that most nearly match half-size prototype sections (Table 1). Beam cover plate dimensions on the model were modified slightly from half scale to make use of commonly available plate thicknesses.

Section properties resulting from the half-scale dimensions follow principles of similitude [39]. Although depths of model beams are one-half those of the prototype, areas are one-quarter, section moduli are one-eighth and moments of inertia are one-sixteenth of those of the prototype. The comparison of section properties in Table 1 indicates good agreement, usually within 10% of scale section property requirements.

Other construction details of the bridge were replicated as nearly as possible to half scale. Angle and bar shear connectors and bearing stiffeners were accurately replicated. Approximately correct camber of model bridge beams resulted from the continuous cover plate welds. Diaphragm connections were modified somewhat from the prototype, primarily to accommodate 1/2-in. diameter bolts rather than half-scale 3/8-in. diameter bolts.

Post-tensioning brackets had to be enlarged beyond half scale because of the diameter of the hollow core prestressing jacks utilized. The enlarged brackets reduced post-tensioning moments slightly, but the reduction was partially offset by the slightly oversized model beam depths.

Dead load stresses in the model were approximately one-half the dead load stresses in the prototype at the time the concrete deck was placed. In order to increase dead load stresses in the model and also to prevent uplift under eccentric loading, rows of sandbags were placed on the composite bridge (Fig. 2(d)). The model sandbag loading did not completely duplicate dead load stresses in the prototype. In the model, the sandbag dead load was applied to the composite bridge whereas in the prototype the entire dead load was applied to the noncomposite steel frame.

Principles of similitude required model live loads to be one-quarter of the prototype live loads in order to duplicate live load stresses. The 5-kip and 10-kip weights used for model loading, therefore, simulated concentrated 20-kip and 40-kip loads on the Appanoose bridge. (The 20-kip load is approximately that of a heavily loaded truck wheel group.)

The model truck load was a three-axle, six-point load, with loading points positioned for a half-size HS-20 truck at maximum eccentricity. The eccentric truck loading was applied to the model bridge through holes cored in the deck. Maximum total truck loads of 25 kips applied to the model constituted a 30 to 40% static overload.

Preliminary computations indicated that the Appanoose County bridge would require about 80 kips of post-tensioning on the exterior beams for strengthening. Model beams, therefore, were post-tensioned to 20 kips normally and to 40 kips to check behavior of the bridge under excessive post-tensioning.

23

2.3. Bracket Configurations

Because of the uncertainty about the type of steel in some of the bridges, it was decided to investigate only bolted connections. However, if the type of steel were known in a given bridge requiring strengthening, some of the brackets investigated could be field welded rather than bolted.

After preliminary bracket tests to evaluate the test setup and loading procedures, three individual bracket tests were conducted. Henceforth, these tests will be designated I, II, and III, indicating the order in which they were performed. Bracket I was half scale and was used as the bracket in the bridge test. Brackets II and III were full scale and were investigated for possible use on actual bridges. Brackets I and III were designed so that the post-tensioning force was applied above the lower flange, thus making the post-tensioning system less susceptible to damage from vehicle impact, debris from flooding, etc. For symmetrical loading, Brackets I and III thus consisted of two parts, one on each side of the beam web. Bracket II was designed so that the post-tensioning force was applied below the bottom flange and thus consisted of only one part. In the following sections the three brackets are described in detail. Although not shown in any of the bracket drawings (Figs. 4, 5, and 6), each bracket configuration requires bearing plates to transmit the force from the tendons to the brackets.

2.3.1. Bracket I

Bracket I was designed for possible use on the bridge model. As a result of its favorable response to load, which will be detailed in

Fig. 5.   Configuration of bracket II.

4"

FILLET
WELDS

FILLET
WELDS

10"

5"

L4x3x3/8   W14x22   L4x3x3/8

Fig. 4.   Configuration of bracket I.

8x8x3/8
STRUCTURAL
TUBE

12"

W33x118

11 1/2"
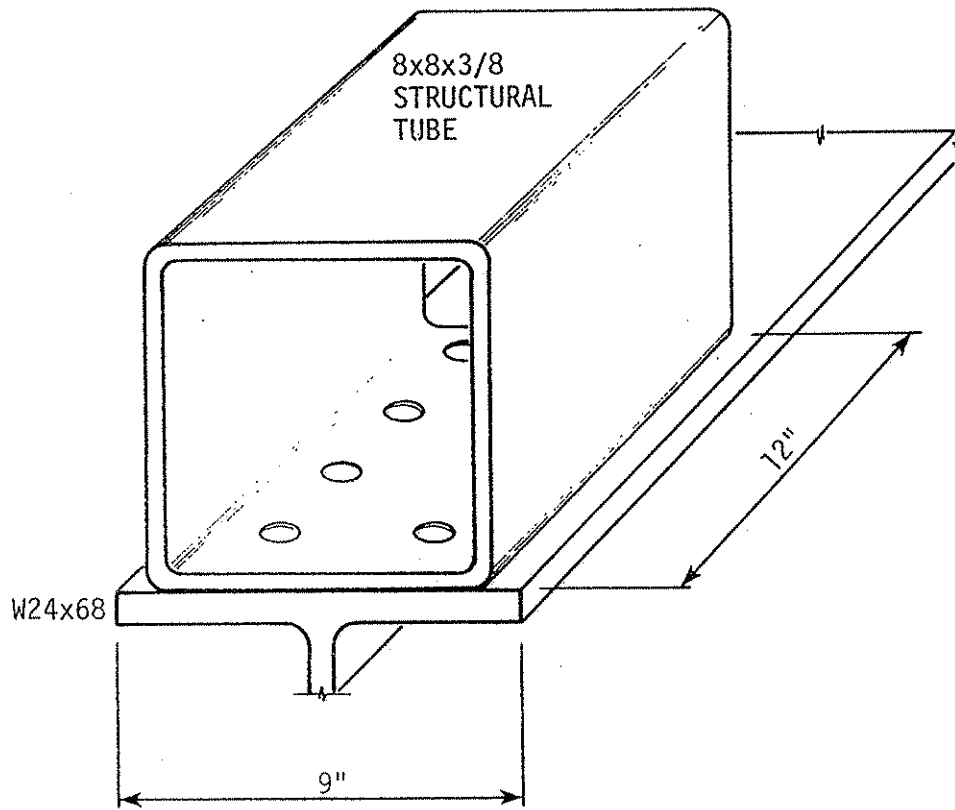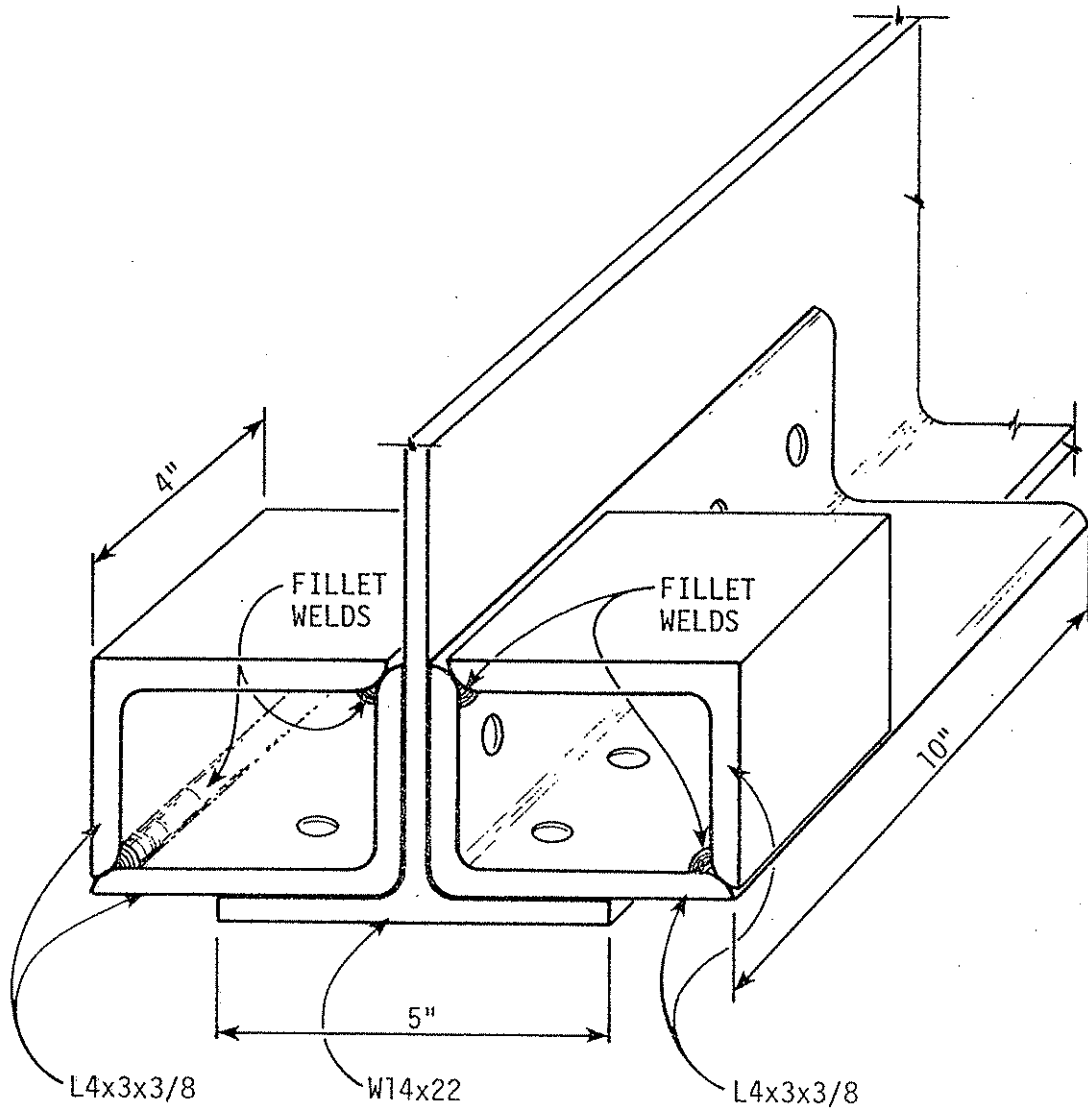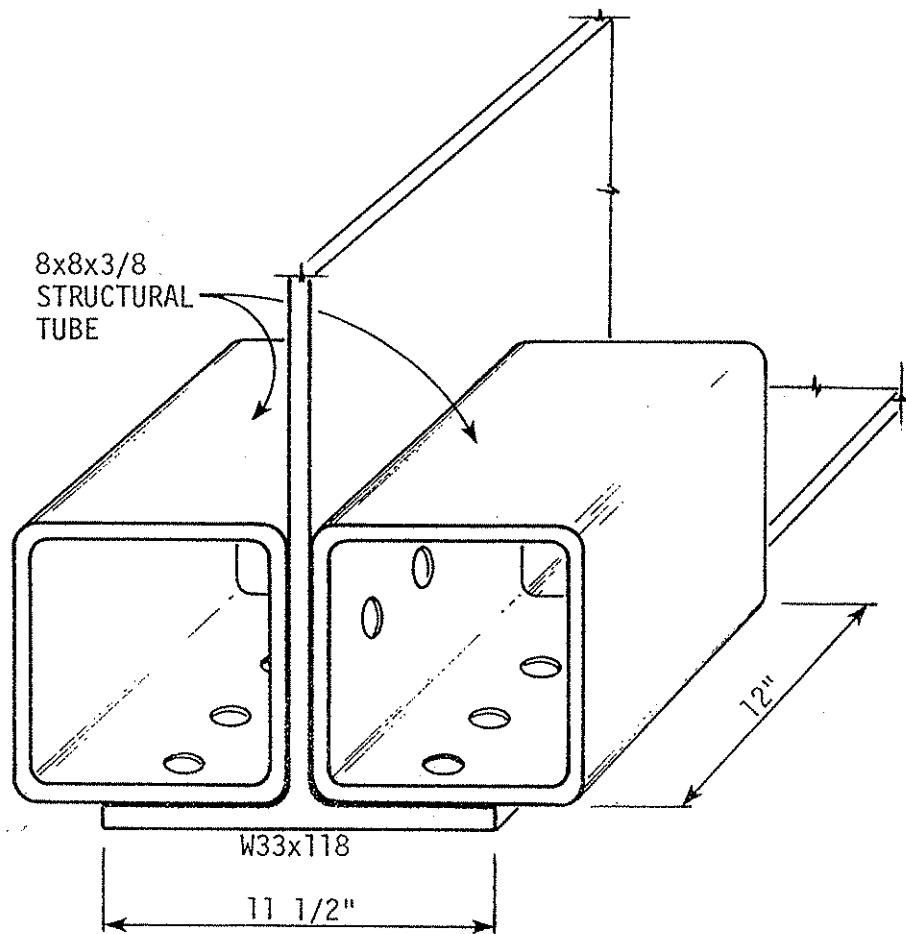
Fig. 6. Configuration of bracket III.

Section 4, Bracket I was used on the bridge model. This connection was designed as a bearing type to carry a load of 88 kips, which is approximately four times the force required to strengthen the bridge model the desired amount. As shown in Fig. 4, each part of Bracket I consisted of two sections of 4 × 3 × 3/8 structural angle welded together, one section 10 in. long and the other 4 in. long. The bracket was then bolted to a 6-ft long section of W14 × 22 wide flange beam which is the same section utilized for the exterior beams in the bridge model. The bracket-to-beam connection employed thirteen A325 bolts 1/2 inch in diameter. Five of the bolts were through the web and the remaining eight (four per side) were through the flange. The angle size used was selected on the basis of strength and size requirements, because the brackets had to be large enough to provide sufficient room for the posttensioning hardware.

2.3.2. Bracket II

Bracket II, shown in Fig. 5, consisted of a single 8 × 8 × 3/8 structural tube 12 in. long. As previously noted, Bracket II is full scale and was attached to the bottom of the beam flange; thus in Fig. 5 the beam is shown inverted from its normal orientation. The bearing-type connection was designed for a load of 80 kips which is approximately the force necessary to strengthen a W24 × 68 bridge beam. Eight A325 7/8-in. diameter bolts were used to attach the structural tube bracket to a 10-ft long W24 × 68; see Fig. 5 for bolt locations. The large tube section employed was necessary to accommodate the large jack required to apply the desired force. As previously stated, the location of

Bracket II requires the prestressing tendon to be positioned in such a way that it is susceptible to damage.

2.3.3. Bracket III

Bracket III, shown in Fig. 6, consisted of two 8 × 8 × 3/8 structural tubes, each 12 in. long, which were bolted to the top of the bottom flange of a 10-ft long W33 × 118 beam. Bracket III was designed as a bearing-type connection for a load of 120 kips, which is approximately the force necessary to strengthen a W33 × 118 bridge beam. To obtain this design load, two jacks 12 in. in diameter were required. Thus, as for Bracket II, the jack size necessitated the use of an 8 × 8 structural tube. The bracket was bolted to the beam with eleven A325 7/8-in. diameter bolts, three through the web in double shear and four through each side of the flange in single shear (see Fig. 6).

2.4. Physical Properties

A series of tests was performed on several representative specimens of the concrete and the steel used in the bridge model in order to determine values of the pertinent material properties. These representative values were then used as needed in the calculations presented in Section 4.

2.4.1. Concrete

Twelve 6 in. diameter × 12 in. long standard ASTM quality test cylinders were made during the pouring of the concrete slab. Because of the cover required on the slab reinforcing steel it was necessary to use a mix in which the maximum aggregate size was 1/4 inch (pea gravel).

All twelve cylinders were subjected to the same curing conditions as the slab. Cylinders were broken at 7 days and 14 days to determine when form work could be removed.

Eight 6 in. diameter × 12 in. long standard ASTM quality test cylinders were made when the curbs were cast on the bridge. Time constraints required that the testing program resume as soon as possible after placement of the curbs, so high early strength cement was used in combination with 3/4 in. maximum diameter limestone aggregate. Table 2 presents the compressive strength and modulus of elasticity of each of the two concretes. The compressive strength values given are the average of three compression tests, and the modulus of elasticity is the average of two tests. Values given were obtained at the completion of the testing program; thus the age of the slab concrete was approximately 220 days while the curb concrete was approximately 30 days.

2.4.2. Steel

Table 3 presents the yield stress, ultimate stress, and modulus of elasticity of each of the steels utilized in the testing program.

The values presented for the reinforcing steel (#3's and #4's) are the average of two tests on each bar size. Stresses given are based on the nominal area of each bar.

Data presented on the prestressing steel are the averages of three tests. As with the reinforcing steel, the stresses are based on the nominal area of the prestressing tendons.

Values given for the wide flange members were obtained from standard ASTM tensile coupons taken from the sections of the actual beams used in the model. For each wide flange section, three specimens (two

Table 2. Physical properties of concrete.

	f'_c(psi)	E(ksi)
Deck	3300	2830
Slab	7450	5080

Table 3. Physical properties of steel.

	σ_y(ksi)	σ_{ult}(ksi)	E(ksi)
Reinforcement			
#3	69.8	110.8	29,110
#4	70.8	109.7	-
Prestressing	-	156.1	24,100
W16 × 26	44.1	66.9	29,990
W14 × 22	44.7	69.4	28,990

from the web and one from the flange) were tested; thus the recorded

values are averages of the three tests.

3. TESTS AND TEST PROCEDURES

This section outlines the details of the specific tests and events that occurred during the conduct of these tests. Each test program (i.e., bracket tests and bridge tests) consisted of several individual tests. In this section, only test setups, instrumentation and events will be outlined; discussion and analysis of results obtained as well as the behavior will be presented in Section 4.

The instrumentation for all tests consisted of electrical-resistance strain gages and mechanical displacement dial gages. In preliminary tests, direct current displacement transducers (DCDTs) were employed for displacement measurement. However, because of problems with the data acquisition system, the DCDTs were replaced with mechanical displacement dial gages, henceforth referred to as deflection dials.

Electrical-resistance strain gages, henceforth referred to as strain gages, utilized on steel were temperature compensated. They were attached to the steel specimens employing recommended surface preparation and adhesive. Strain gages used on the concrete were likewise mounted with recommended adhesive after the concrete surface had been properly prepared. Three-wire leads were used to minimize the effect of the long lead wires and any temperature changes. All strain gages were waterproofed using a minimum of two coats.
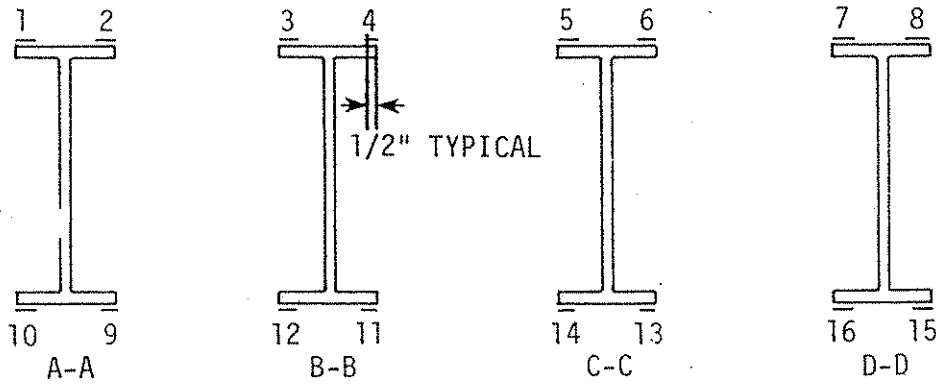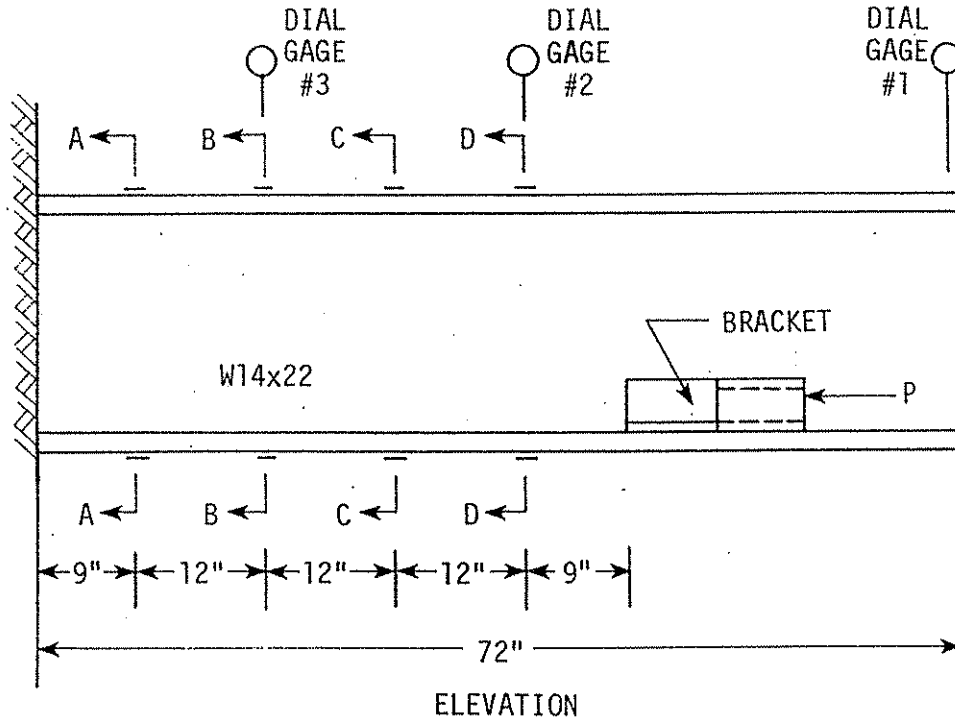
Strain gages used in the bracket tests were read by using a Vishay portable switching unit and strain indicator and were recorded by hand. Strain gages used in the bridge tests were read and recorded using a data acquisition system. Deflections measured by deflection dials were read and recorded by hand in all tests.

3.1. Bracket Test Setup and Procedure

Bracket I was loaded in increments of 5 kips, while Brackets II and III were loaded in 20-kip increments. Hydraulic jacks were used to apply the post-tensioning force in all bracket tests. Load was monitored by both hydraulic pressure and strain gage readings. As loading progressed, strains and displacements were recorded after each load increment. When any significant deformation occurred, photographs were taken. After the design load was reached and data were recorded, the specimens were loaded to failure without taking additional data. When failure occurred, photographs were taken to show the final deformed state. The specimens were then disassembled to determine the effects of the loading on the brackets, beams, and bolts. Individual bracket strains, deflections, failures, etc. are presented in Section 4.

3.1.1. Bracket Test I

As may be seen in Fig. 7, Bracket I was tested while attached to a cantilever beam. Also shown are the locations of the strain gages and dial gages. A total of 16 strain gages and three dial gages were used in the test. Figure 8 is a photograph of the test setup at the start of the test. As may be observed by comparing Figs. 7 and 8, the bracket and beam were tested in an inverted position for ease of testing. The brackets were mounted near one end of the beam, while the other beam end was welded to a plate which in turn was bolted to the tie-down floor thus providing a cantilever beam. Post-tensioning force was applied to the brackets utilizing grade 75 number 9 reinforcing bars stressed by hollow-core hydraulic jacks (see Fig. 8). Each reinforcing bar was

Fig. 7. Strain and displacement gage locations for bracket I.
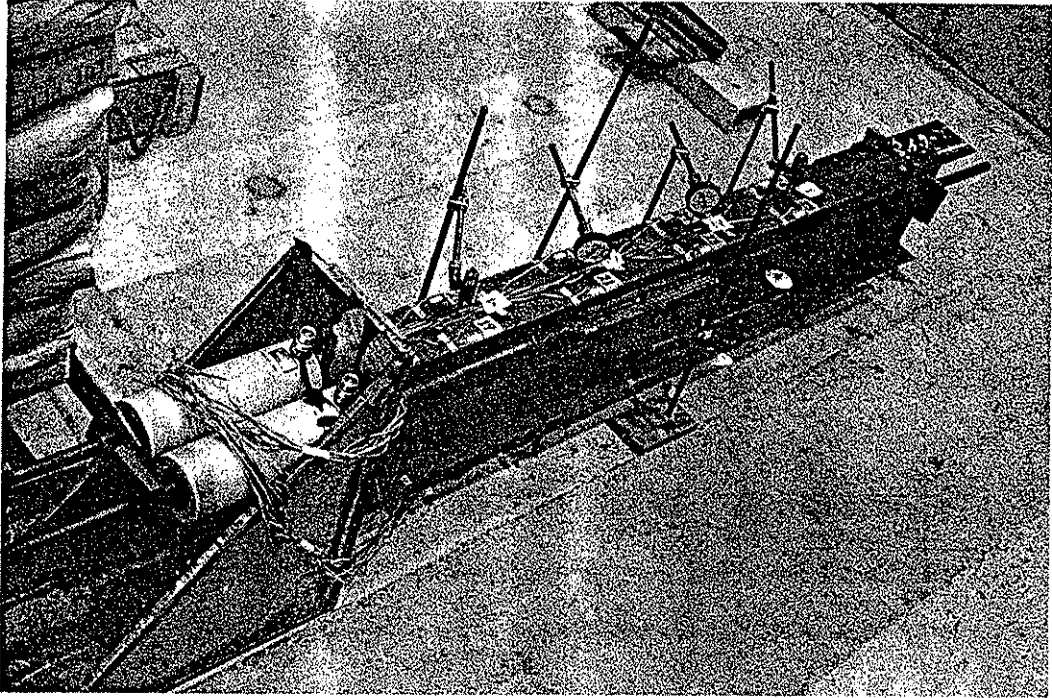
Fig. 8.   Bracket I test set-up.

instrumented with two strain gages to cancel bending strains and measure only axial strains. This allowed individual measurement of the force in each reinforcing bar. Each reinforcing bar had approximately the same force because the two hydraulic jacks applying the force were connected in parallel.

3.1.2. Bracket Test II

Bracket II, as may be seen in Fig. 9, was tested while attached to a simply supported beam. Figure 9 also indicates the location of the eight strain gages and three dial gages used in the test. The actual test setup is shown in Fig. 10. In this figure the test bracket is at the far end; attached to the near end is another section of structural tube similar to the test bracket except that it was designed for a higher load, thus insuring that failure would occur in the test bracket. The post-tensioning force was applied by stressing a single 1-3/8 in. diameter Dywidag Threadbar anchored between the test bracket and the other section of structural tube. The Dywidag Threadbar was instrumented similarly to the reinforcing bars used in the testing of Bracket I to measure only axial force.

3.1.3. Bracket Test III

The test of Bracket III, shown in Fig. 11, was similar to that of Bracket II in instrumentation and support conditions. As in the test of Bracket II, eight strain gages and three dial gages were used for data collection. Figure 12 is an overall view of the test setup prior to testing. As in test Bracket II, post-tensioning force was applied by stressing 1-3/8 in. diameter Dywidag Threadbars anchored between the test bracket and another section of structural tubing bolted to the beam.
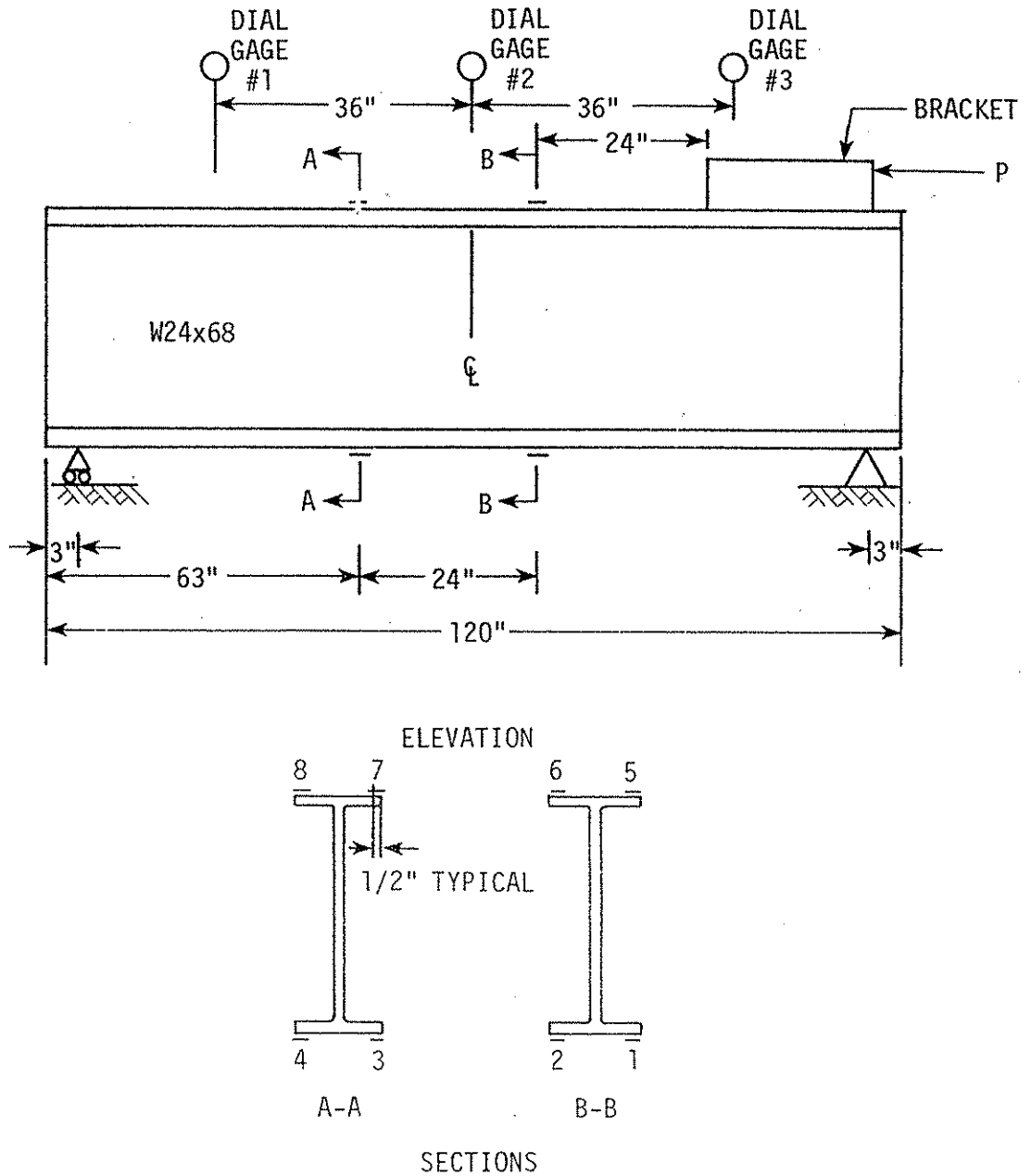
Fig. 9. Strain and displacement gage locations for bracket II.
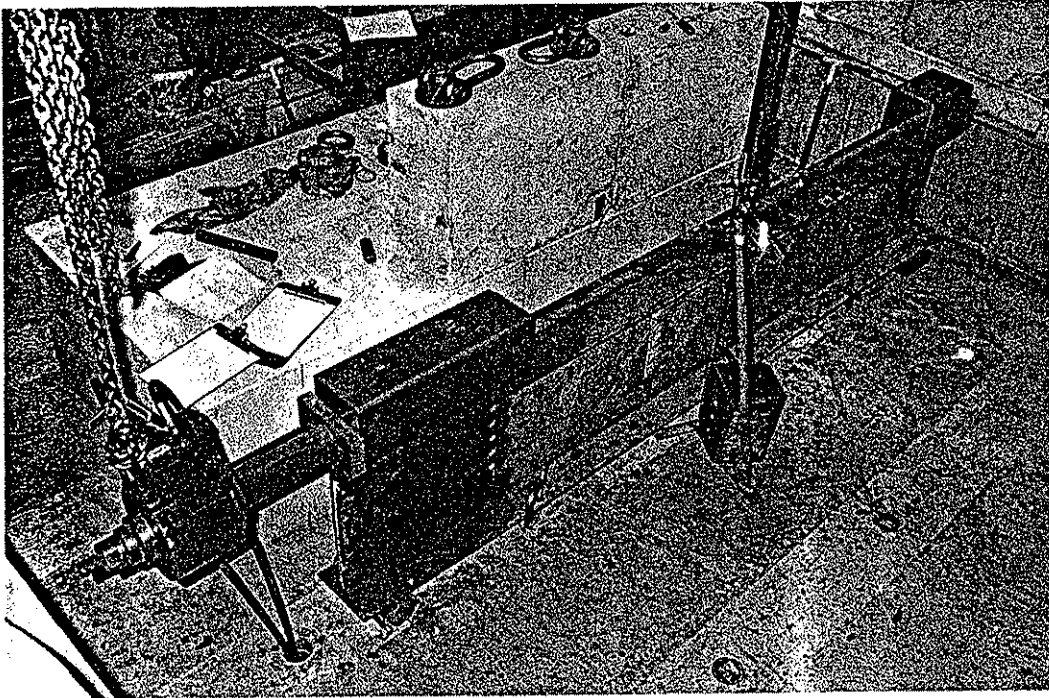
Fig. 10. Bracket II test set-up.
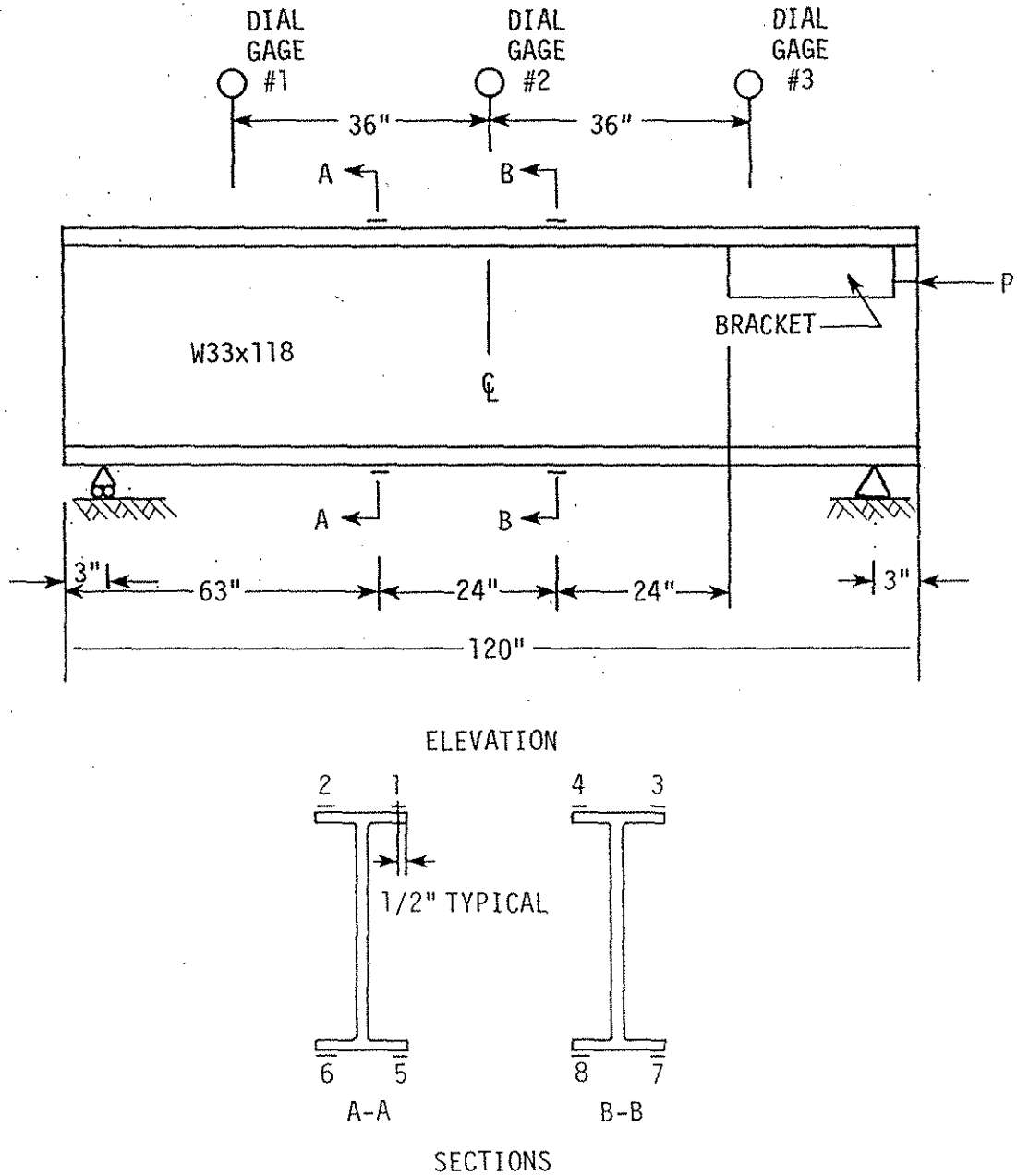
Fig. 11. Strain and displacement gage locations for bracket III.
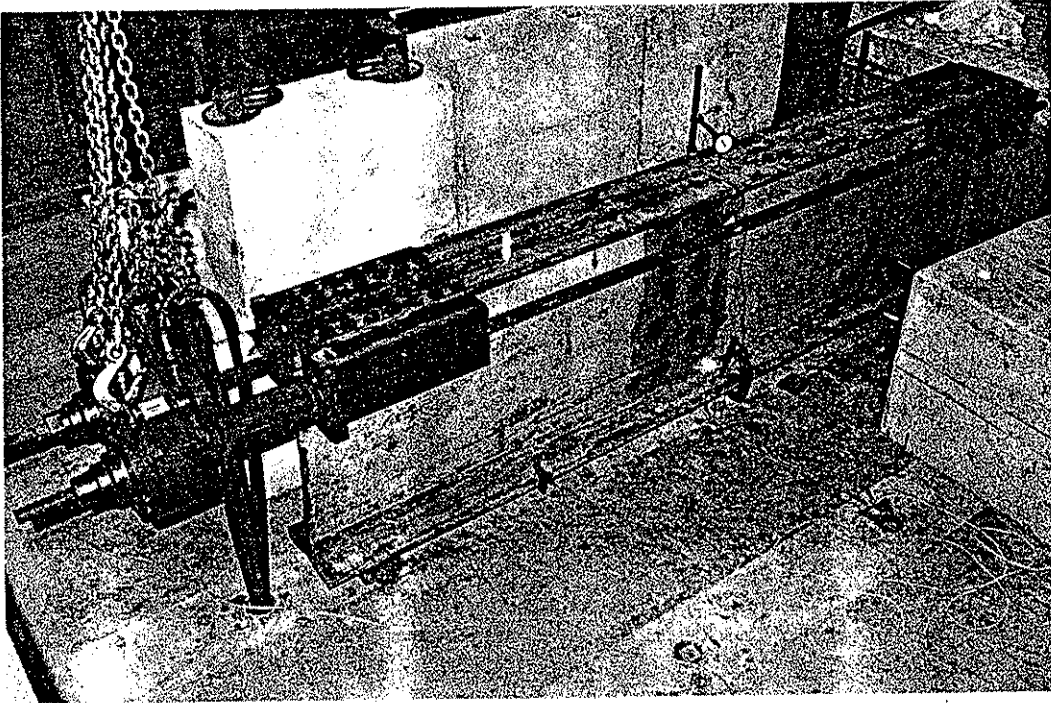
Fig. 12.   Bracket III test set-up.

The bracket was designed for less load than the other structural tube, thus insuring failure in the bracket. Because of the bracket configuration and the force required, two Dywidag Threadbars and thus two hydraulic jacks were required. Both tendons were instrumented, as in previous bracket tests, to measure only axial force.

3.2. Bridge Tests

As has previously been mentioned, numerous tests were performed on the bridge; several of these tests were subdivided. Variables included magnitude and location of post-tensioning force, magnitude and location of vertical load, presence or absence of curbs, presence or absence of diaphragms.

Figure 13 indicates the location of the strain gages used on the steel beams. At each of the 13 sections instrumented, four strain gages were oriented with their axes parallel to the axis of the beam. Two of the four gages were on the top flange of the beam and two were on the bottom flange. At sections where there were no cover plates, such as sections 1 and 6, the gages were placed 1/2 inch in from the flange edge; at sections where there were cover plates, such as sections 3, 4, 8, etc., the gages were placed 1/4 inch in from the edge of the cover plate. As may be seen, the majority of instrumented sections were on Beams 1 and 2; however, the centerline and quarter-point sections of Beams 3 and 4 were also instrumented. Strain gages were also mounted on five of the six interior diaphragms; however time has not permitted analysis of this data as yet.

PLAN VIEW OF FRAME
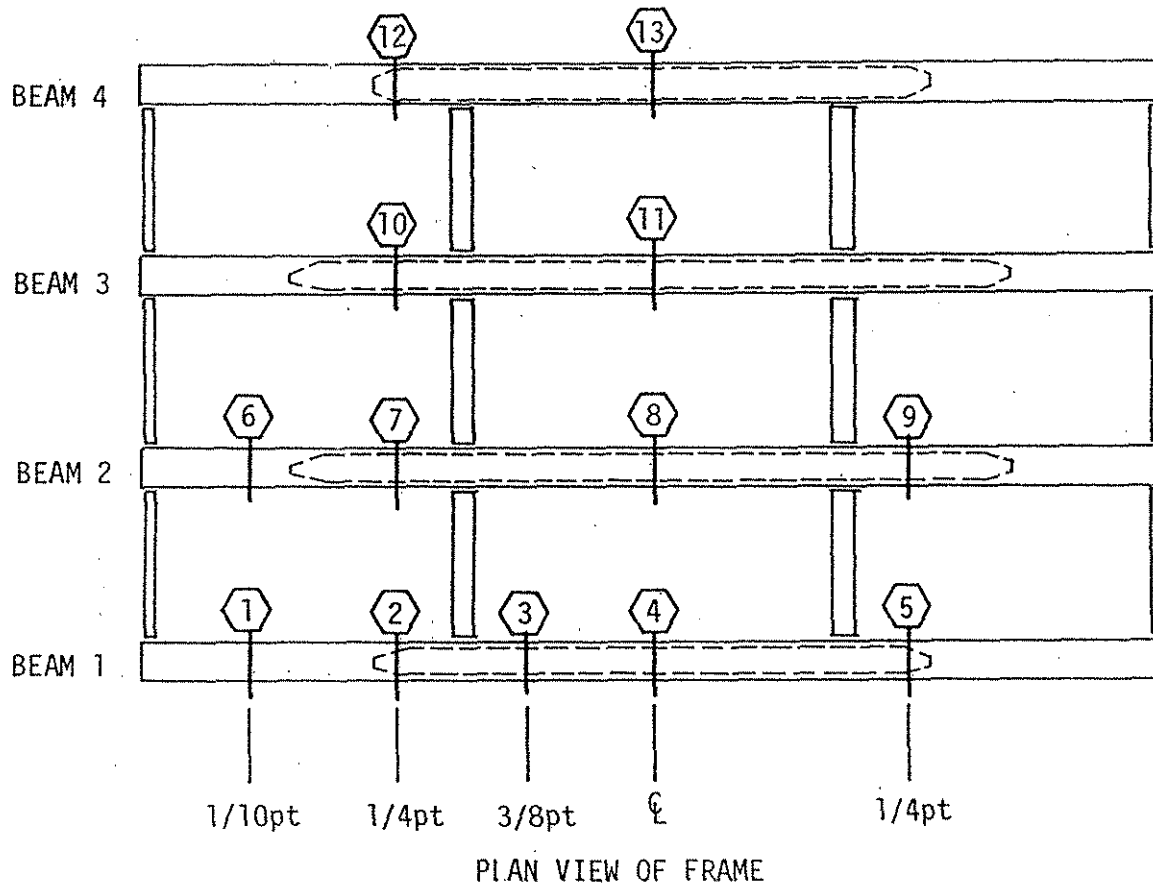
Fig. 13.   Location of strain gage sections.

Each of the 5/8 in. diameter Dywidag Threadbars used for post-tensioning the bridge was instrumented with two longitudinal strain gages connected to cancel bending strain and sense twice the axial strain, thus improving sensitivity.

Strain gages were also mounted on the concrete slab at the quarter-point sections and the centerline section. Two problems were encountered with these gages. When post-tensioning forces were applied to the steel beams, the bridge deck was in tension. In several instances this tension stress resulted in cracks in the concrete which passed through the strain gages, destroying them. The other problem with the concrete strains was their small magnitude, which was a result of the loading being applied. Thus the results obtained were of questionable reliability and were not used in further evaluations.

The locations of the dial gages used for measurement of bridge movement are presented in Fig. 14. Dial gages oriented for measurement of vertical movement have been labeled with a "V"; those for detecting horizontal movement (as on Beams 1 and 4) have been designated with an "H." As one would expect, horizontal movement for the vertical load and post-tensioning load was either zero or essentially zero. Dial gages at the centerline of supports on Beams 1 and 4 were so placed to determine if the beams lifted off their supports when loading was applied to the opposite side of the bridge. The magnitude of vertical loading was scaled so that lift-off did not occur during any of the composite bridge tests, although it did occur during preliminary testing of the steel frame.

To determine the effectiveness of the diaphragms, an attempt was made to test the steel frame prior to placement of the concrete deck.

PLAN VIEW OF FRAME
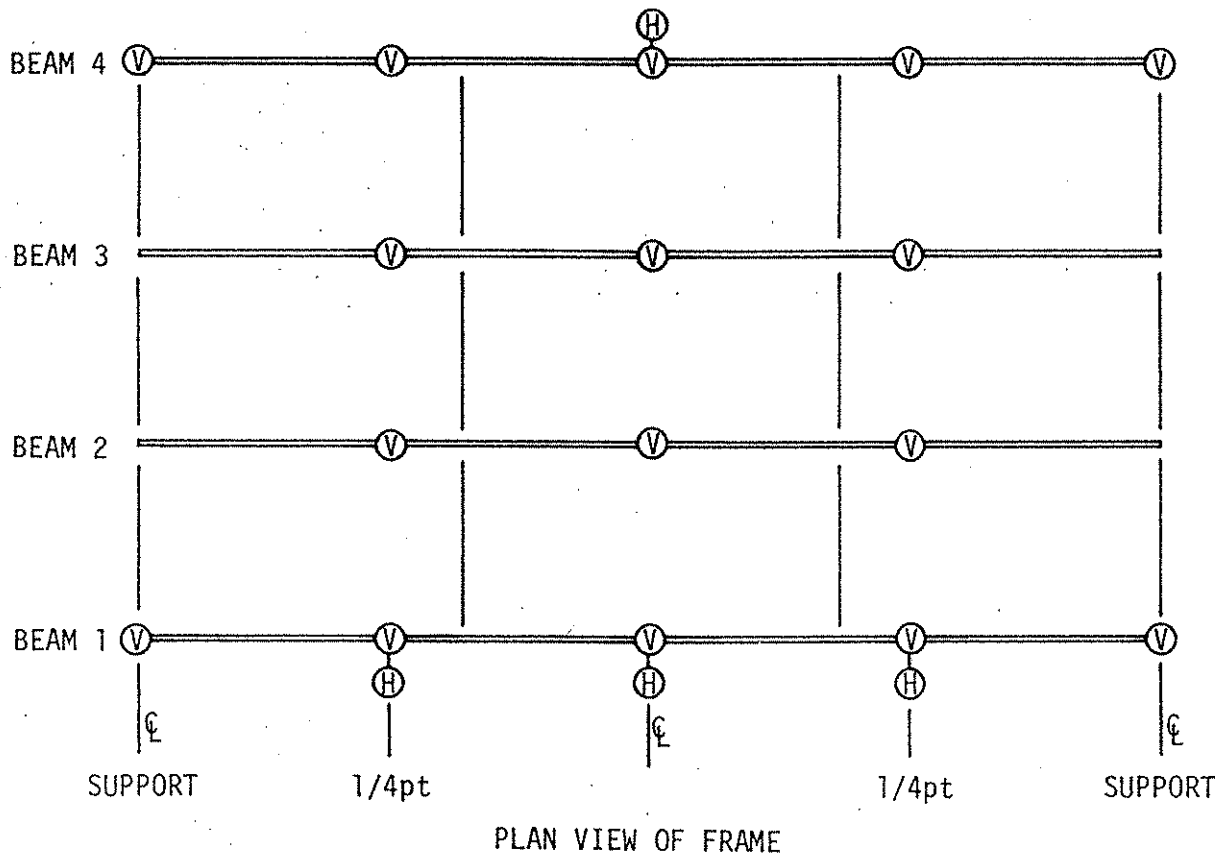
Fig. 14.   Location of deflection dials.

This testing was unsuccessful for the following reasons. If load of sufficient magnitude was applied to produce measurable strains, one or the other of the exterior beams would lift from its supports since there was not sufficient dead load (frame weight) to keep it in place. As soon as one of the beams came off the supports, the original boundary conditions changed (i.e., three beams rather than the original four now supported the load). Also the beam that was off the supports became an additional load for the other three beams to support. The resulting frame was not of interest as it had no practical significance.

Table 4 lists the combination of variables in each of the 18 different tests. As may be seen, the various combinations make it possible to isolate the effects of the several variables. Clarification of the various loading positions, truck loading, post-tensioning schemes is presented in Figs. 15 and 16 and Table 5.

For clarity, the bridge testing program will be presented in three sections: vertical load tests (tests 1-4 in Table 4), post-tensioning tests (tests 5-13) and tests involving a combination of vertical load and post-tensioning (tests 14-18). Note that test numbers do not indicate the order in which the tests were performed.

In tests where it is indicated that there were no diaphragms, such as in tests 4, 12 and 13, the interior diaphragms were unbolted, rotated 90 degrees and lowered to the bottom flanges of the main beams; thus they were essentially noneffective.

3.2.1. Vertical Load Tests

Tests involving only vertical loading are designated in Table 4 as tests 1-4. In Table 4, the numbers from 1 to 14 listed under the

le 4. List of tests--combinations of loading, curbs, and diaphragms.

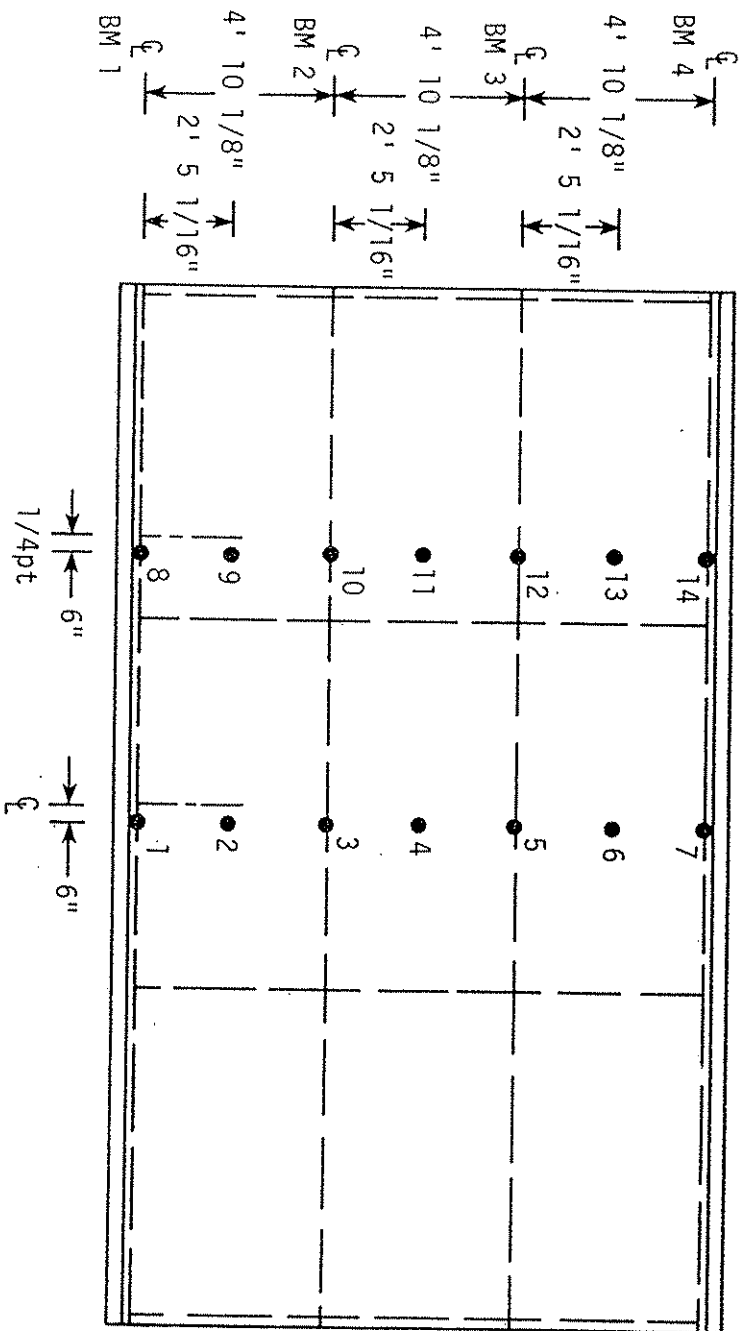| Test number	Post-Tensioning Scheme				Vertical Loading																						T†	Curbs	Diaphragms
					5 kips @														10 kips @										
	1	2	3	4	1	2	3	4	5	6	7	8	9	10	11	12	13	14	1	3	5	7	8	10	12	14*	T†	Curbs	Diaphragms
1					•	•	•	•	•	•	•	•	•	•	•	•	•	•	•	•	•	•							•
2																											•		•
3					•	•	•	•	•	•	•								•	•	•	•						•	•
4					•	•	•	•	•	•	•	•	•	•	•	•	•	•	•	•	•	•	•	•	•	•		•	
5	•																												•
6				•																									•
7		•																											•
8			•																										•
9	•																											•	•
10				•																								•	•
11		•																										•	•
12	•																											•	
13				•																								•	
14	•				•	•	•	•	•	•	•								•	•	•	•							•
15	•																										•		•
16				•	•	•	•	•	•	•	•								•	•	•	•							•
17				•																							•		•
18	•				•	•	•	•	•	•	•								•	•	•	•						•	•

sitions at which load was applied (see Fig. 15).

:mulated truck load (see Fig. 18).

PLAN VIEW OF BRIDGE DECK

Fig. 15. Location of vertical load points.

PLAN VIEW OF BRIDGE DECK
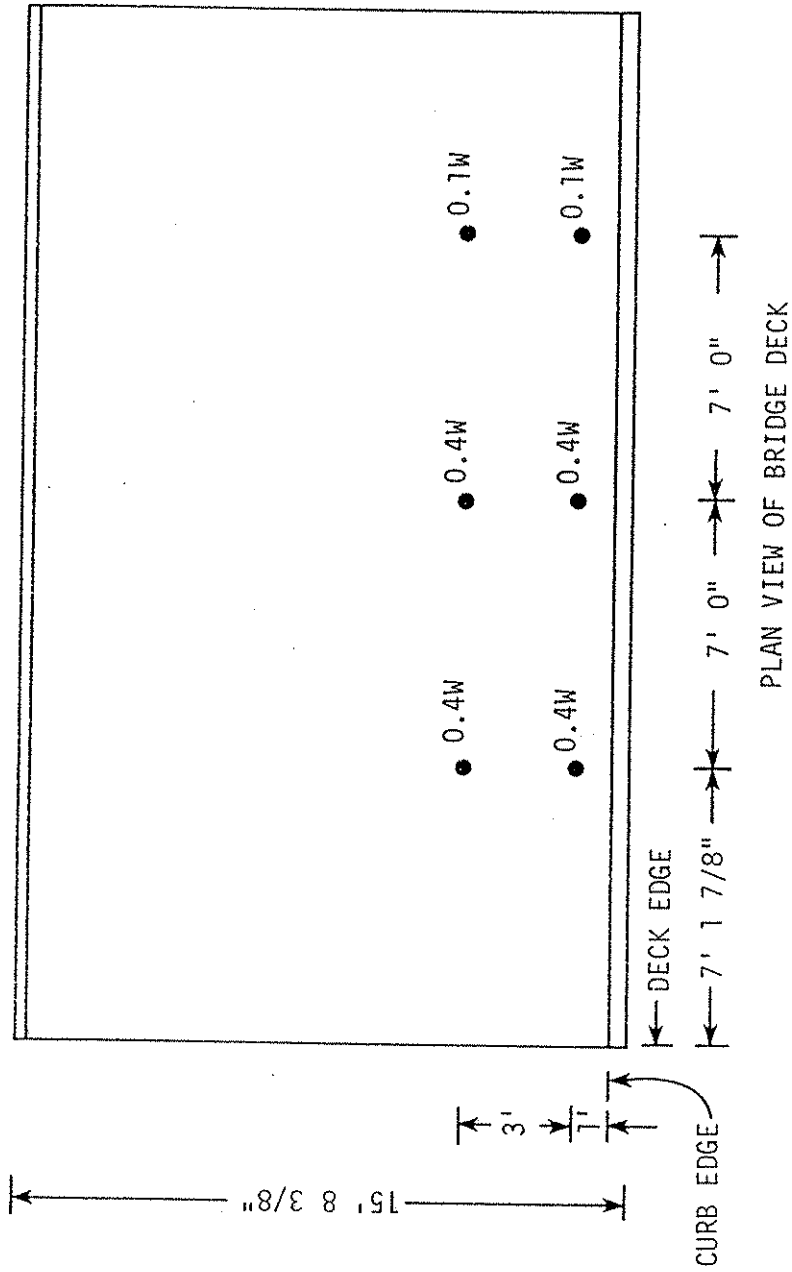
Fig. 16. Location of truck loading.

Table 5.   Post-tensioning configurations.

Post-tensioning Scheme	Configuration			
	Beam			
	1	2	3	4
1				
Order	1			1
2				
Order	1			2
3				
Order	1	2	3	4
4				
Order	1	2	2	1

vertical loading heading represent 14 different positions at which, depending upon the test in question, concentrated load was applied; locations of the 14 points are given in Fig. 15. Note that load points are 6 in. off centerline of span and 6 in. off the quarter point of span to avoid the concrete strain gages. A load of 5 kips or 10 kips was applied to the various load points. As may be noted in Table 4, 10 kips were applied only at positions over the beams, since the concrete deck did not have sufficient strength to support a load of this magnitude. Application of the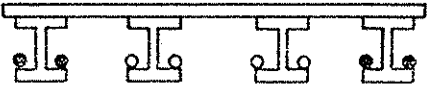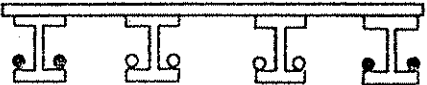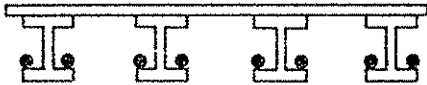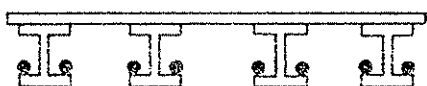 5-kip and 10-kip force was achieved by use of concrete weights, one of which measured 4 ft × 4 ft × 2-1/4 ft. The other weight had a different bottom configuration, so that it could be placed accurately upon the desired location.

The concrete weights were placed on 9 in. × 9 in. × 3 in. neoprene pads, thus approximating a concentrated load. Each block weighed approximately 5 kips; thus two fastened together produced the desired 10 kips weight. The actual weight of the lower block and bearing pads was 4950 lbs (previously and henceforth referred to as 5 kips); the weight of the two blocks and bearing pads together was 10,040 lbs (previously and henceforth referred to as 10 kips). In all theoretical calculations the true or actual block weight was used.

Figure 17 shows the 10-kip load at load position 3; the worker at the edge of the bridge is recording deflection data.

The procedure for each of the vertical load tests was to:

1. Record "zero" strain readings for all strain gages utilizing the data acquisition system; read and record initial readings of all dial gages.
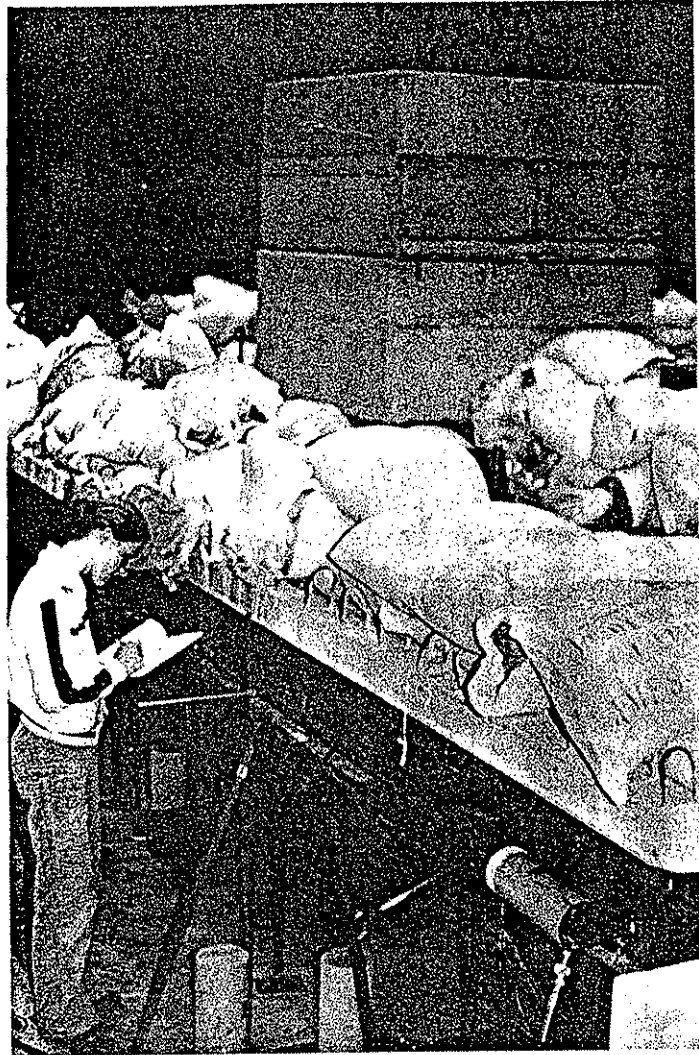
Fig. 17.   Typical vertical load test—10-kip
concrete weight at position 3.

2. Apply load of desired magnitude (5 kips or 10 kips) at desired location.

3. Take strain gage and dial gage readings as in step 1. Record any behavioral indications.

4. Remove load from bridge and take second "zero" strain gage reading as in step 1. (This was necessary because of the "zero shift" problem associated with the data acquisition system.)

5. Repeat steps 1 and 2 until the load has been placed at the desired number of locations.

The other vertical load test undertaken was to subject the bridge to a simulated truck load; this type of loading is indicated by "T" in Table 4. The position of the simulated truck loading, henceforth referred to as the truck, is shown in Fig. 18. The truck has been positioned on the bridge at the design distance from the curb to produce the maximum moment in the span. The wheel load and spacing shown are in proportion to an HS-20 truck.

Holes were bored through the deck at each of the "wheels." Steel rods were placed through the holes and secured against steel plates and 9 in. × 9 in. × 3 in. neoprene pads which were centered over the holes. Under the bridge, the rods were anchored to the tie-down floor through a system of structural tubes and additional steel rods. In the loading system under the bridge were hydraulic jacks and load cells for applying and measuring load respectively.

Inadvertently the ratio of load on back axles to load on front axles was 2 to 1 rather than the desired 4 to 1 as shown in Fig. 16.
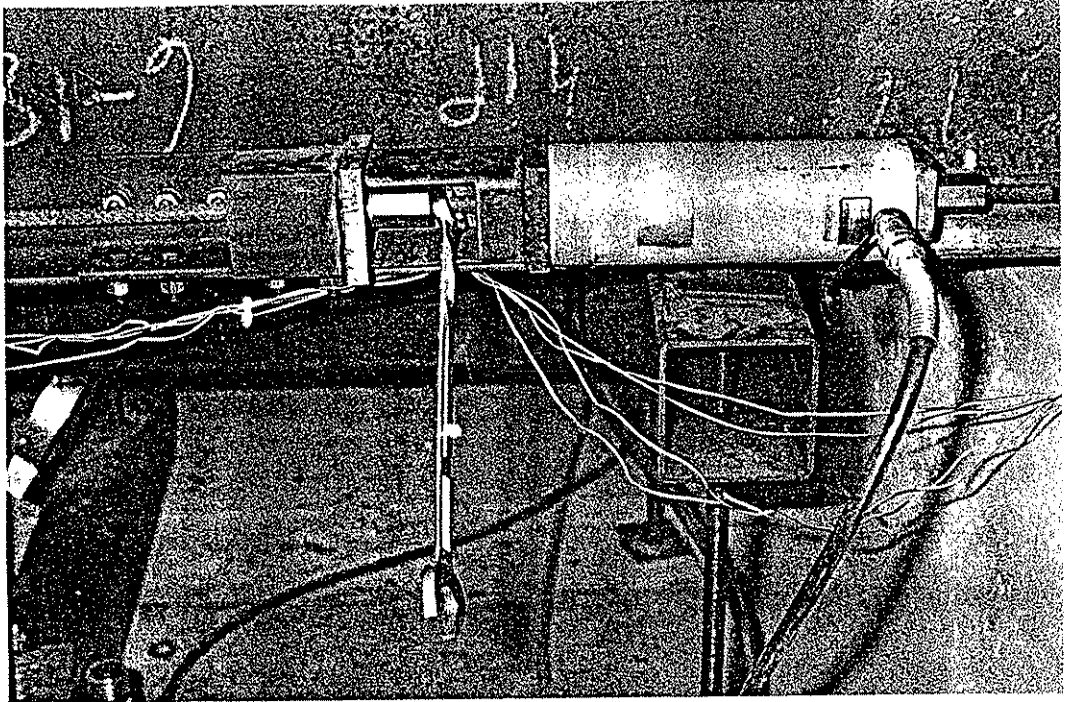
Fig. 18.   Photograph of post-tensioning jack in position.

55

Load was applied to the bridge in increments of 2 kips to the rear

axles and 1 kip to the front axle until an overload condition existed.

The testing procedure followed was the same as previously stated except

that, rather than moving the concentrated load to another position,

another increment of truck loading was added.

3.2.2. Post-Tensioning Tests

Tests involving only post-tensioning loading are listed in Table 4

as tests 5-13. In Table 4, numbers from 1-4 are listed under the post-

tensioning scheme heading; Table 5 describes the various post-tensioning

schemes utilized. As may be seen, the only difference between schemes 1

and 2, henceforth referred to as PTS-1 and PTS-2, in which only the

exterior beams are post-tensioned, is the order of post-tensioning.

Likewise the only difference between PTS-3 and PTS-4 in which all beams

are post-tensioned is the post-tensioning sequence.

Post-tensioning force was applied to the various beams, utilizing

60 kip capacity hollow-core hydraulic jacks. Fig. 18 illustrates one

of the jacks in position. If it was desired to post-tension beams and

collect data at various post-tensioning load levels, such as in tests 5,

9 and 12, the procedure was to apply the desired force with the hydraulic

jacks, collect the desired data and release the force. However, for other

load cases, such as tests 6, 10 and 13, it was necessary to lock the

force on some of the beams before post-tensioning the others.

Locking the force in a given beam was accomplished as follows.

First, the approximate desired force was applied to the post-tensioning

tendons by the hydraulic jack acting against the chair (see Fig. 19).

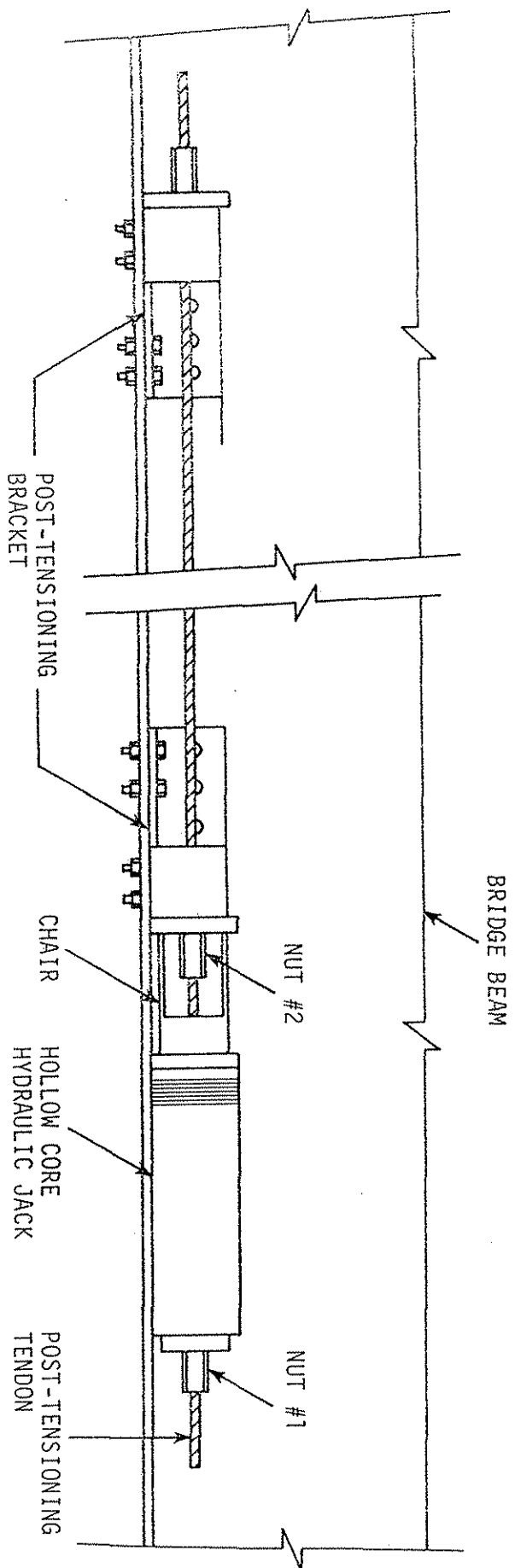Nut 2 was then tightened, so that a force slightly higher than desired

POST-TENSIONING
BRACKET

POST-TENSIONING
BRACKET

CHAIR

NUT
#2

HOLLOW CORE
HYDRAULIC JACK

NUT
#1

POST-TENSIONING
TENDON

BRIDGE BEAM

Fig. 19. Post-tensioning system in position.

56

was in the rod to offset seating losses. All nuts utilized were cold worked before using, thus making possible more accurate prediction of seating losses. The hydraulic jacks were then released and the force was locked in the rod (and thus the beam) by nut 2 seated against the post-tensioning bracket. All post-tensioning tendon forces were determined by measuring the strain in the tendon.

The previously presented test procedure (taking of initial strain "zeros," dial reading, applying force, etc.) was again utilized, the only difference being in the type and location of loading applied.

From initial calculations it was found that the Appanoose County bridge required approximately 80 kips of post-tensioning force to be applied to each of the exterior beams (Beams 1 and 4) to counterbalance the desired amount of strain in the exterior beam bottom flanges. Thus the model bridge required 20 kips in each exterior beam to produce the desired results.

The loading procedures followed on each of the four schemes (see Table 5) was as follows:

In PTS-1, force was applied to Beams 1 and 4 in increments of 4 kips per beam until 36 kips (1.8 times that required) per beam was reached.

In PTS-2, force was applied in increments of approximately 4 kips to Beam 1 up to 34 kips and then released. A force of 20 kips was then locked in Beam 1 and the force in Beam 4 increased by 4-kip increments to 34 kips. Force in Beam 4 was then released and a force of 20 kips locked in.

In PTS-3, a force of 20 kips was first locked in Beam 1; 20 kips were locked in Beam 2. Next, 20 kips were locked in Beam 3; finally 20 kips were locked in Beam 4.

In PTS-4, 20 kips were locked in Beams 1 and 4. Next the force in Beams 2 and 3 was increased to 34 by increments of approximately 4 kips. Force to Beams 2 and 3 was then released and 20 kips were locked in each interior beam (Beams 2 and 3).

In the previous discussion of the various post-tensioning schemes, it was stated that 20 kips were locked in the various beams. Because of the variability of seating losses, this obviously was the value desired, not necessarily the value obtained. However, in no instance was a force less than 20 kips locked in a beam, and in all cases the force locked in did not exceed 20 kips by more than 1.5%.

3.2.3. Combination Tests--Vertical Load Plus Post-Tensioning Force

Tests involving a combination of vertical load and post-tensioning are designated in Table 4 as tests 14-18. These tests involved both vertical loading (concentrated load at various points as well as truck loading) plus post-tensioning forces. As Table 4 indicates, only two post-tensioning schemes were used--namely PTS-1 where 20 kips are locked in Beams 1 and 4 and PTS-4 where 20 kips are locked in all beams. Loading procedures, data collection procedures, etc. were the same as those presented in Sections 3.2.1 and 3.2.2. In each of the tests (14-18), the post-tensioning forces were applied and locked in prior to the addition of vertical load. Instrumentation on the post-tensioning tendons permitted measurement of force changes in the tendons as location and magnitude of the vertical force was changed.

4. TEST RESULTS AND ANALYSIS

In Section 3 the details of the test program and the actual events that occurred during the conduct of the tests were presented. In subsequent sections of this chapter the experimental results will be summarized and compared with theoretical results. Also presented is an analysis of the significance of the various variables investigated. For clarity each test program will be discussed separately.

4.1. Bracket Test Results and Analysis

Earlier, the bracket descriptions (Section 2.3) and bracket test setups (Section 3.1) were presented. The following sections will present behavior information and data obtained in each of the bracket tests. Experimental results obtained are then compared to values obtained from theory. One measure of the effectiveness of the brackets in transmitting the applied force to the beam is the relationship of measured and theoretical strains and displacements in the beam.

The beam in each bracket test was essentially an eccentrically loaded column with the only lateral load present being the weight of the beam. This is a nonlinear problem; i.e., the deflection with respect to the axial load is nonlinear when transverse load is held constant and axial load is increased. However, for values of axial load that are relatively small compared to the buckling load of the beam-column, the relationship is essentially linear. Therefore, if the axial load applied to the beam-column is small compared to the buckling load of the beam-column, the aforementioned nonlinearity may be neglected.

In all the bracket tests, the loads applied were less than 5% of the buckling load of the beam-column. Thus, a numerical integration procedure, such as Newmark's Method can be used to calculate beam deflections.

Theoretical deflections presented in the following sections were determined utilizing Newmark's Method of numerical integration. The axial load-deformation effect (P-Δ effect) was found to be extremely small (due to the magnitude of the loads applied and the beam-column size) and so was not included in the theoretical strains calculated. The theoretical strains thus are simply a combination of the flexural and axial load effects.

4.1.1. Behavior of Bracket I

Bracket I (see Fig. 4) was attached to a cantilever beam and loaded with two number 9 reinforcing bars and two 60-kip capacity hollow-core hydraulic jacks up to maximum capacity of the test setup (120 kips) with no sign of distress or deformation of the bracket. This load was approximately 1.4 times the bracket design load or approximately six times the required strength for use on the bridge model. Thus, it was decided that Bracket I, although somewhat overdesigned, would be used on the bridge model.

Figure 20 presents representative samples of theoretical and experimental compressive strains for Bracket I. Gage locations are shown in Fig. 7. Inspection of the beam before testing revealed a small eccentricity about the weak axis. Neglecting this resulted in the theoretical curve labeled Theory #1 in Fig. 20. As may be seen, compression gages at the same sections, i.e., 3 and 4, 5 and 6, etc., are considerably different and do not compare favorably with this curve.
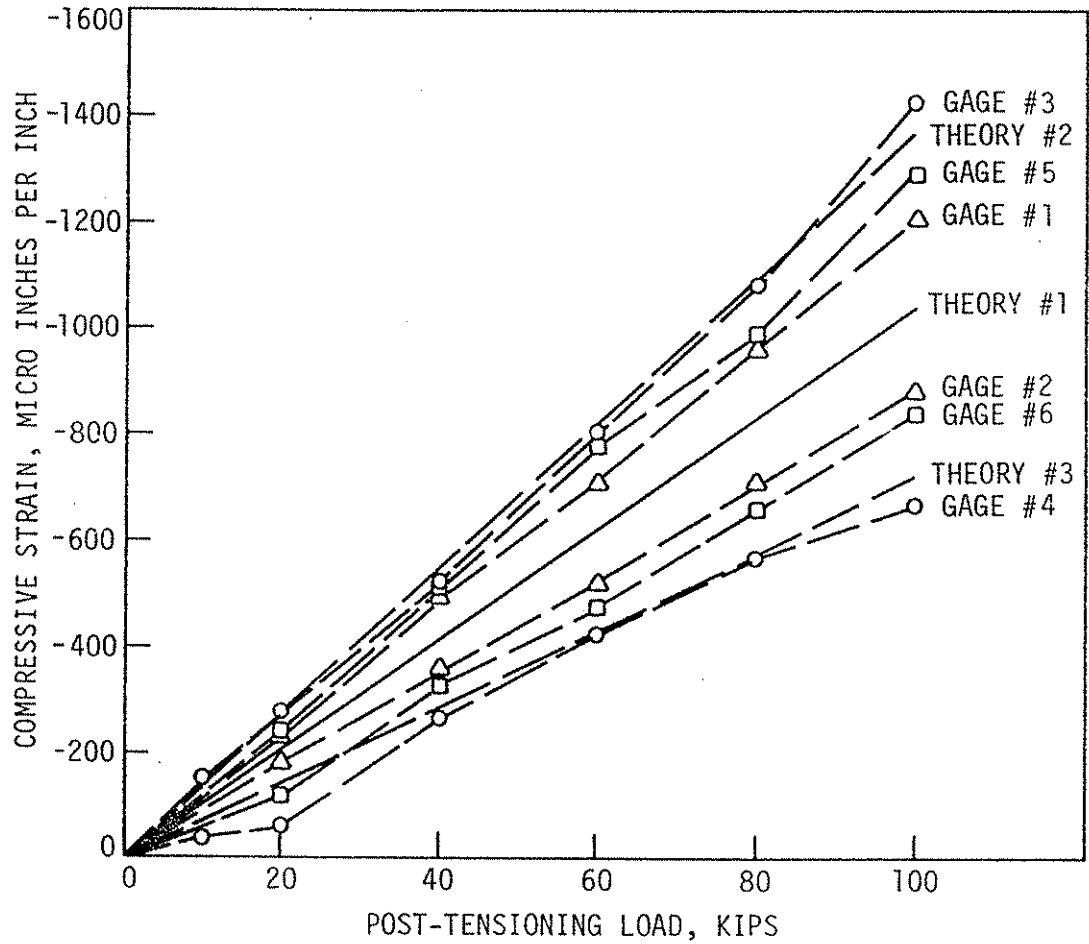
Fig. 20.   Post-tensioning load vs. compressive strain for bracket I.

Taking weak axis bending into account produces curves labeled Theory #2 and Theory #3. As may be seen, when weak axis bending is included there is good agreement between experimental and theoretical strains.

Theoretical and experimental deflections at the free end of the cantilever beam (dial gage #1, see Fig. 7) used in Bracket I are presented in Fig. 21. At low loads there is considerable difference between experimental and theoretical values; however, at higher loads—above 60 kips—there is a very good comparison. One possible explanation for the difference at low loads is that as the hydraulic jacks were seated against the end of the beam, the entire beam underwent rotation, thereby giving the negative deflections shown in Fig. 21. Another problem in the comparison of theoretical and experimental results at low loads is the beam support. Theoretically it is assumed to be fixed; however, this was only approached in the laboratory test.

Because the limit of the loading system was 120 kips, it was not possible to force failure in or even to distress Bracket I. Therefore, it was decided to remove some of the bolts connecting the bracket to the beam, thus forcing a failure in the remaining bolts. After bolts 1, 5 and 9 were removed (see Fig. 22) the bracket was loaded to 100 kips with no apparent deformation or distress. Bolt 11 was then removed, but the bracket loaded to 100 kips with no problems. Removal of bolts 2, 6, and 10, leaving six of the original thirteen bolts, resulted in failure of four of the remaining six bolts in shear (bolts 7, 8, 12 and 13) at a load of approximately 100 kips. After the bolt failure, the bracket had very little deformation. The performance of Bracket I with less
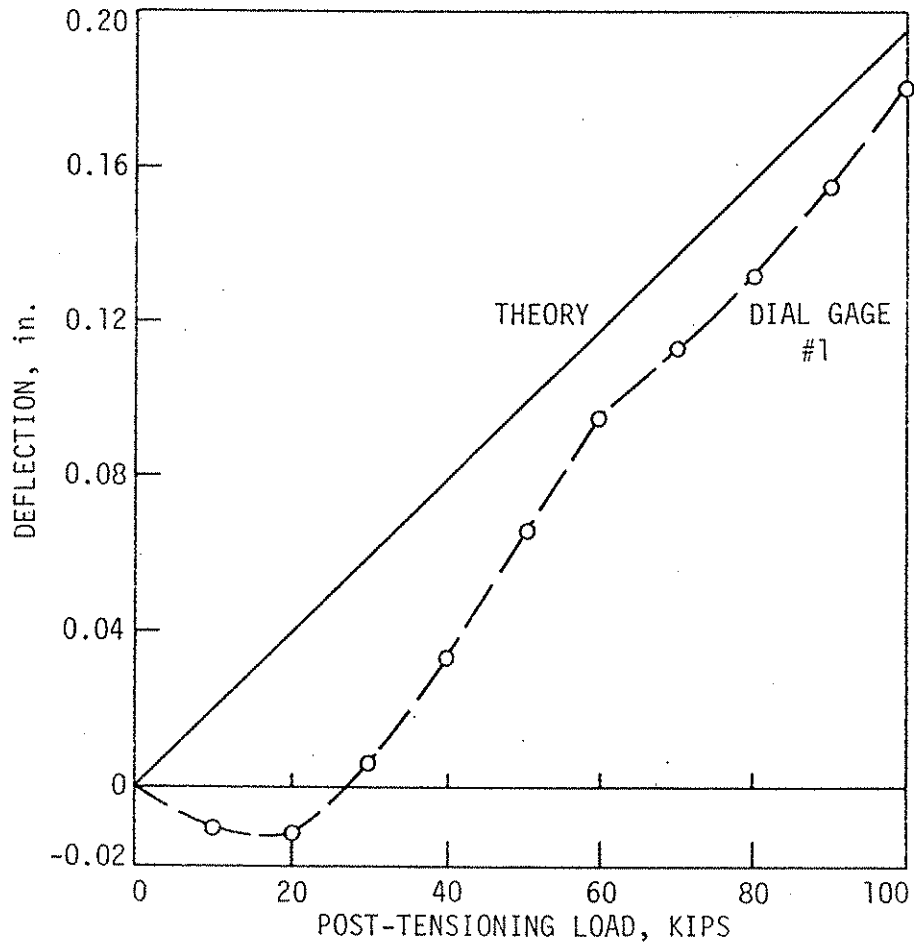
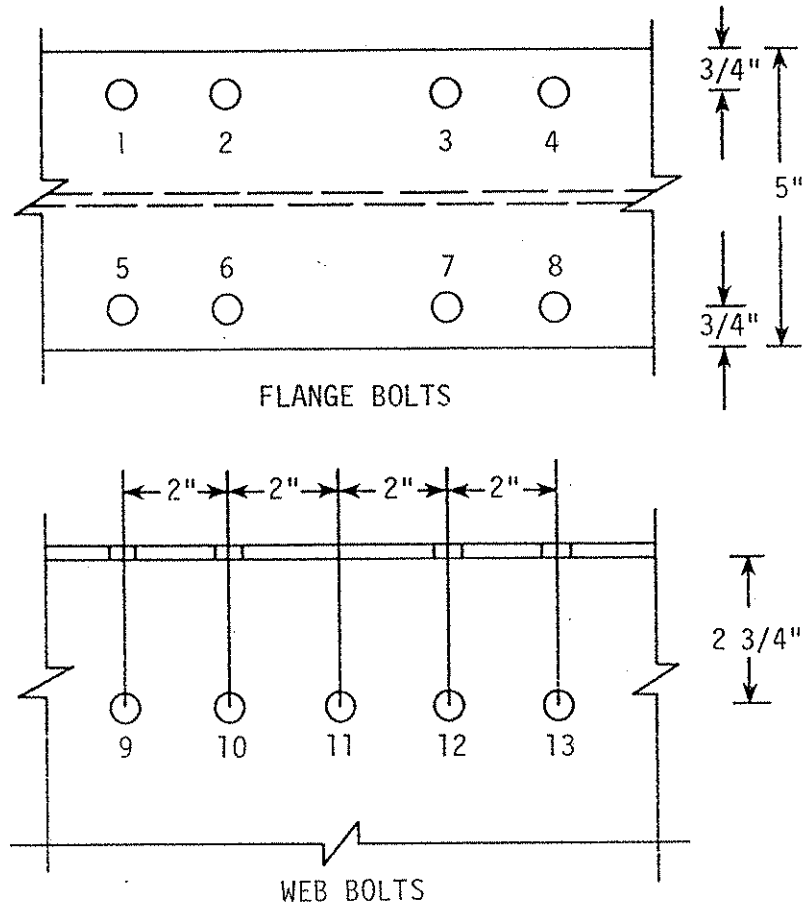Fig. 21.   Post-tensioning load vs. deflection, dial gage 1,
for bracket I.

Fig. 22. Bolt locations for bracket I.

than half the designed number of bolts in place reinforced the decision to utilize it on the model bridge.

4.1.2. Behavior of Bracket II

Bracket II (see Fig. 5) which was designed for a post-tensioning force of 80 kips, was attached to a simply supported beam (see Figs. 9 and 10). Force was applied to the bracket by a Dywidag hydraulic jack with a capacity of 220 kips, stressing a 1-3/8 in. Dywidag Threadbar whose ultimate strength was 237 kips. Load was applied to the bracket in 20-kip increments, with strains and deflections recorded after each load increment, until the design load was reached. At this level the bracket and beam displayed no apparent distress or deformation. Loading was then continued in increments of 20 kips up to 140 kips, at which time deformation of the beam flange was noted.

Loading was again increased, but it was possible to reach only 142 kips as the beam flange and bracket continued to deform. The final deformed beam and bracket are shown in Fig. 23.

Failure occurred in the beam flange to which the bracket was bolted, rather than in the bracket. Other than the deformation of the bracket that resulted from its being bolted to the beam flange, there was no damage to either the bracket or the bolts.

At loads considerably larger than the design loads, the bracket performed with no problems. However, to improve its load carrying ability at higher loads, one or both of the following modifications could be made. If beam stiffeners were provided in the vicinity of the bracket, the stiffness added to the beam flanges probably would prevent the type of failure that occurred. Also, increasing the bracket length
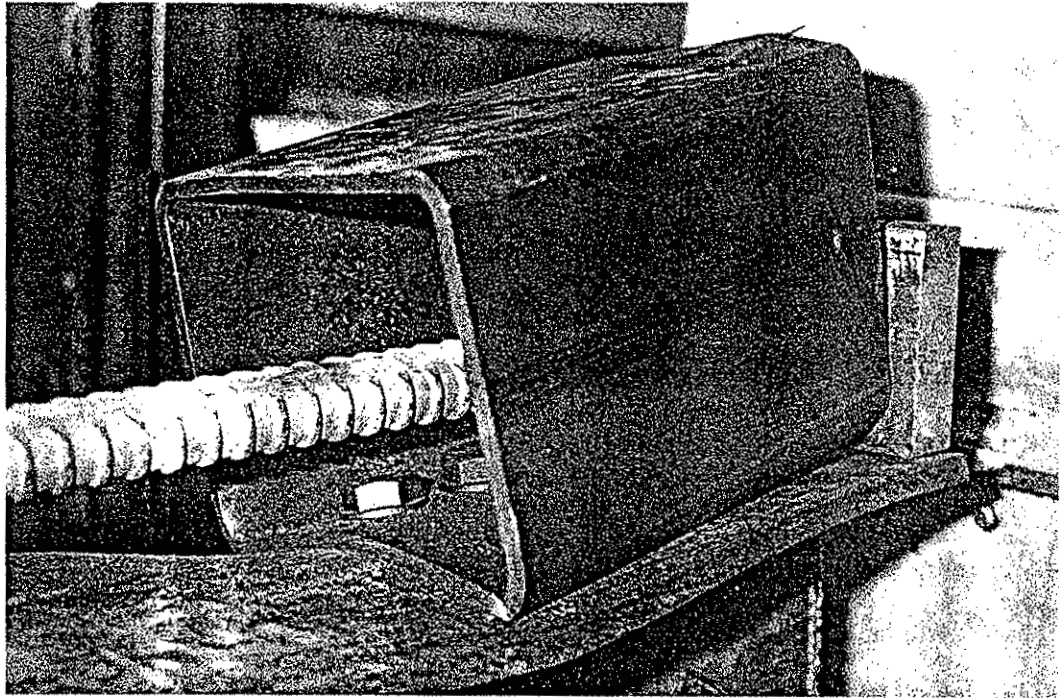
Fig. 23. Failure deformation of bracket II and beam flange.

would provide more beam flange to resist the bending and thus would also be likely to prevent the failure that occurred.

Although Bracket II did experience large deformations (and thus failure), the failure was not sudden and it occurred at approximately 1-3/4 times the design load. As with Bracket I, there was good agreement between the theoretical and experimental strains and deflections.

4.1.3. Behavior of Bracket III

Bracket III (see Fig. 6), designed for a load of 120 kips, was tested while attached to a simply supported beam (see Fig. 11). Post-tensioning force was applied through two 1-3/8 inch diameter Dywidag Threadbars (each with an ultimate strength of 237 kips) stressed by two 220-kips capacity Dywidag hydraulic jacks. Load was incrementally increased to 80 kips at which time it was noticed that both brackets were separating from the web. As loading continued, the brackets continued to separate from the web; at 120 kips the brackets began to pull away from the flanges. Both these deformations continued until the maximum load of 149 kips was reached, at which magnitude plastic deformation of the brackets began. The failure of the bracket, shown in Fig. 24, was the result of severe deformations of the bracket. Inspection of the connection after failure revealed no bolt damage.

Failure occurred at approximately 2/3 of the design load, thus making Bracket III unacceptable. The performance of Bracket III could be improved in two ways. The use of additional bolts, although not required for transmitting force from the bracket to the beam, would provide more support to the structural tube and thus prevent some of its deformation which led to failure. Use of bearing plates that covered
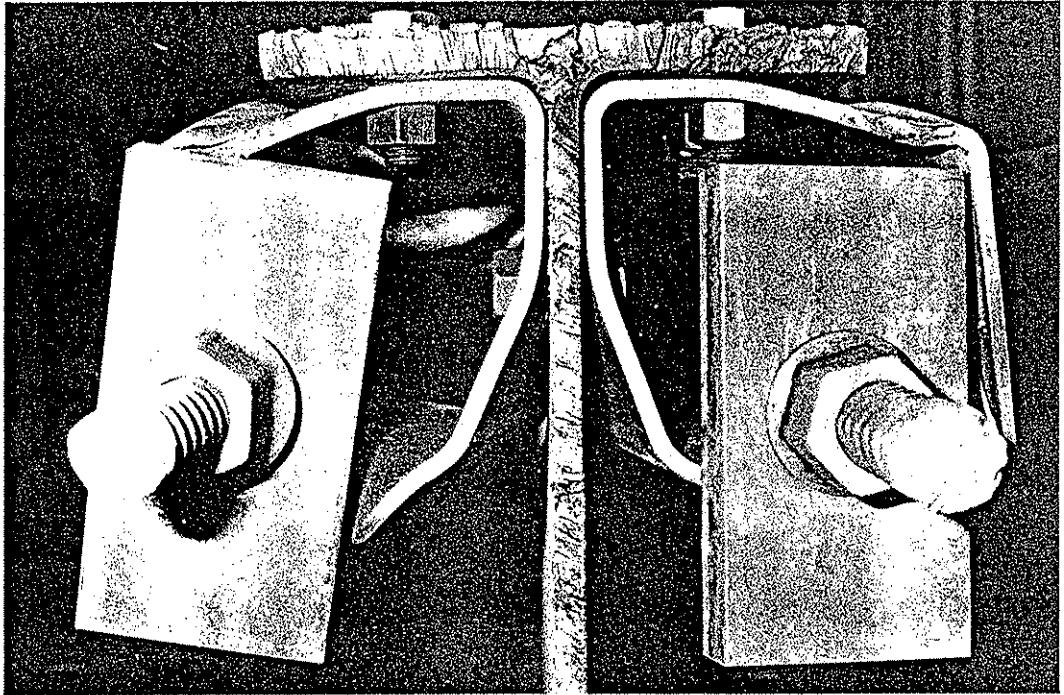
Fig. 24.   Deformation of failed bracket III.

the entire end of the bracket would provide a more uniform force transfer to the bracket and also reduce the eccentricity about the minor axis. Both of these effects would improve the performance of Bracket III.

In the opinion of the researchers, the aforementioned modifications to Bracket III would make it more than adequate for field use. However, before actually using this bracket, the suggested modifications should be made and the bracket tested.

The agreement between theoretical and experimental strains and deflections below 80 kips was found to be quite good considering the magnitude of strains being measured. Above 80 kips there is considerable deviation which could be the result of several factors. At loads above 80 kips the bracket was deforming. This deformation continually changed the location of the application of load, thus affecting the strain in the beam. Also, deformation of the left and right portions of the bracket were not symmetrical, which suggests the possibility of weak axis bending. Another reason for the difference between the experimental and theoretical strains could be the means by which load was applied. Load was applied by two separate jacking systems thus making it extremely difficult to keep the force on the left and right equal. Any variation in force from the left to the right side would produce weak axis bending.

4.2. Orthotropic Plate Theory

Orthotropic plate theory and its use in bridge deck analysis is well known. The beam, diaphragm and slab bridge deck assembly is

replaced, for purposes of analysis, by an orthogonal, anisotropic plate of uniform thickness but with elastic properties different in two orthogonal directions. The bridge deck can then be represented by a fourth order linear differential equation.

The differential equation can be solved by various methods. Sanders and Elleby [43] utilized a Levy series solution. That solution, programmed in FORTRAN, is used for all theoretical load distributions in this study. The solution depends on the flexural parameter, θ, and the torsional parameter, α. (Both parameters for model and prototype are presented in Table 1.) Results of the series solution are obtained in terms of moment coefficients across the midspan cross section of the deck. Each coefficient represents the ratio of the moment at that point to the average moment at the bridge cross section. Utilizing numerical integration to determine the area under the moment coefficient curve over the width tributary to a particular bridge beam yields the fraction of the total longitudinal bridge moment applied to the beam.

Because of the complexity of the bridge model, several approximations were necessary. Because the exterior and interior beams are not of the same stiffness, the width of the bridge was reduced for analysis using the ratio of exterior beam stiffness to interior beam stiffness as suggested by Sanders and Elleby [43]. The reduced width affects the flexural parameter, θ, and hence the orthotropic plate solution. Within the reduced exterior beam width, load positions were scaled accordingly.

The varying stiffness along beams due to absence or presence of cover plates was neglected. Since the central halves or more of the bridge beams were cover plated, the stiffnesses of the composite beams

with cover plates were used in the orthotropic plate parameters. This procedure should introduce little error since beam deflections with full- or partial-length cover plates are quite similar.

Moment fractions obtained for midspan by orthotropic plate theory were assumed to apply over the entire bridge span, although that is not strictly correct. In general, the variation in moment fractions among beams is less near the supports than at midspan and hence some error is introduced as noted in Section 4.5.

The basic orthotropic plate solution is obtained for a concentrated load applied perpendicular to the bridge deck at midspan. Axial forces and moments due to post-tensioning are, of course, different loading conditions. A review of plate coefficients [4] showed that, at least for axial forces, axial force coefficients would be similar to moment coefficients for the midspan concentrated load. As an approximate check on the experimental results, moment fractions for post-tensioning and axial force fractions for post-tensioning were assumed to be the same as the moment fractions for vertical load. On the basis of results to date, orthotropic plate theory is acceptable for preliminary designs of post-tensioning systems.

4.3. Strain and Deflection Data Interpretation

Both strain and deflection data were used to compute fractions of moment distributed among the model bridge beams for vertical loading and for post-tensioning. Computations required section properties for the composite bridge beams. A review of the strains measured on top

and bottom beam flanges indicated that neutral axis locations were almost always lower than those predicted on the basis of AASHTO's effective flange widths. The lower neutral axis could be caused at least partially by slab shrinkage, as suggested by Hondros and Marsh [28]. The neutral axis also moved upward when concentrated vertical loads were placed on or adjacent to the beam under consideration, again as observed by Hondros and Marsh. In the authors' judgment, the most accurate data interpretation would be achieved using average neutral axis locations for beams near concentrated loads. Those average locations were then used to obtain effective slab widths and relative section properties.

Bottom flange strain data were substantially larger and hence more reliable than other strain data. Bottom flange strains are proportioned to beam moment fractions as indicated below:

$$f = \frac{Mc}{I} = \frac{M}{S}$$

and $\qquad f = E\varepsilon,$

therefore $M = (\varepsilon S)\ (E)$

where

f = stress

M = moment

S = section modulus

ε = strain

E = modulus of elasticity

Because the modulus of elasticity is constant for all beams,

$$M \propto \varepsilon S$$

For the relative distribution of moment among beams, only relative section moduli need be considered. Moment fractions may then be computed as indicated below for Beam 1:

$$MF_1 = \frac{\varepsilon_1 S_1}{\Sigma \varepsilon S}$$

where

MF_1 = moment fraction for Beam 1,

ε_1 = bottom flange strain in Beam 1,

S_1 = bottom flange relative section modulus for Beam 1, and

$\Sigma \varepsilon S$ = sum of εS products for all beams.

The process described above can be used for any bridge cross section for which strains are available.

Deflection data were interpreted by a more complex computation. Deflection at a bridge cross section is also proportional to moment:

$$\delta = c \frac{PL^3}{EI}$$

and $M = q\, PL$

therefore $\delta = cq\, ML^2/EI = k\, ML^2/EI$

and $M = (\delta\, I/k)\, (E/L^2)$

where

δ = deflection

P = load

L = span

E = modulus of elasticity

I = moment of inertia

c, q, and k = constants for any given loading condition

E and L are constant for all beams, hence

$$M \propto \delta \frac{I}{k}$$

Only relative moments of inertia need be considered. To account for partial-length cover plates, an effective relative moment of inertia was computed separately for interior and exterior beams assuming a midspan concentrated unit load.

The k constants were computed for each beam for each load type and position assuming a 45 degree load spread. The 45 degree load spread has little theoretical basis, especially for the model or prototype, because of the small value of the plate torsional parameter [16]; but it did provide good correlation with experimental results.

Moment fractions were then computed like those for strains:

$$MF_1 = \frac{\delta_1 \; I_1/k_1}{\Sigma \delta \; I/k}$$

where

MF_1 = moment fraction for Beam 1,

δ_1 = deflection of Beam 1,

I_1 = relative, effective moment of inertia for Beam 1,

k_1 = deflection constant for Beam 1 loading, and

$\Sigma\delta$ I/k = sum of δ I/k products for all beams.

Throughout Sections 4.4.2, 4.5, 4.6 and 4.7, the bridge beam moment fractions indicated by dotted lines on figures are those obtained from orthotropic plate theory. The theoretical moment fractions correlate well with moment fractions obtained experimentally and, consequently, orthotropic plate theory may be used for preliminary design of composite bridge strengthening schemes. Because of the complexity of orthotropic plate theory, however, it would be appropriate in future phases of research to develop simplified methods of analysis and design for office use.

4.4. Effects of Post-Tensioning

Post-tensioning had a variety of effects on the model bridge both during and after stressing of the tendons. Effects of the post-tensioning are discussed in Section 4.4.1. Primary effects of the post-tensioning after application are discussed in Section 4.4.2, and a secondary effect, the change in tension in the tendons during application of load to the post-tensioned bridge, is discussed in Section 4.4.3.

4.4.1. Analysis of Various Post-Tensioning Schemes

Results presented and discussed in this section are for the tests (5-13 in Table 4) that involved only the application of post-tensioning forces to the bridge. Only experimental results are presented in the following paragraphs; comparisons between experimental results and theoretical results will be presented in later sections.

Figure 25 illustrates variations in bottom flange strains at the span centerline, if PTS-4 is employed with no curbs present and with diaphragms in place (test 6, Table 4). As may be seen with 20-kip post-tensioning force initially locked in the exterior beams (Beams 1 and 4), the strain in the exterior beams and interior beams would be approximately equal if a post-tensioning force of approximately 15.75 kips was applied to the interior beams (Beams 3 and 4). The linear variation of bottom flange strain with post-tensioning force for both the interior and exterior beams may also be seen.

Table 6 gives the change in post-tensioning force applied to a given beam as a result of post-tensioning other beams. Note that when Beams 2 and 3 are stressed with 20 kips (PTS-4), Beams 1 and 4 experience a loss of 1.29% and 1.15% respectively. This percentage is obviously dependent upon the initial magnitude of prestress on Beams 1 and 4. The loss of force to Beams 1 and 4 is due to the elastic shortening of the bridge and deflection of the bridge as a result of post-tensioning Beams 2 and 3.

Bottom flange strains for Beams 1-4 resulting from post-tensioning only one beam--in this case Beam 1--are presented in Fig. 26. Note that when Beam 1 is post-tensioned (thus the bottom flange is in compression) the bottom flange of the other exterior beam (Beam 4) is in tension. The compressive strains in Beam 3 appear to be essentially independent of the applied post-tensioning. Figure 27 illustrates the variation in bottom flange strains when 20 kips are locked on Beam 1 and the post-tensioning force is applied to Beam 4. Note that when approximately 19.5 kips are applied to Beam 4, the resulting strains in the exterior
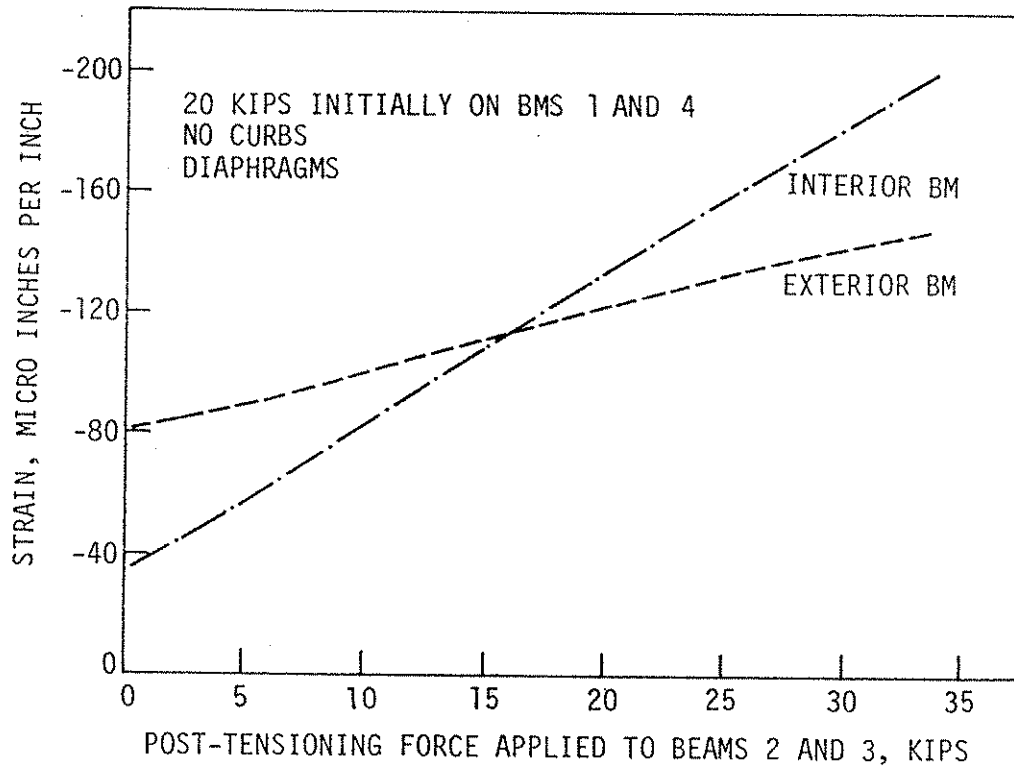
Fig. 25.   Span centerline bottom flange strain vs. post-tensioning
force applied to beams 2 and 3 (PTS-4).

Table 6. Variation in post-tensioning force due to application of additional post-tensioning force.

Post-Tensioning Scheme	Post-Tensioning Order	Post-tensioning Force Applied to Beam			
		1	2	3	4
4	First	20.22 kips	0	0	20.07 kips
	Second	1.29% loss	20 kips	20 kips	1.15% loss
2	First	20.10 kips	0	0	0
	Second	0.59% gain	0	0	20 kips
3	First	20.16 kips	0	0	0
	Second	1.74% loss	20.15 kips	0	0
	Third	1.64% loss	1.14% loss	20.02 kips	0
	Fourth	1.14% loss	1.14% loss	1.60% loss	20.12 kips

79
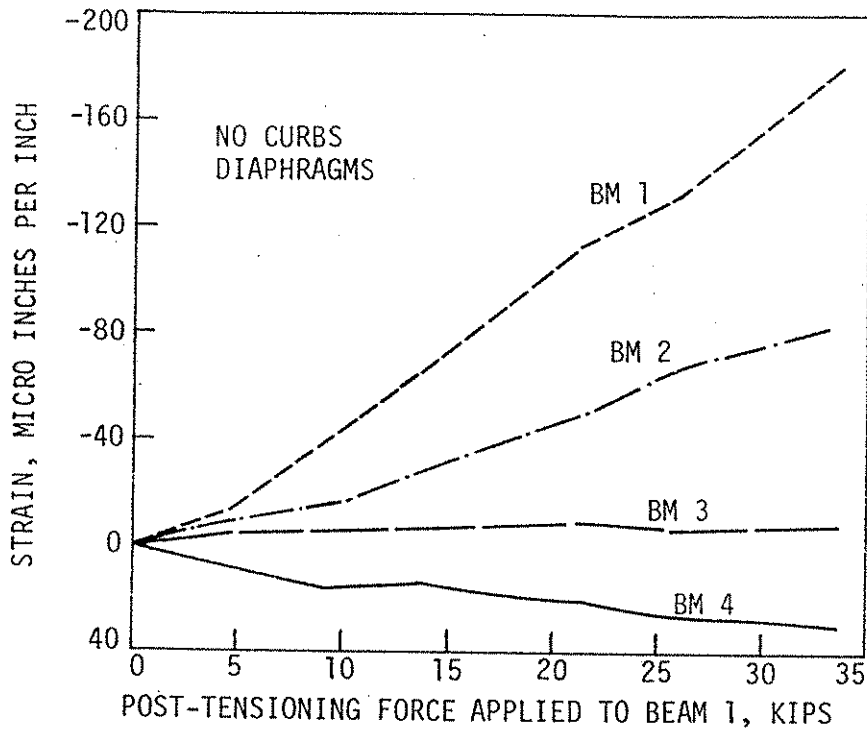
Fig. 26. Span centerline bottom flange strain vs post-tensioning
force applied to beam 1.
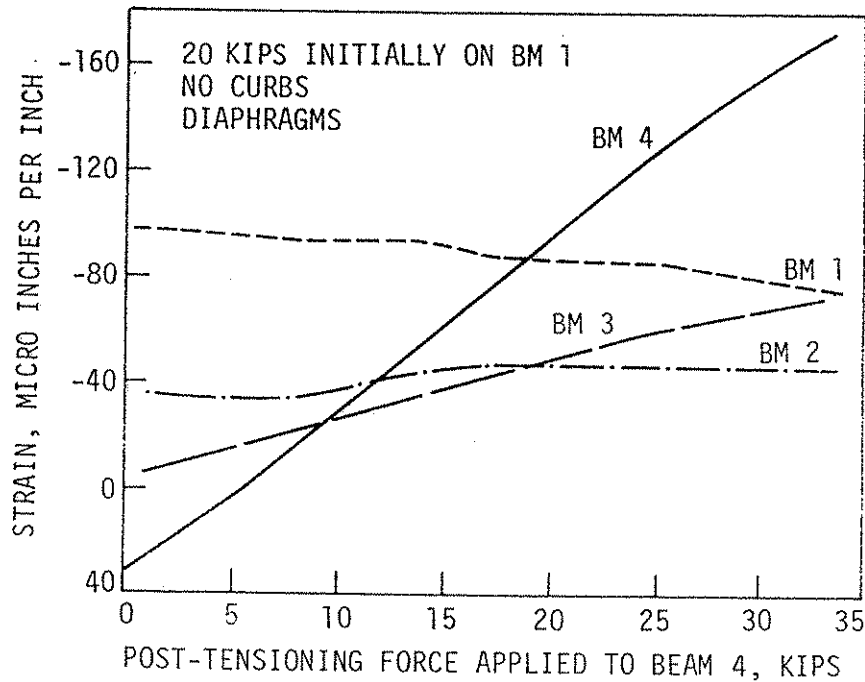
Fig. 27. Span centerline bottom flange strain vs post-tensioning
force applied to beam 4.

beams are equal and the strains in the interior beams are equal. This suggests that, when post-tensioning a given bridge, if not enough equipment is available for stressing all beams simultaneously, satisfactory results can be obtained by post-tensioning beams individually. The deflection of the bridge as a result of post-tensioning Beam 1 first and then Beam 4 (PTS-2) is shown in Fig. 28. Note the downward deflection of Beam 4 when Beam 1 is post-tensioned and the downward deflection of Beam 1 when Beam 4 is stressed. Maximum deflection occurring as a result of post-tensioning Beams 1 and 4 with 20 kips each occurred at the centerline of Beams 1 and 4 and was 0.066 inches.

Table 6 indicates that when PTS-2 is applied to the bridge there is actually a small gain in the force being applied to Beam 1. Figure 29 illustrates the variation in the centerline bottom flange strain resulting from using PTS-3--post-tensioning beams one at a time in the following order: Beam 1, Beam 2, Beam 3 and Beam 4. A post-tensioning force of 20 kips was locked on each beam; but, because of losses, one would not expect a symmetrical strain distribution (Beam 2 same as Beam 3, etc.). However, as may be seen, after Beam 4 is stressed the symmetry of the strain is very good. Losses are very small as a result of the magnitudes for post-tensioning being applied (see Table 6). In Table 6, losses are based on the initial post-tensioning force on the beam. For example, as other beams are post-tensioned, the loss in Beam 1 decreases; in other words, post-tensioning Beams 3 and 4 actually increases the force on Beam 1. As may be seen, although the effect is still very small, the most significant change in the post-tensioning force on a given beam occurs when the beam adjacent to it is post-tensioned. Bridge deflection
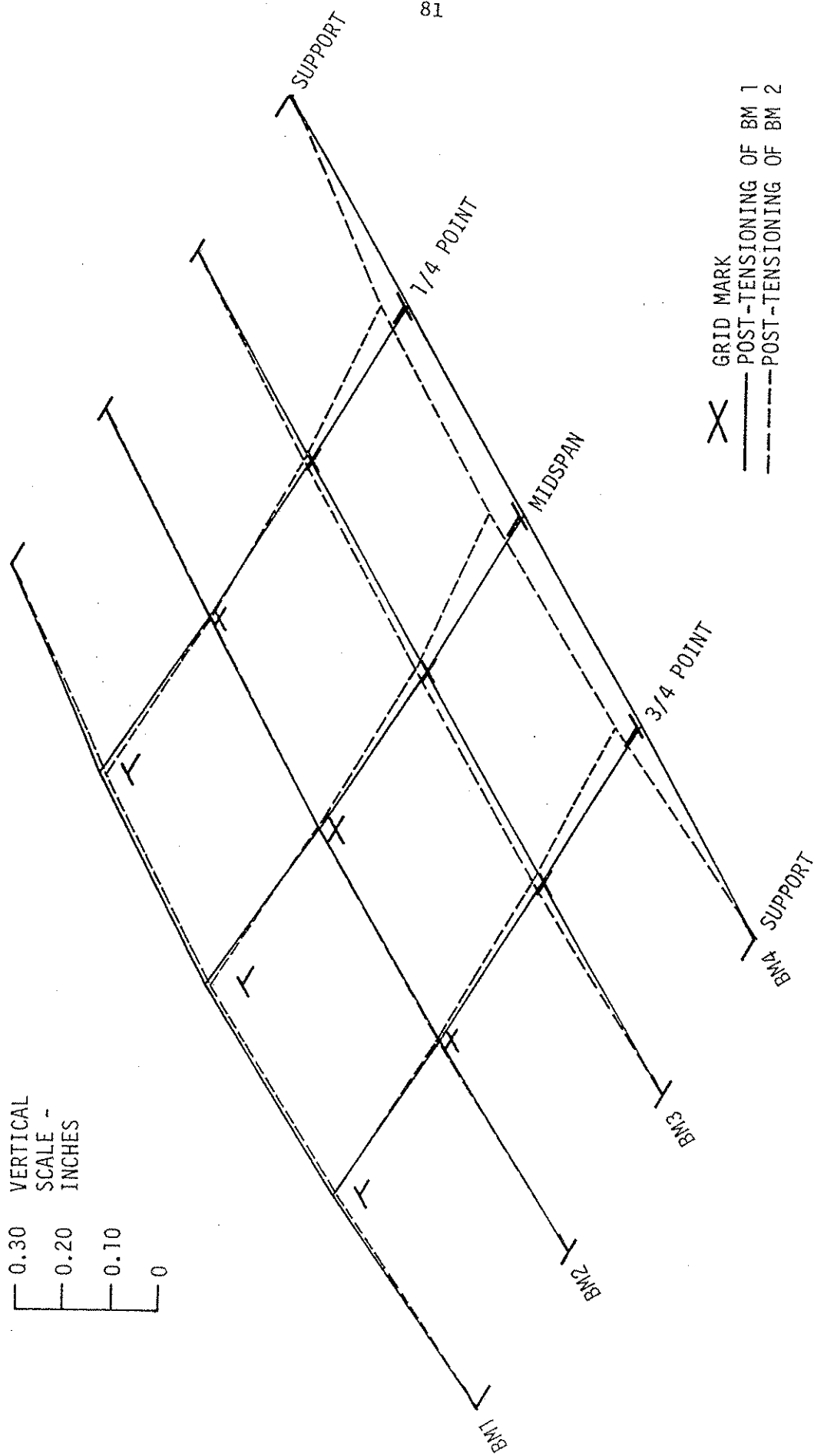
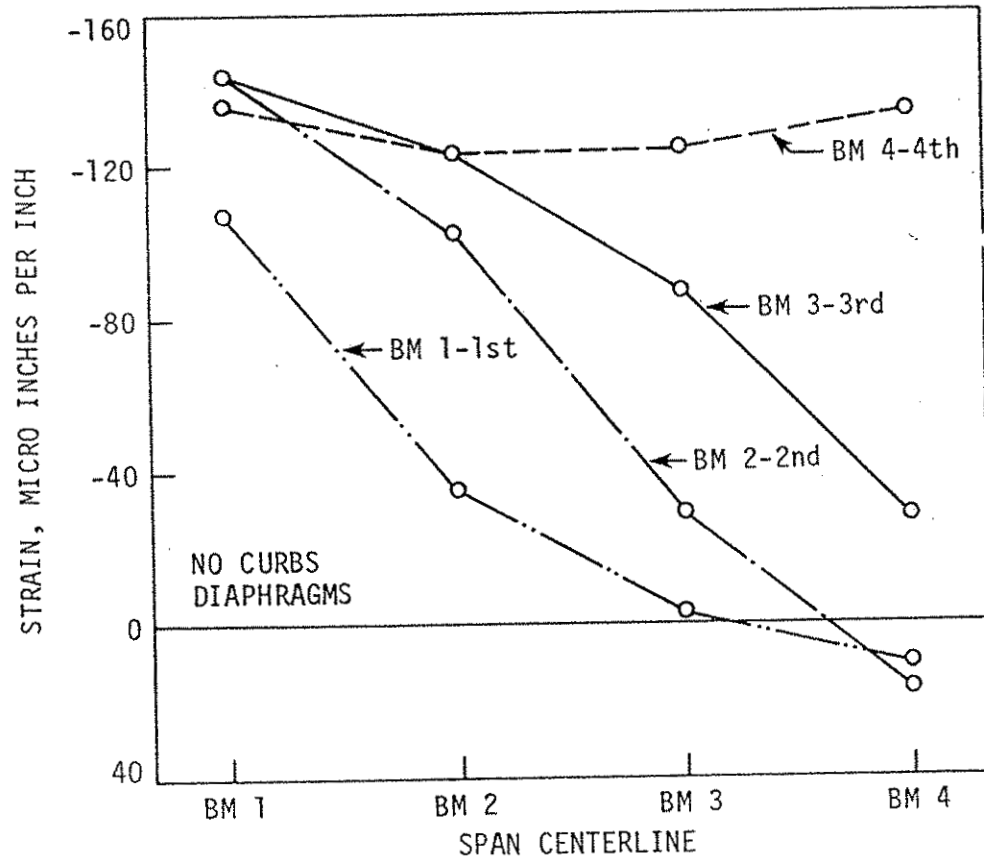Fig. 28. Deflection of bridge due to PTS-2 at magnitude of 20 kips per beam.

82

Fig. 29. Variation in span centerline bottom flange strain as beams are post-tensioned with 20 kips in order beam 1, 2, 3, 4 (PTS-3).

resulting from the four bridge beams being post-tensioned in order is shown in Fig. 30. As may be seen, the greatest change in deflection of a given beam occurs when that beam is post-tensioned. This is especially true for the exterior beams.

Overlooking losses, the only difference between PTS-3 and PTS-4 is the order in which the post-tensioning was applied. The span centerline bottom flange strains for these two systems are compared in Fig. 31. As may be seen, the difference is very small: PTS-3 results in slightly higher strains in the exterior beams, while PTS-4 results in slightly higher strains in the interior beams. Figures 32(a) and 32(b) present the centerline deflection for each of the two post-tensioning systems. Although the deflection patterns are very different while the various beams are being post-tensioned, there is little difference in the deflection patterns after all beams have been post-tensioned.

The effect of varying the post-tensioning force on Beams 2 and 3 while the force on Beams 1 and 4 is held constant is shown in Fig. 33. The curve labeled "0 k" illustrates the strain in the four beams resulting from stressing Beams 1 and 4 to 20 kips each. As may be seen, essentially any practical strain level may be achieved, depending on the force applied to Beams 2 and 3.

The following paragraphs describe the effects of curbs and diaphragms on two of the post-tensioning systems used: PTS-1 and PTS-4.

With PTS-1 being applied to the bridge, the effects of curbs and diaphragms for interior and exterior beams are shown in Fig. 34. For the exterior beams, the strains found in the bottom flange were what one would expect. The smallest strain occurred when curbs were absent
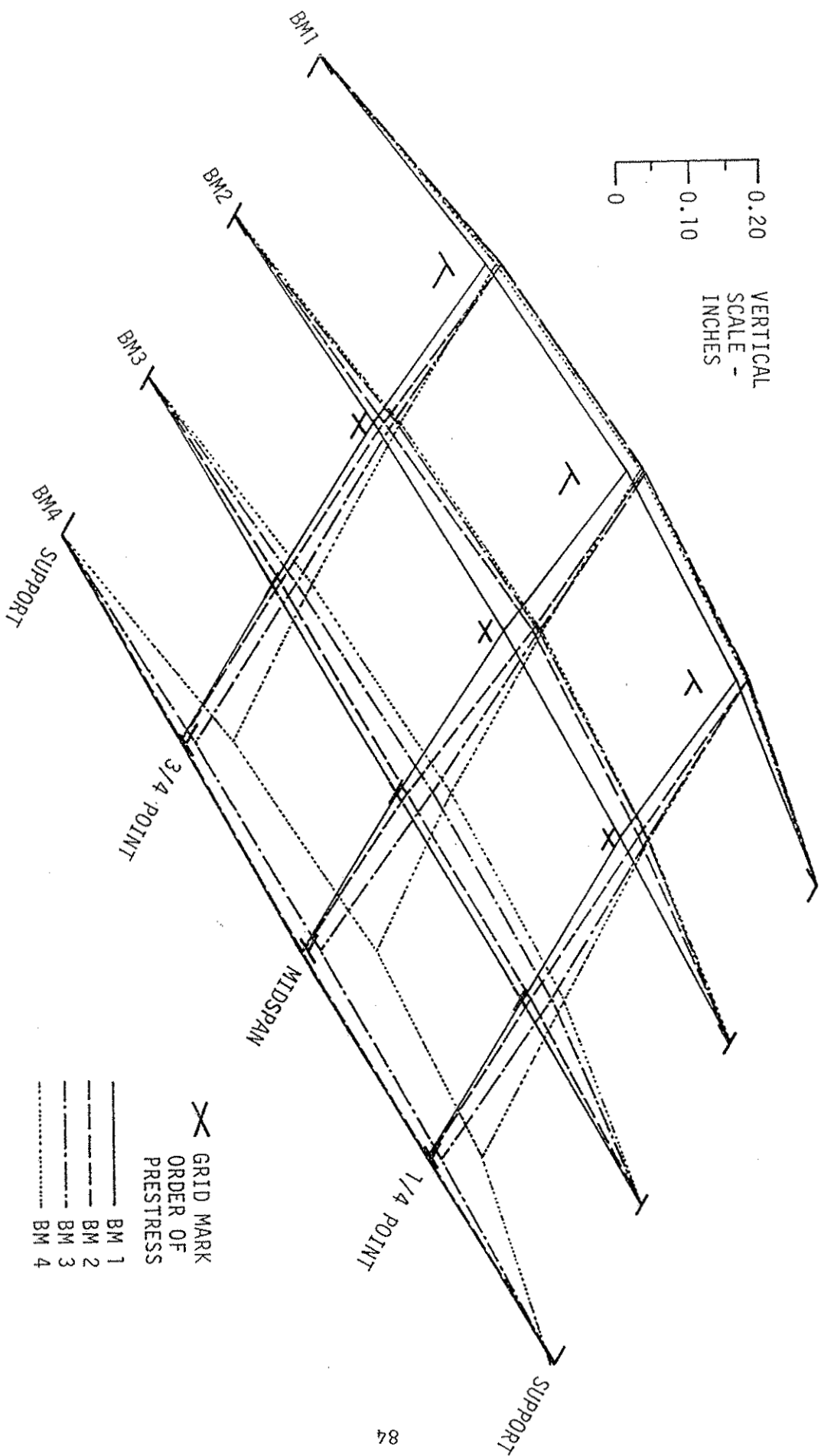
VERTICAL
SCALE -
INCHES

0.20
0.10
0

BM1
BM2
BM3
BM4
SUPPORT
3/4 POINT
MIDSPAN
1/4 POINT
SUPPORT

GRID MARK
ORDER OF
PRESTRESS

BM 1
BM 2
BM 3
BM 4

Fig. 30. Deflection of bridge due to PTS-3 at magnitude of 20 kips per beam.
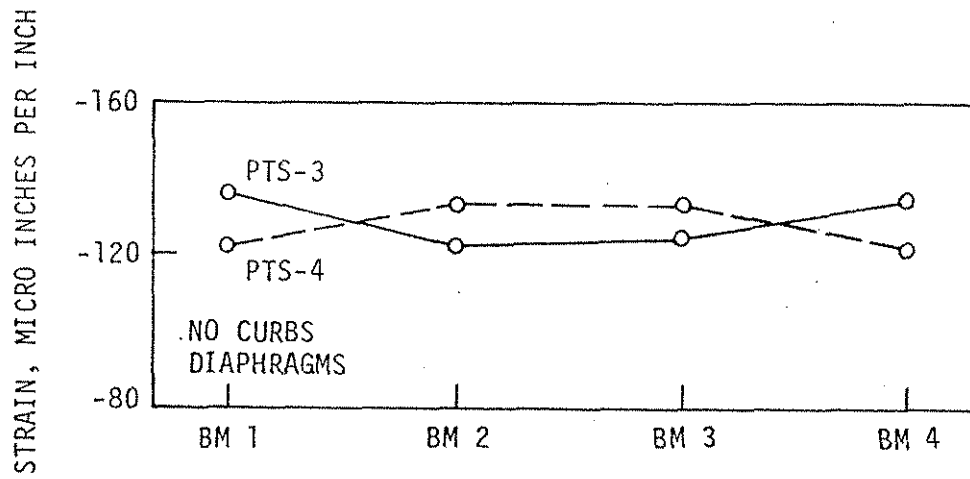
85

Fig. 31. Comparisons of span centerline bottom flange strains resulting
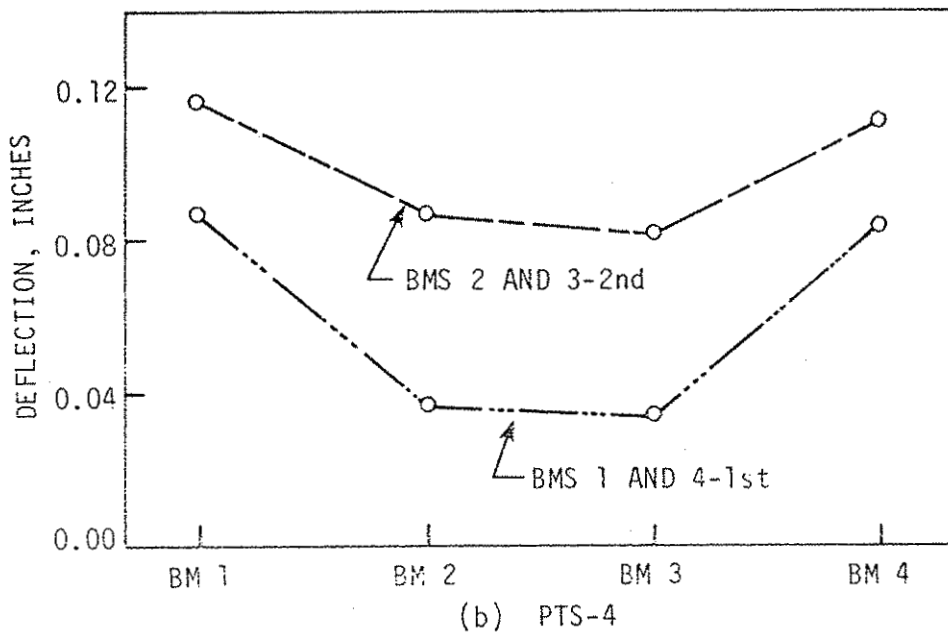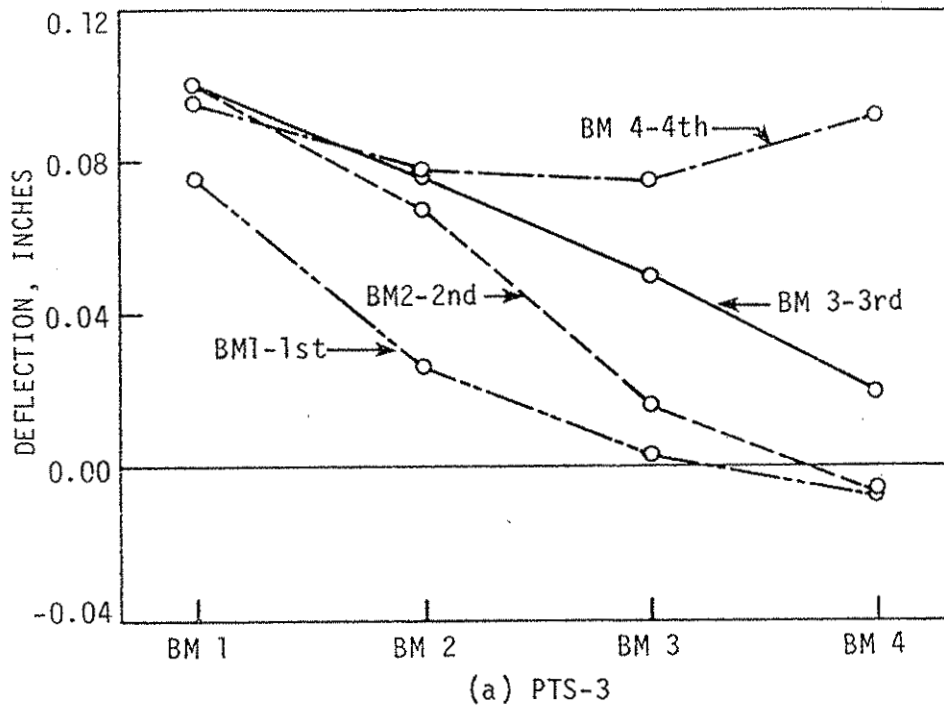from PTS-3 and PTS-4.

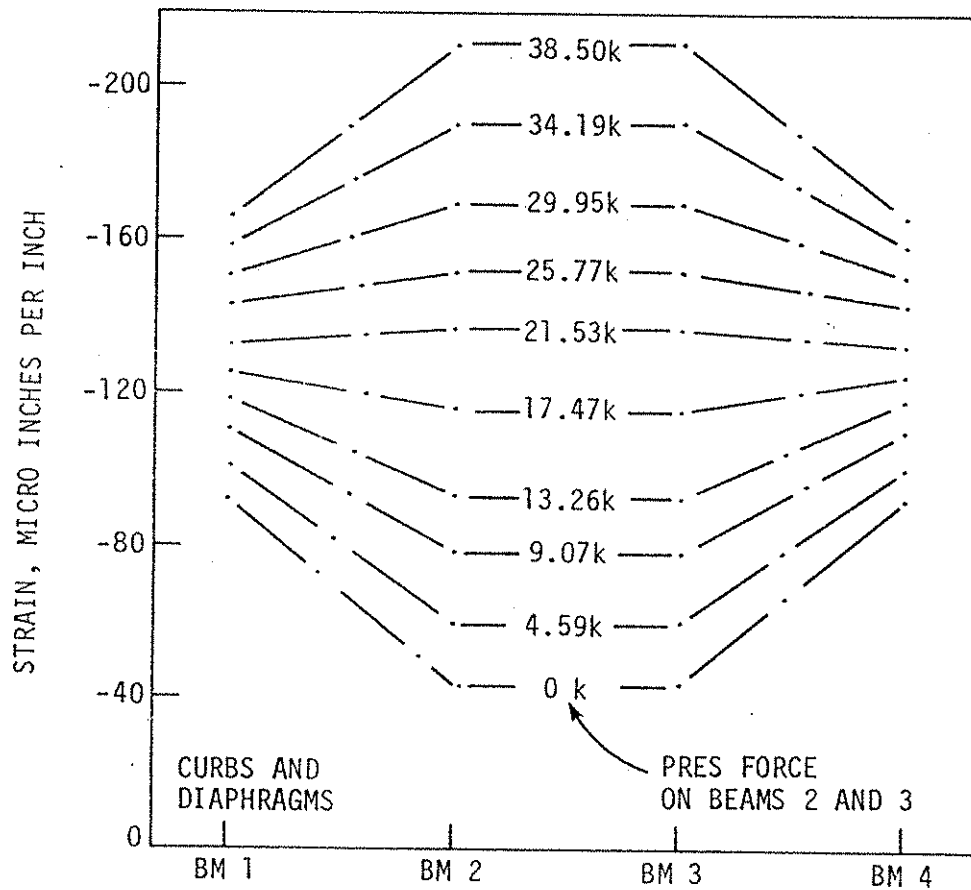Fig. 32. Centerline deflection of bridge due to PTS-3 and PTS-4 at magnitude of 20 kips per beam.

Fig. 33. Variation in beam bottom flange strain as post-tensioning
force is increased on beams 2 and 3 (PTS-4).
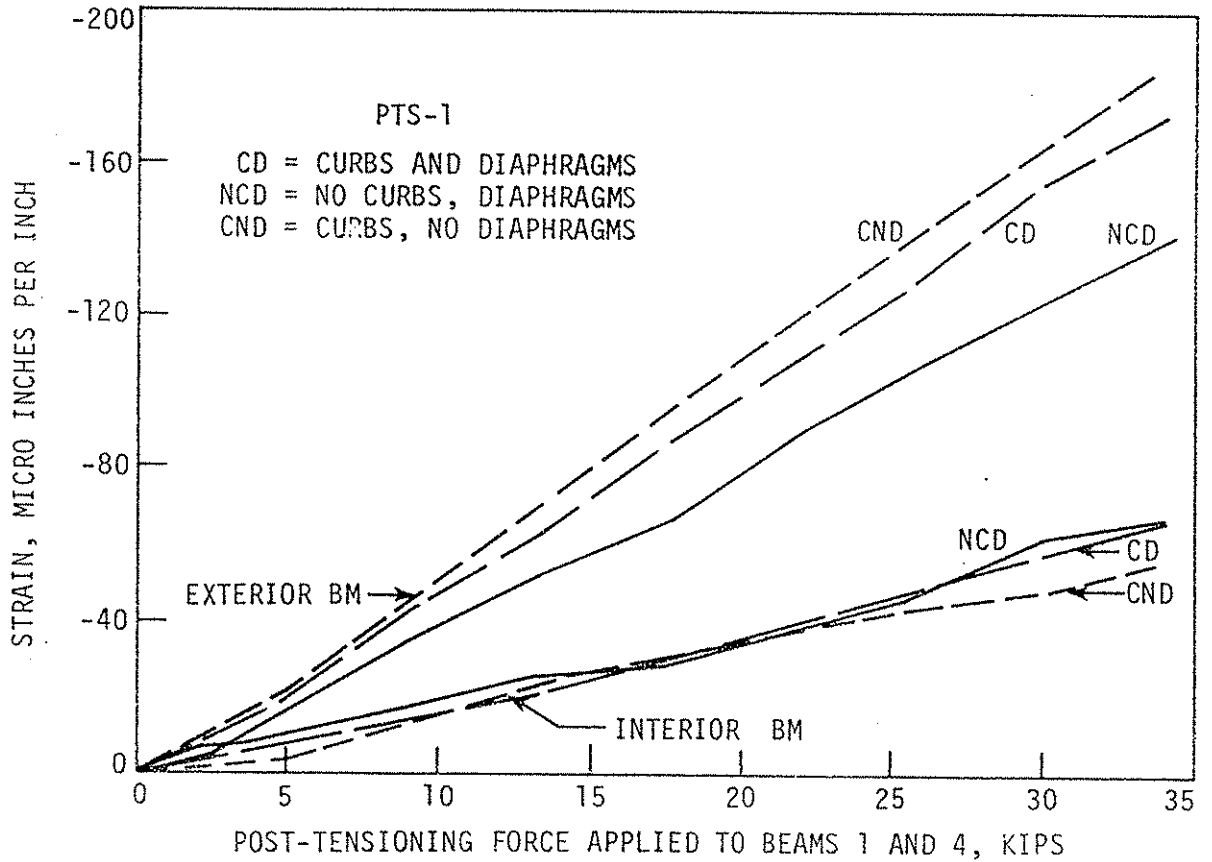
Fig. 34. Variation in span centerline bottom flange strains, PTS-1, due to curbs and diaphragms.

(thus a weaker section) and diaphragms were present (diaphragms assist in distributing load to adjacent beams). The greatest strain was obtained when curbs were present (stronger section) and diaphragms were not in place (thus no distribution to next beams). Between these two limits was the case which would normally be found in the field: curbs and diaphragms both in place. For interior beams, curbs and diaphragms have little effect. However, if diaphragms are removed less load is distributed to the interior beam and thus more remains in the exterior beams.

Figure 35 presents the effects of curbs and diaphragms on the strain in exterior and interior beams when PTS-4 is applied to the bridge. Results are essentially the same as when PTS-1 was applied to the bridge. For exterior beams, maximum strain occurs when curbs are present and diaphragms are removed; minimum strain occurs when diaphragms are in place and curbs are removed. The most common case, curbs and diaphragms both in place, lies between the two extremes. As for interior beams, curb and diaphragm effects are still small, although they are more significant than when PTS-1 was applied. Except for post-tensioning forces in the 0-10 kips range, the maximum strain in the interior beams occurs when there are no curbs and diaphragms are in place.

4.4.2. Moment Distribution

Throughout this section and subsequent sections, moment fractions in the figures are for beams at midspan unless otherwise noted. In the various figures, moment fractions computed from strains are depicted by solid dots; moment fractions computed from deflections are shown as open dots; orthotropic plate theory moment fractions are indicated by dotted lines.
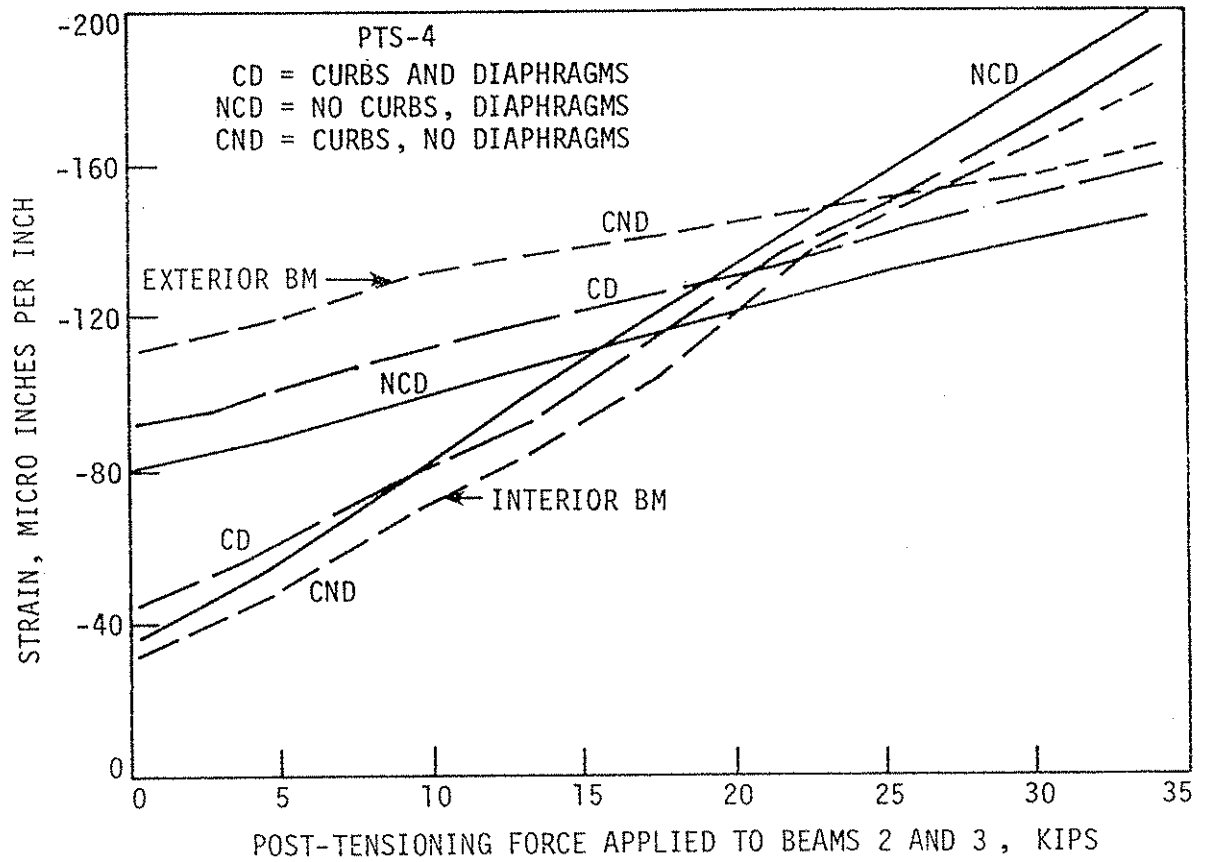
Fig. 35. Variation in span centerline bottom flange strains, PTS-4:
20 kips applied at beams 1 and 4, due to curbs and diaphragms.

Figure 36 presents the moment fractions for model bridge beams for the three successive stages of PTS-4. The first stage, Fig. 36(a), is the same as PTS-1. As can be determined from the figures, in PTS-1 a larger fraction of the post-tensioning remains with the exterior beams than is distributed to interior beams. In PTS-4, Fig. 36(c), however, the interior beams take the larger share of the post-tensioning moments. In general, the moment fractions computed by orthotropic plate theory for applied concentrated vertical load correlate very closely with moment fractions computed from post-tensioning strain or deflection data.

Post-tensioning the model bridge did not significantly affect the vertical load distribution among the four bridge beams. Figures 37 and 38 compare moment fractions for the bridge before and after post-tensioning. Figures 37(a) and (b) when compared with (c) and (d) (PTS-1) and (e) and (f) (PTS-4) show no difference as a result of either post-tensioning scheme. Likewise, Fig. 38 for the simulated truck loading indicates no difference in beam moment fraction before and after post-tensioning.

The model bridge deflected shapes in Figs. 39 and 40 qualitatively illustrate the effects of PTS-1 and PTS-4. The difference in deflection patterns in each figure is caused only by the post-tensioning and is not a result of a different load distribution. In Fig. 39, there is a greater difference in deflection for the exterior beams then for the interior beams, as might be expected from the fact that the exterior beams retain a larger fraction of the post-tensioning. Similarly, the larger difference in interior beam deflection in Fig. 40 could be anticipated
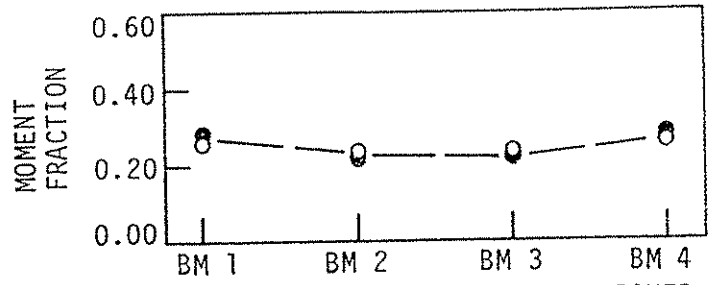
(a) BEAMS 1 AND 4 POST-TENSIONED,
SIMILAR TO PTS-1 (TEST 6)
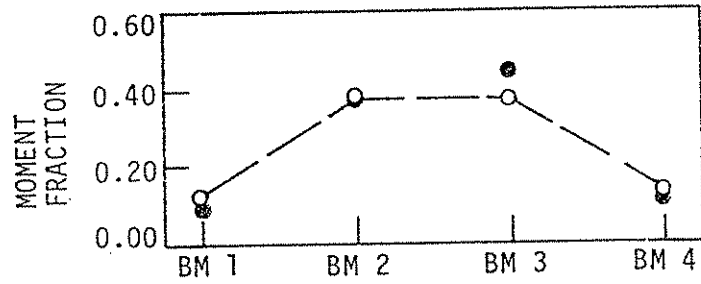
(b) BEAMS 2 AND 3 POST-TENSIONED (TEST 6)
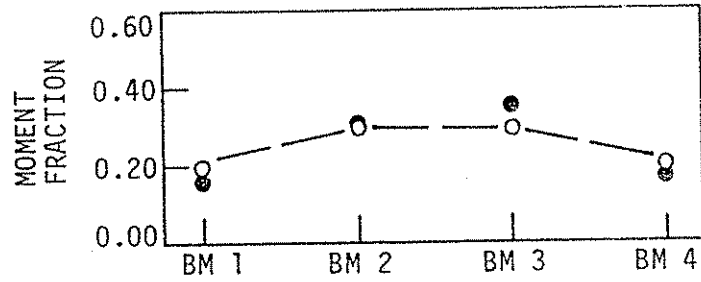
(c) ALL BEAMS POST-TENSIONED, PTS-4 (TEST 6)

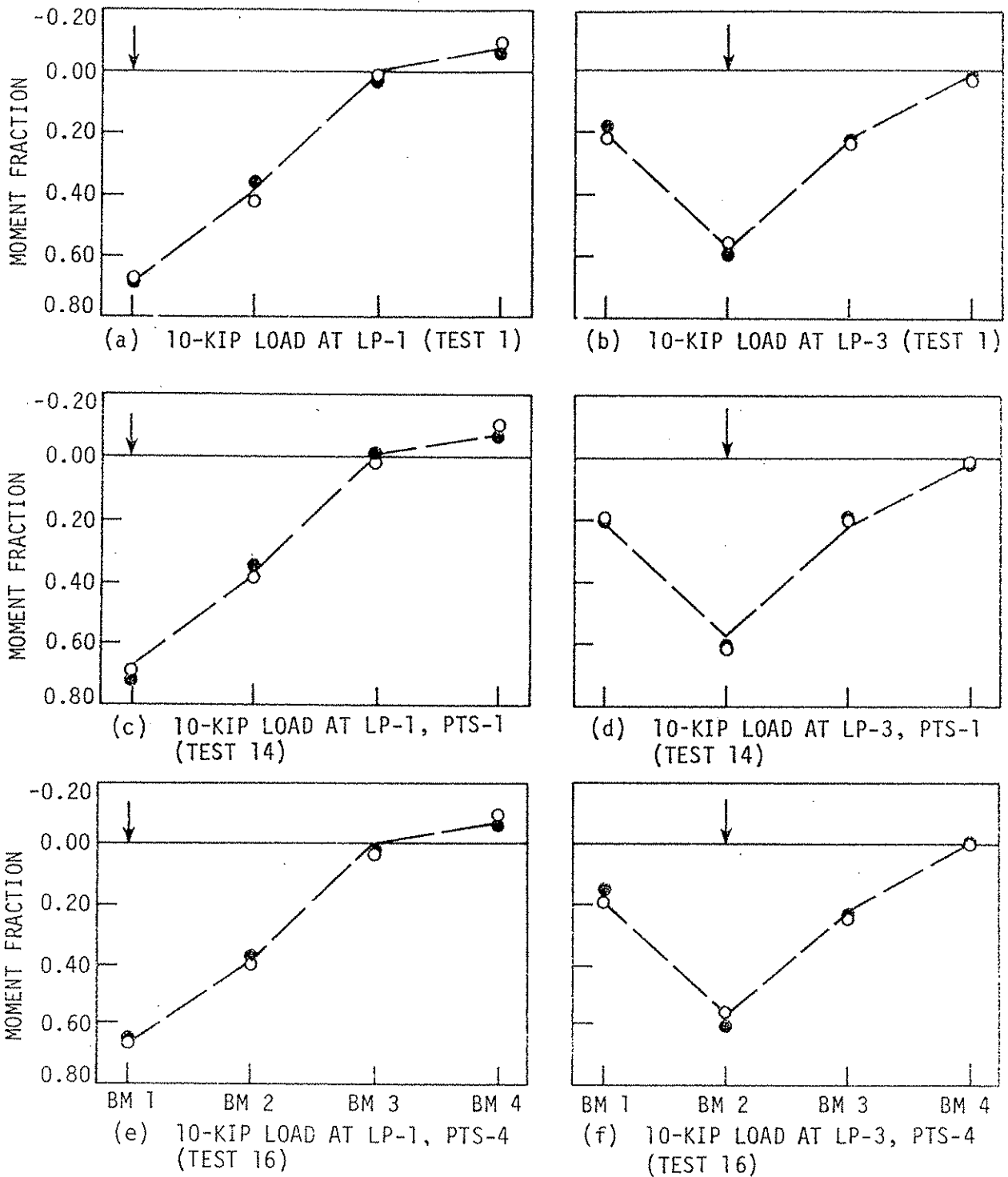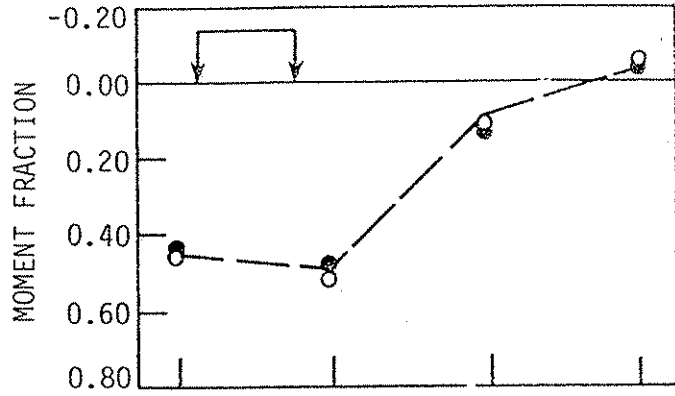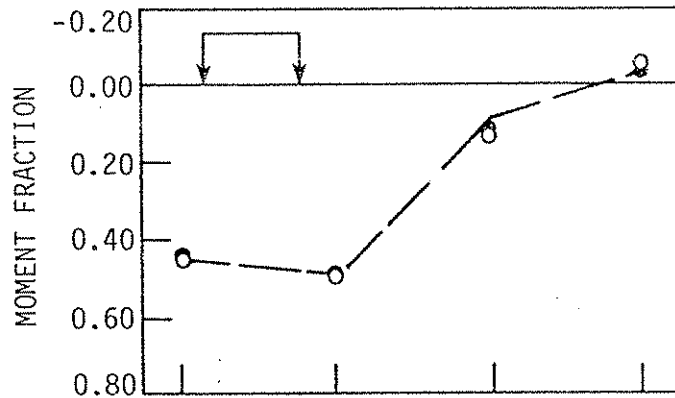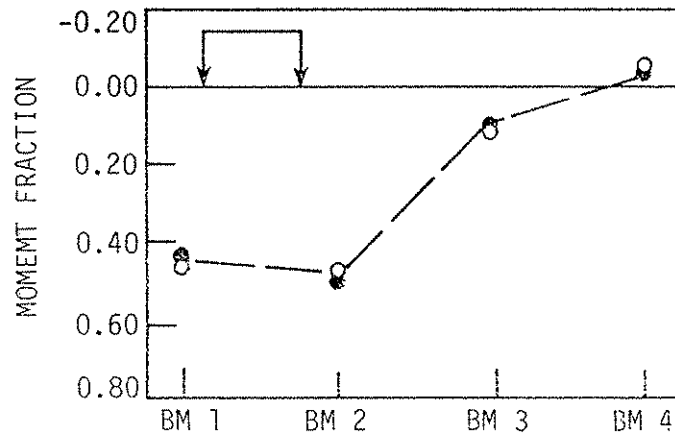Fig. 36. Moment distribution due to post-tensioning (PTS-4).

Fig. 37. Moment distribution due to vertical load before and after post-tensioning.

Fig. 38.   Moment distribution due to truck load before and after post-tensioning.
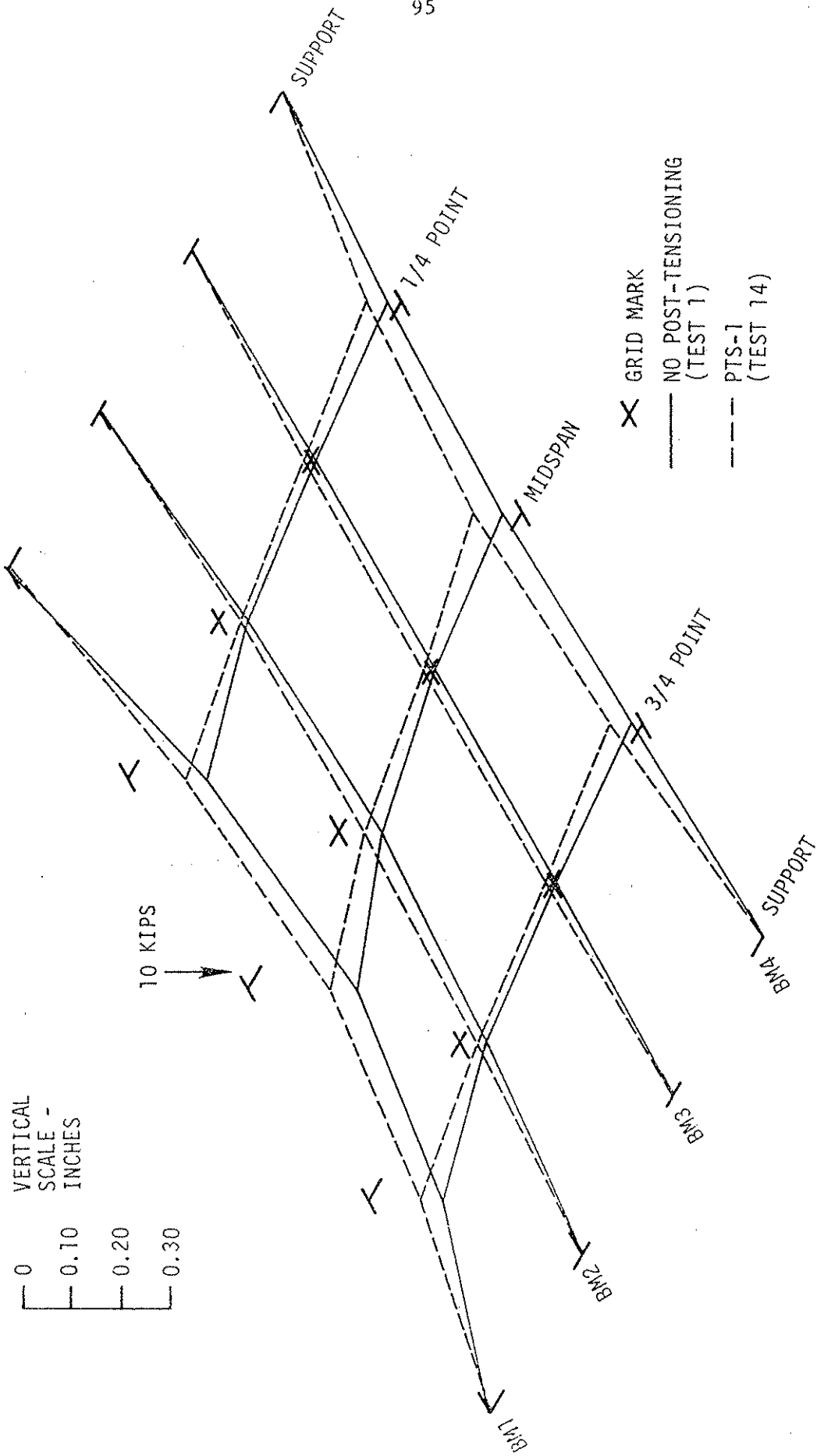
Fig. 39. Deflected shape for model bridge, 10-kip load at IP-1, without and with PTS-1.
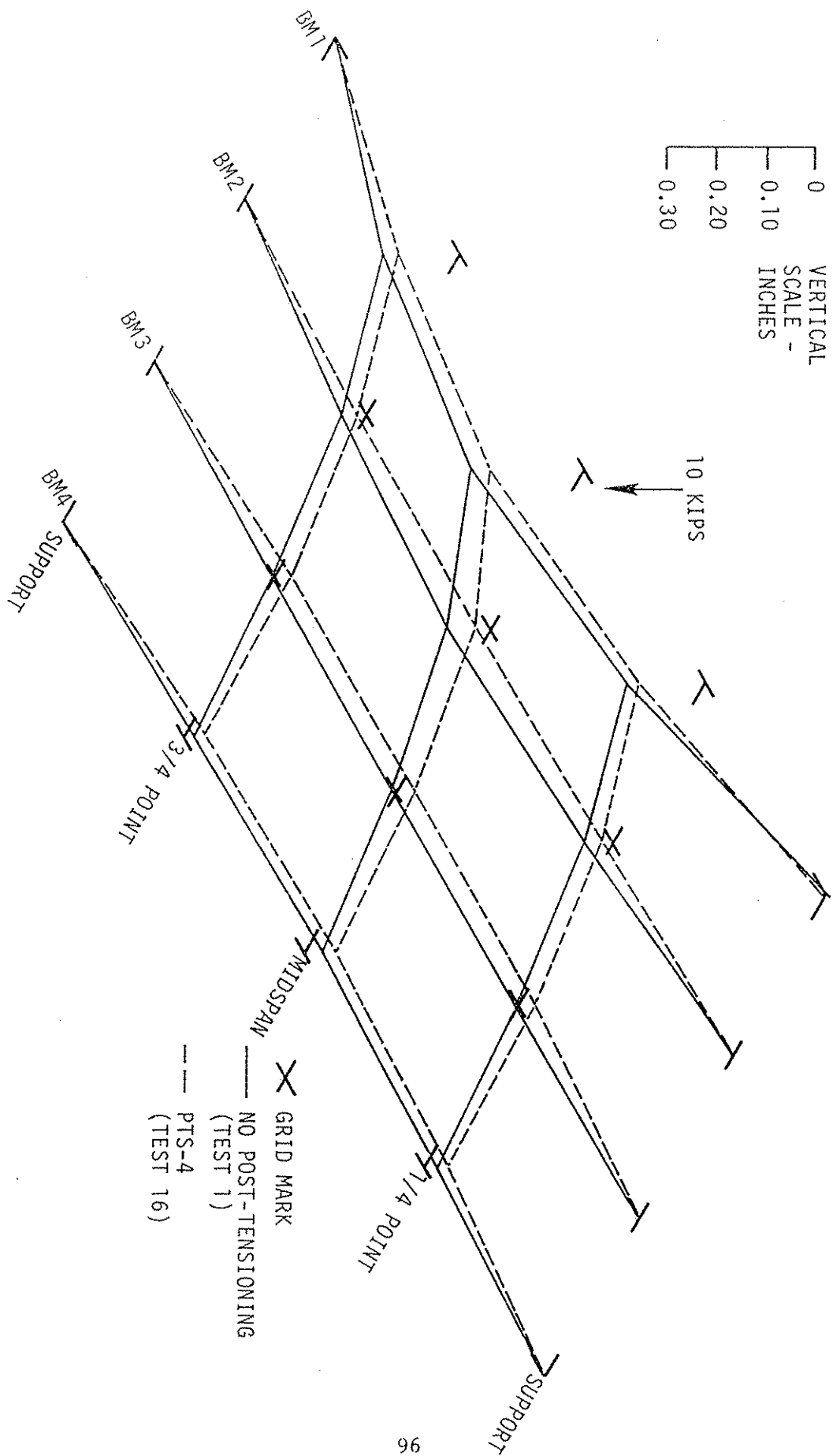
Fig. 40. Deflected shape for model bridge, 10-kip load at LP-1, without and with PTS-4.

on the basis of moment fractions for PTS-4. The deflection effects described above are more directly compared for the two post-tensioning schemes with truck loading in Fig. 41. Deflected shape lines cross between exterior and interior beams because the deflection patterns account for the two different post-tensioning schemes.

The effects of post-tensioning can be shown in another manner, as given in Figs. 42 and 43. Each figure is a bar graph of the strain history of the bottom flange cover plate at midspan of the bridge as 10-kip concentrated loads and two post-tensioning schemes were applied. In each figure there is a series of four steps--created by placing the 10-kip load at LP-1, LP-3, LP-5 or LP-7--repeated at three different levels: no prestress, PTS-1 and PTS-4.

For the exterior beam, Fig. 42, the application of PTS-1 removes a tensile strain of approximately 100 microinches per inch or about 20% of the total strain. A lesser reduction in tensile strain occurs when PTS-4 is applied to the bridge.

For the interior beam, Fig. 43, the application of PTS-1 (even though post-tensioning was applied only to exterior beams) reduced tensile strain by approximately 30 microinches per inch. A larger reduction in tensile strain occurred when PTS-4 was applied.

For both beams, the application of post-tensioning did reduce midspan tensile strains. In no case did the post-tensioning cause a final strain at midspan that was compressive. A compressive strain could occur, however, if a greater magnitude of post-tensioning force were applied.

A third method for illustrating the effects of post-tensioning is given in Figs. 44 and 45. Both figures show strain computed on the
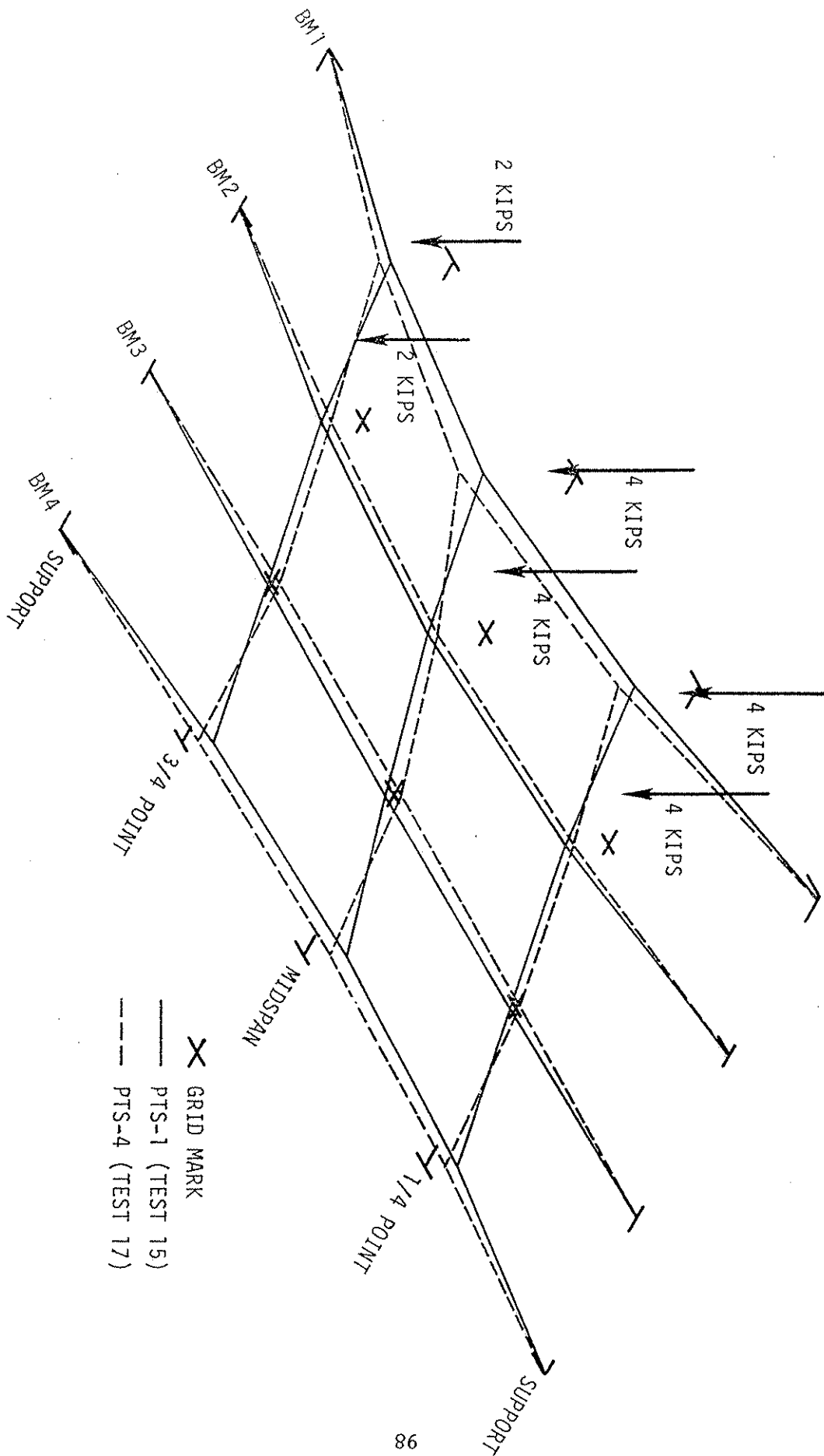
Fig. 41. Deflected shape for model bridge, truck load, PTS-1 and PTS-4.
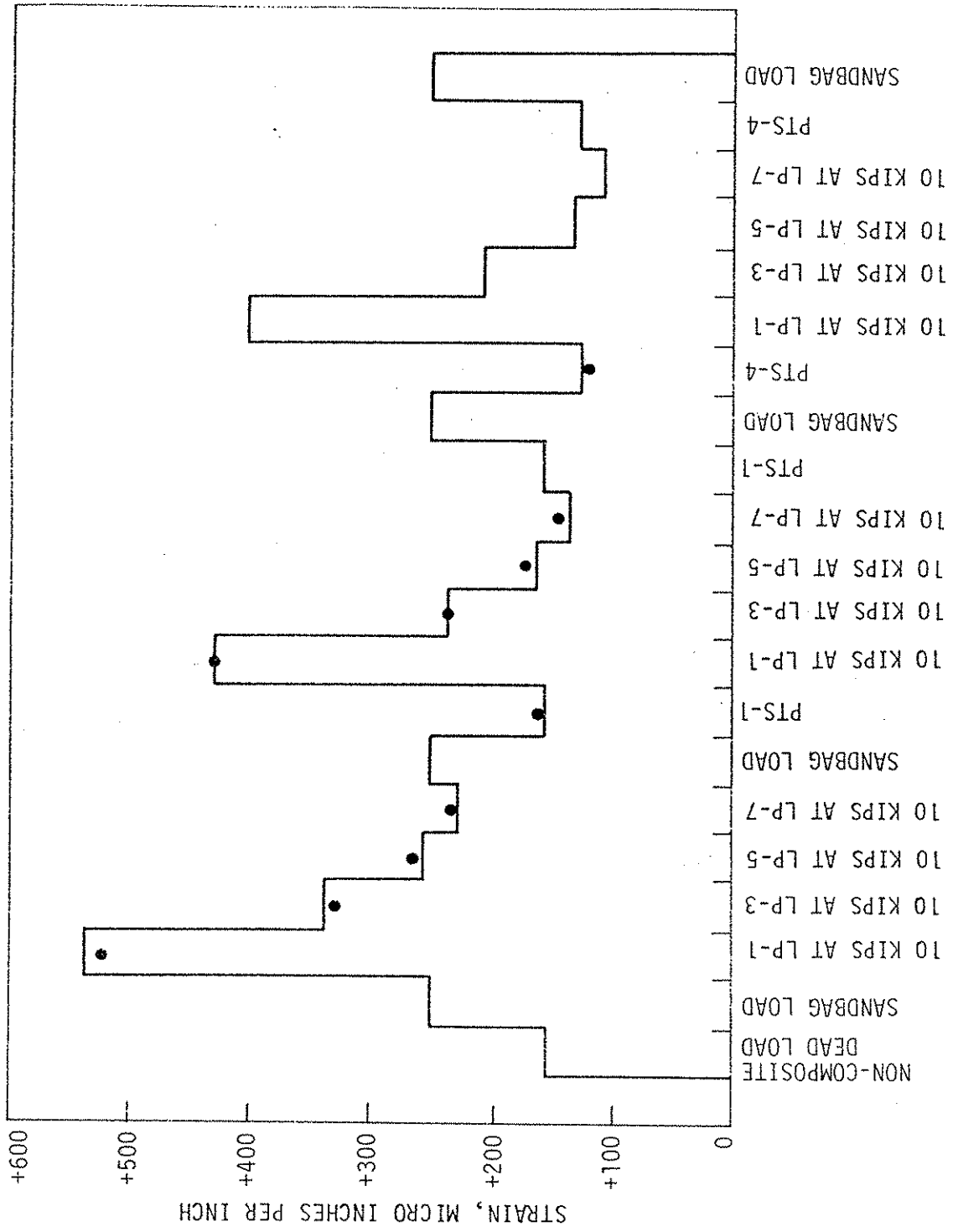
Fig. 42. Bottom flange cover plate strain history at midspan, exterior beam 1(tests 1, 5, 14 and 10)

Fig. 43. Bottom flange cover plate strain history at midspan, interior beam 2 (tests 1, 5, 14 and 10).
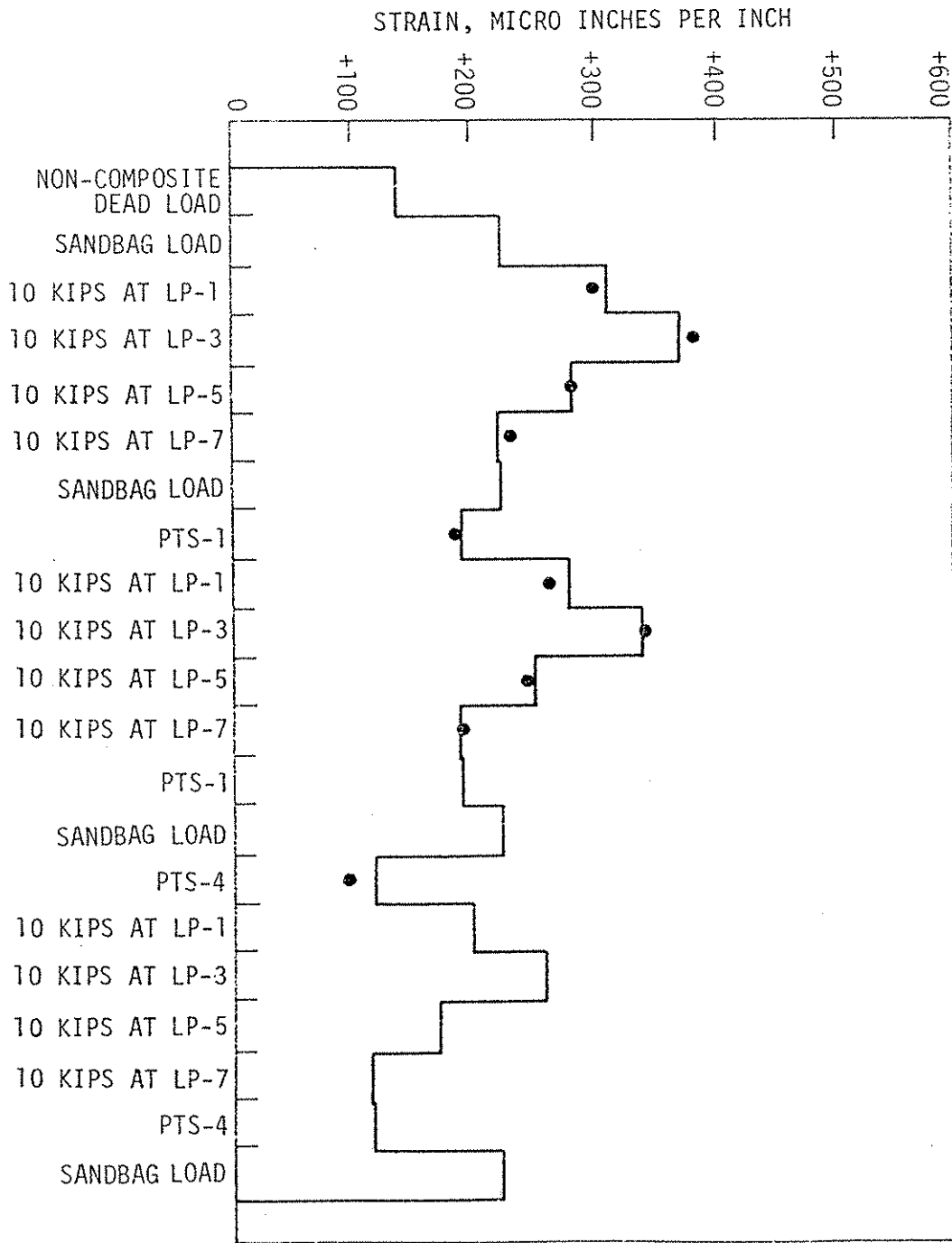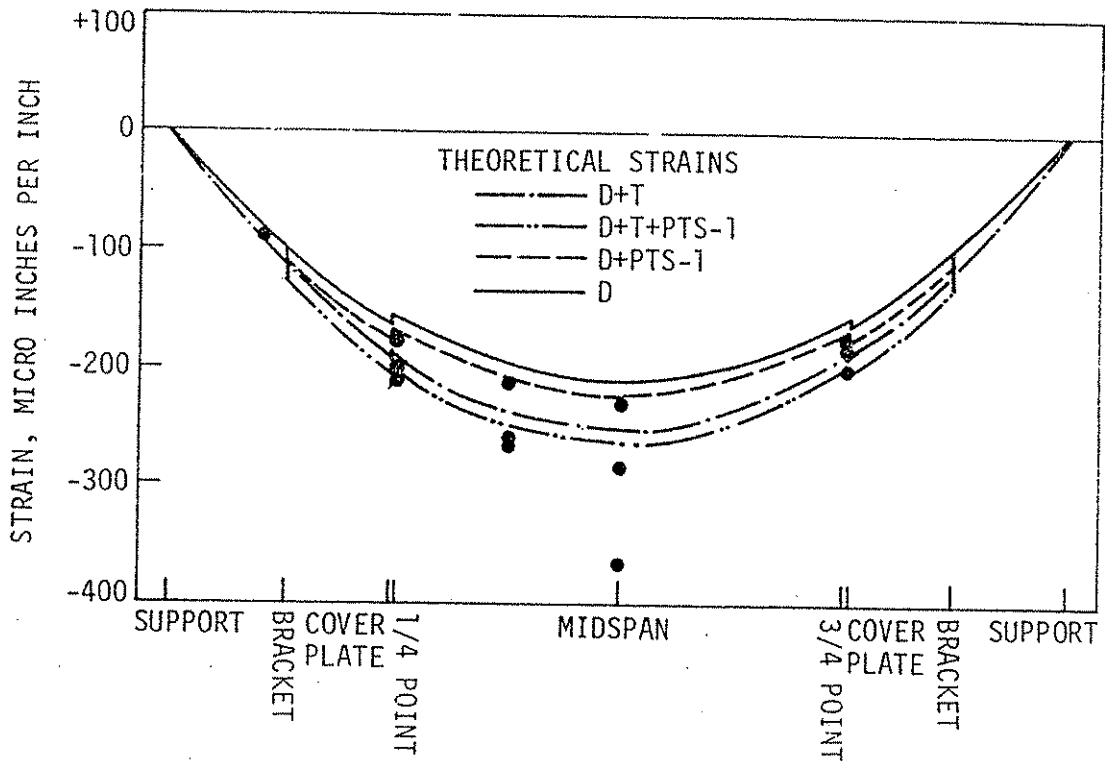
(a)   TOP FLANGE STRAINS (TESTS 2 AND 15)

Fig. 44.   Flange strains for exterior beam 1 without curbs on bridge.
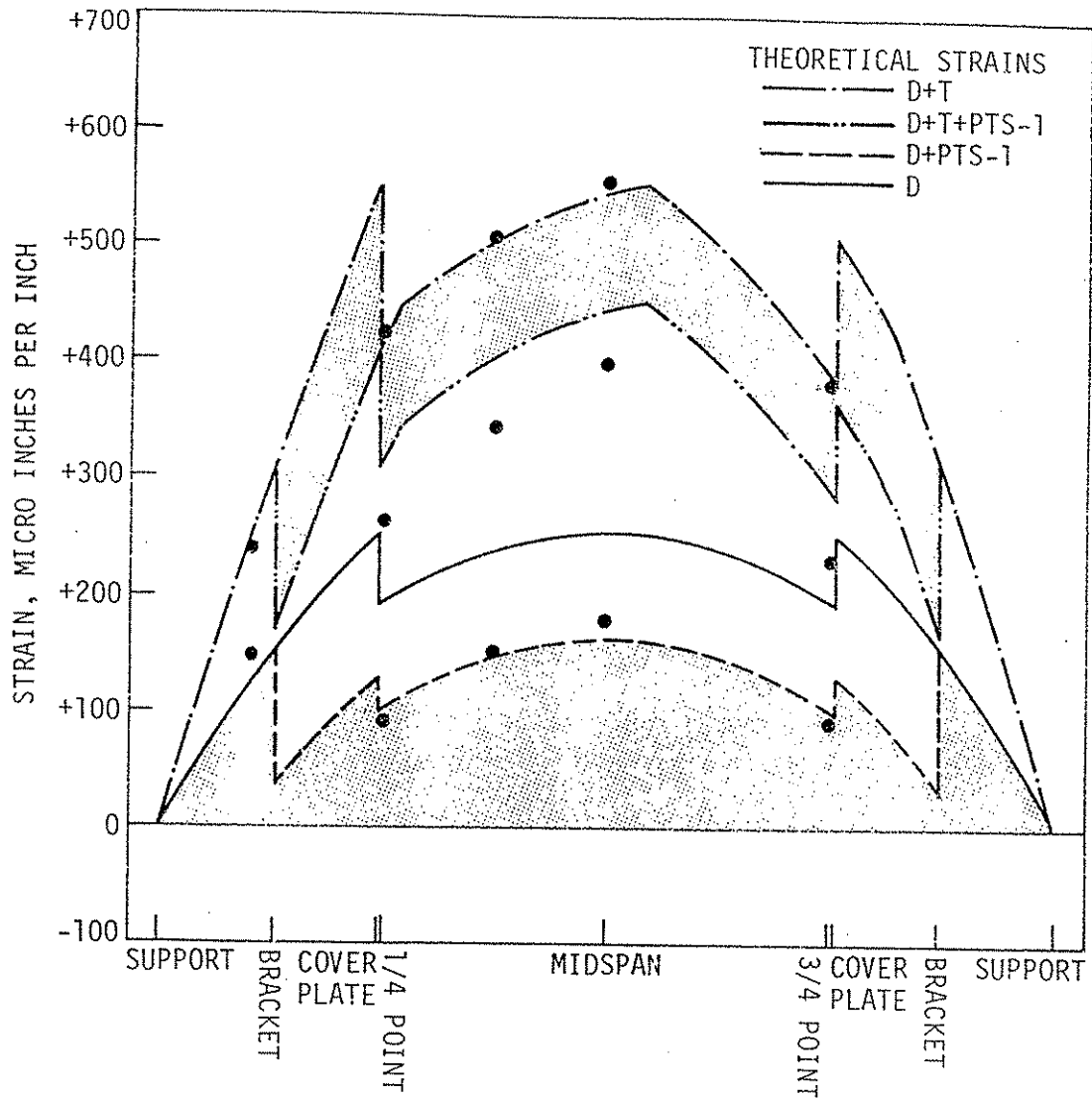
(b) BOTTOM FLANGE/COVER PLATE STRAINS (TESTS 2 AND 15)

Fig. 44. Concluded.

(a) TOP FLANGE STRAINS (TESTS 2 AND 15)

Fig. 45. Flange strains for interior beam 2 without curbs on bridge.

(b)   BOTTOM FLANGE/COVER PLATE STRAINS (TESTS 2 AND 15)

Fig. 45.   Concluded.

basis of AASHTO's effective slab widths, orthotropic plate theory and strain measured in beam flanges or cover plates. The loading stages shown progress from dead load to the final combination of dead load, PTS-1, and eccentric truck load.

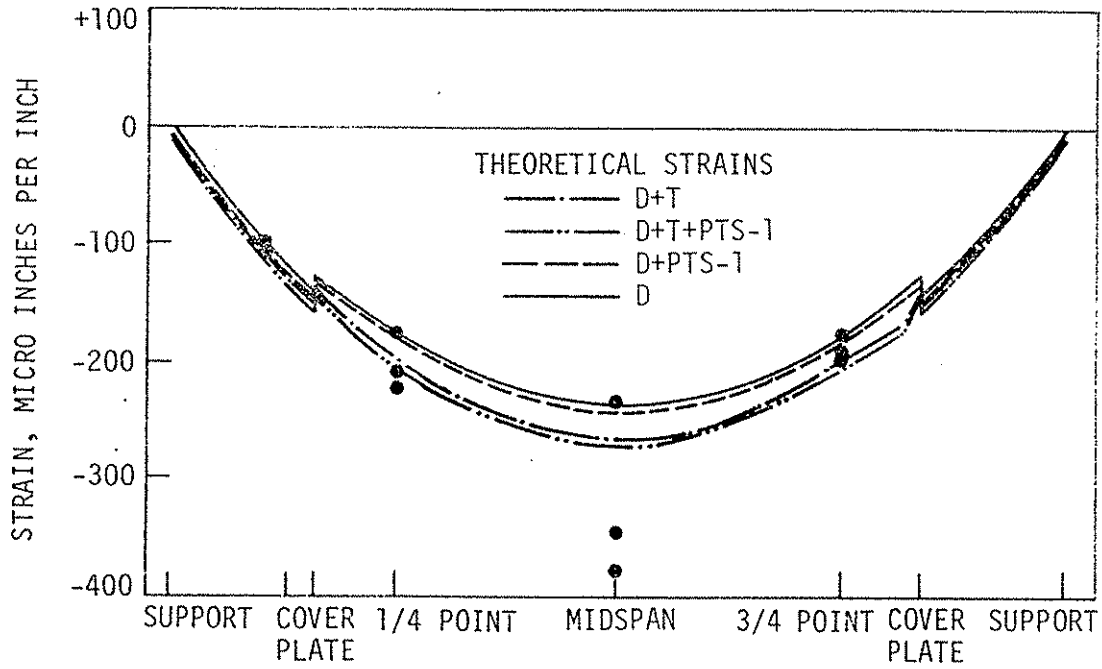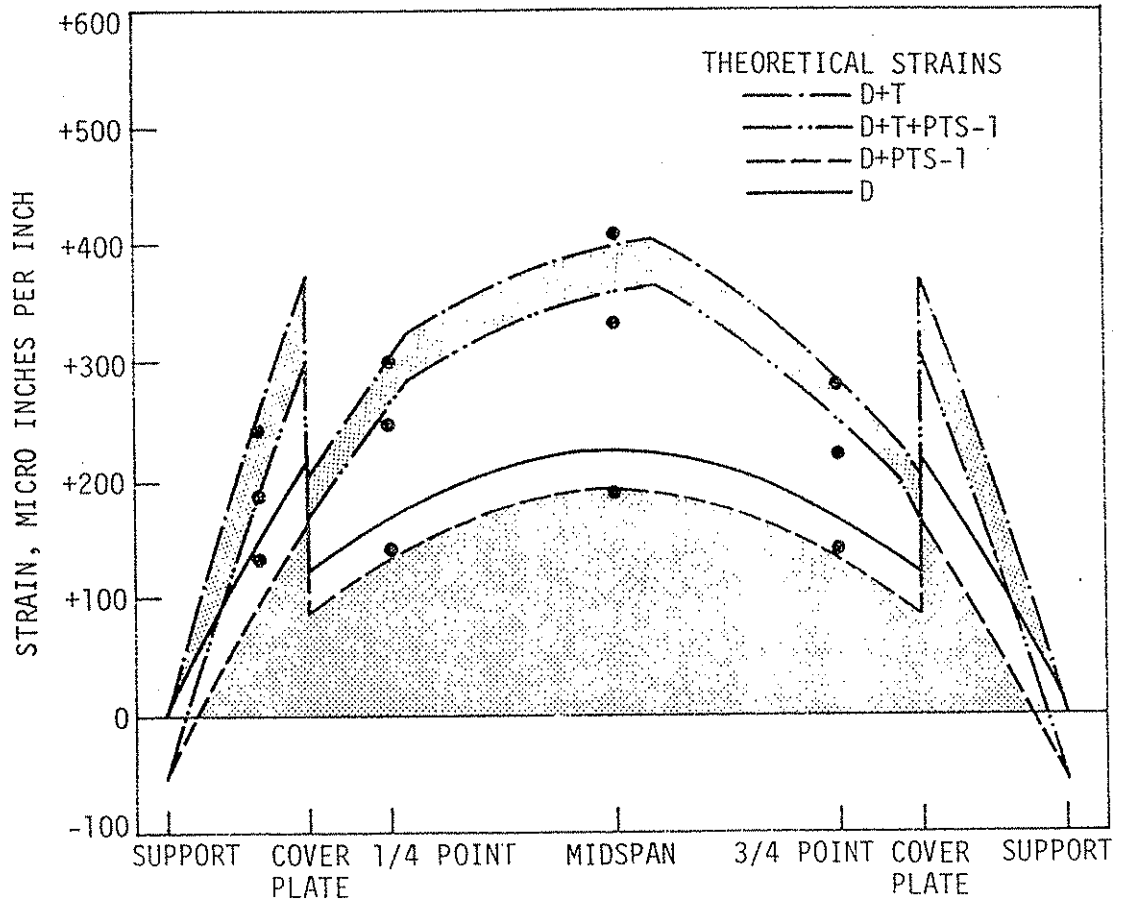Figures 44(a) and 45(a) show that dead load causes most of the strain in Beam 1 and Beam 2 top flanges. The truck load and PTS-1 cause little change in strain since those loads are applied to the composite section, which has a neutral axis reasonably close to the top flange. The measured strains correlate well with computed strains, except at mid-span. The unusual discrepancy in strains at midspan could be caused by some localized effect at the gages or could be caused by neutral axis shift. The discrepancy does not appear in bottom flange cover plate strains.

Figures 44(b) and 45(b) show that PTS-1 and truck load do significantly affect bottom flange cover plate strains. For the exterior beam, Fig. 44(b), the simulated truck load causes about half of the total strain, and PTS-1 reduces the total strain on the order of 20%. For the interior beam, Fig. 45(b), PTS-1 causes less reduction in total strain since the interior beam actually is not post-tensioned but receives the effects of post-tensioning through distribution by the deck and dia-phragms. In both figures referred to above, the shaded band across the top represents the amount of tensile strain removed, and the white band across the center represents the envelope of tensile strains to which the beam would be subjected after strengthening by post-tensioning.

The bottom flange or cover plates for Beams 1 and 2 are not sub-jected to compression from application of post-tensioning, except

perhaps near the supports of Beam 2. The tension there may or may not

exist, depending on distribution of the post-tensioning from Beam 1.

If post-tensioning forces were increased, some regions of compression

would be created along the bottoms of bridge beams.

In Fig. 44(b) there are four noticeable vertical discontinuities.

The two nearest the supports are due to application of post-tensioning

force at the brackets, and the two near midspan are due to cover plate

cutoffs. Since the brackets apply force over a finite length and since

the cover plates terminate over a length of 9 inches, the discontinui-

ties actually are more gradual than shown in the figure. Figure 44(b)

does indicate the five locations of potential maximum strain: brackets,

cover plate cutoffs, and midspan. It is apparent that bracket locations

can be adjusted somewhat to fit strengthening need and jacking clearances.

Figures 44(b) and 45(b) both show reasonable correlation between

experimental and computed strains. The greatest error, about 15% of

the total strain, occurs for the combination of dead load, truck, and

PTS-1. Experimental values seem to indicate that the post-tensioning

has a greater effect than computed and, thus, that the computations give

conservative results.

4.4.3. Δ-T Analysis

After a composite beam is post-tensioned, the post-tensioning

tendons become part of the beam structure, thereby rendering the post-

tensioned portion of the beam statically indeterminate to the first

degree. As applied load is increased or decreased on the beam, the

force in the post-tensioning tendons will change. In this study the

change in force is referred to as Δ-T effect.

By means of the principle of strain energy (Castigliano's Theorem), Hoadley derived an equation for Δ-T effect [27]. The authors have extended Hoadley's Δ-T equation to the partial length cover plate condition encountered in the model bridge beams. As the Δ-T formula in Fig. 46(b) indicates, the change in tendon tension is dependent on the moment due to loads applied after post-tensioning but is independent of the magnitude of the original post-tensioning force.

Figure 47 illustrates the Δ-T force in the post-tensioning tendons on model bridge Beam 1 as 10 kip concentrated loads were applied at the bridge centerline. The lines in the figures representing theory are computed using both orthotropic plate theory and the Δ-T formula. Moment fractions determine the quantity of moment applied to Beams 1 and 4, the two post-tensioned beams in PTS-1. The Δ-T equation can be used to compute the change in tension for the two beams. Moment fractions from orthotropic plate theory finally determine the Δ-T effect for Beam 1. The process described above generally yielded results within 10% of the values measured by strain gages mounted on the post-tensioning tendons.

A comparison of Figs. 47(a) and 47(b) indicates little difference in Δ-T effect caused by presence or absence of curbs. The total change in tendon tension is small, about 10% of the load actually applied to Beam 1 and a small percentage of the post-tensioning force applied to the beam. Because the Δ-T effect is small and serves to increase post-tensioning only when live load is applied, it could conservatively be neglected in design or credited against long-term prestress losses.
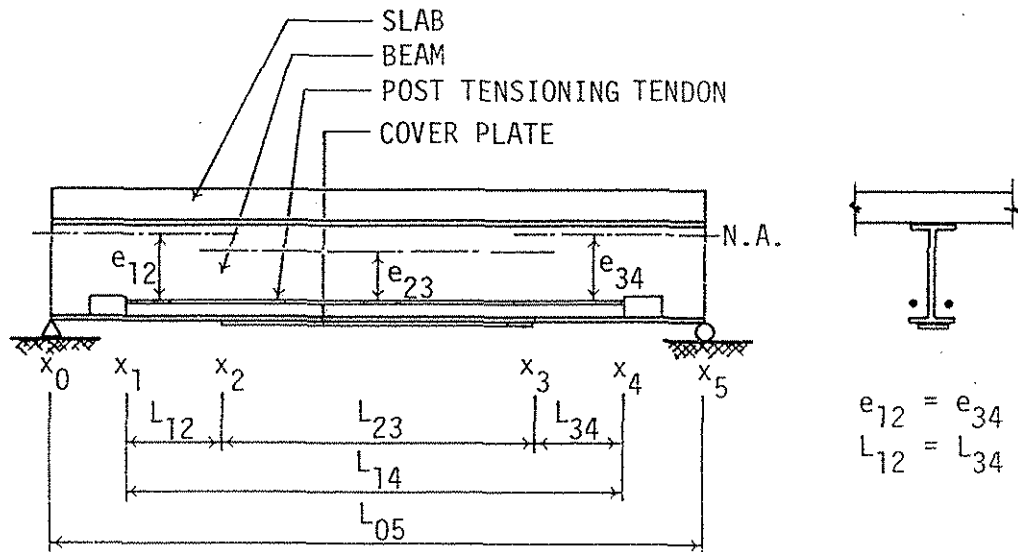
(A)   POST-TENSIONED COMPOSITE BEAM

$$\Delta T = \frac{\dfrac{e_{12}}{EI_{12}}\left(\displaystyle\int_{x_1}^{x_2} M\,dx + \int_{x_3}^{x_4} M\,dx\right) + \dfrac{e_{23}}{EI_{23}}\displaystyle\int_{x_2}^{x_3} M\,dx}{\dfrac{2e_{12}^{2}L_{12}}{EI_{12}} + \dfrac{e_{23}^{2}L_{23}}{EI_{23}} + \dfrac{2L_{12}}{A_{12}E} + \dfrac{L_{23}}{A_{23}E} + \dfrac{L_{14}}{A_R E_R}}$$

(B) ΔT FORMULA

WHERE M = MOMENT DUE TO LOADS APPLIED AFTER
           POST-TENSIONING

e = ECCENTRICITY OF PRESTESS

A = AREA OF TRANSFORMED COMPOSITE
     SECTION

I = MOMENT OF INERTIA OF TRANSFORMED
     COMPOSITE SECTION

E = MODULUS OF ELASTICITY OF TRANSFORMED
     COMPOSITE SECTION

A_R = AREA OF POST-TENSIONING TENDONS

E_R = MODULUS OF ELASTICITY OF TENDONS
     POST-TENSIONING

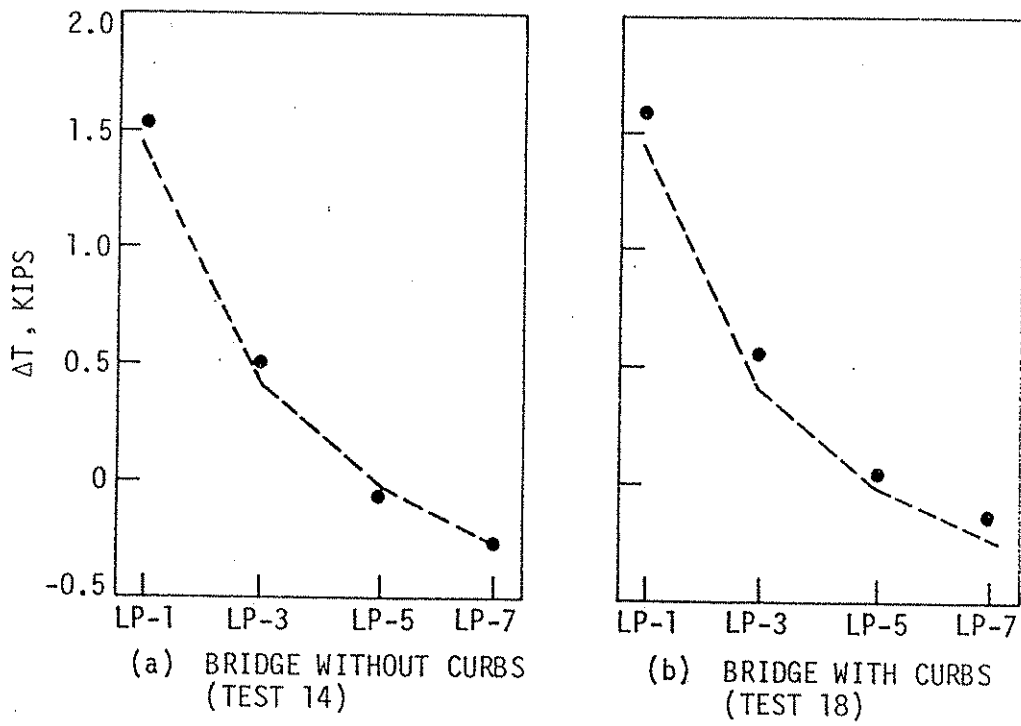Fig. 46. ΔT for composite beam with cover plate.

Fig. 47. ΔT in exterior beam 1 tendons for 10-kip load at midspan load points.

4.5. Effect of Vertical Loads

As a check on the symmetry of the model bridge and as a check on instrumentation, concentrated loads were placed on both sides of the longitudinal centerline of the bridge. Thus, the results from a 10-kip load at LP-1 should mirror the results for a load at LP-7. The strain gage and deflection dial data generally were in good or excellent agreement for mirror image cases; hence, only results for LP-1 and LP-3 are presented in this report.

Although data were gathered for both 5-kip and 10-kip loads, the data for 10-kip loads were judged to be less affected by zero shift and other instrumentation problems. Therefore, vertical load results are presented only for the 10-kip loads.

From Figs. 48(a) and (b) it is apparent, as could be expected, that the loaded beam always carries the largest share of the load. Eccentric loads to the left of LP-3 on the figures cause negative moment in the exterior beam on the right side of the bridge. The simulated truck load for which moment fractions are shown in Fig. 48(c) gives results similar to those for a combination of the individual loads at LP-1 and LP-3. Actually, the theoretical moment fractions for the truck were obtained using a combination of two separate midspan concentrated loads at the truck wheel line positions.

In Section 4.2 it was stated that the distribution of moment varies from section to section in the bridge span but is similar to the distribution at midspan. Figures 49(a), (b), (c), and (d) show the moment fractions at bridge quarter points obtained experimentally, plotted
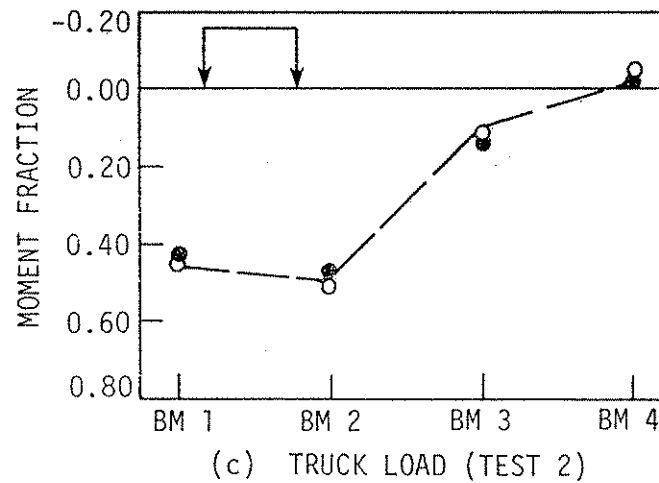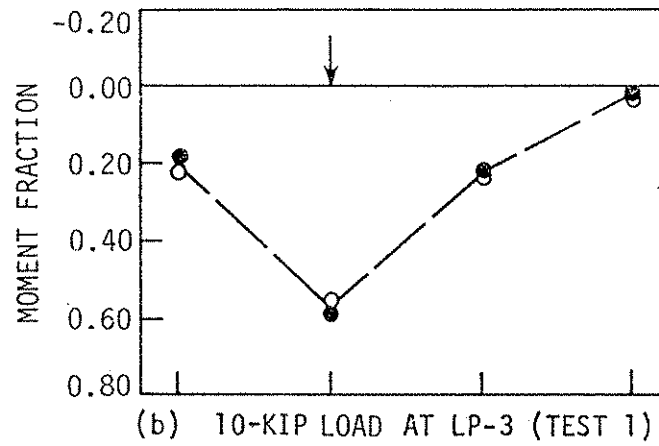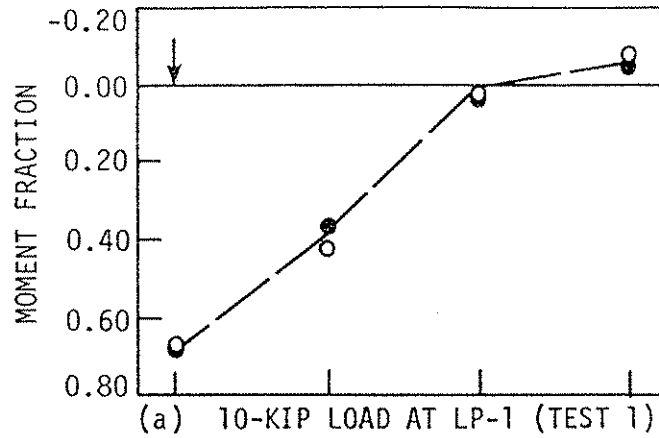
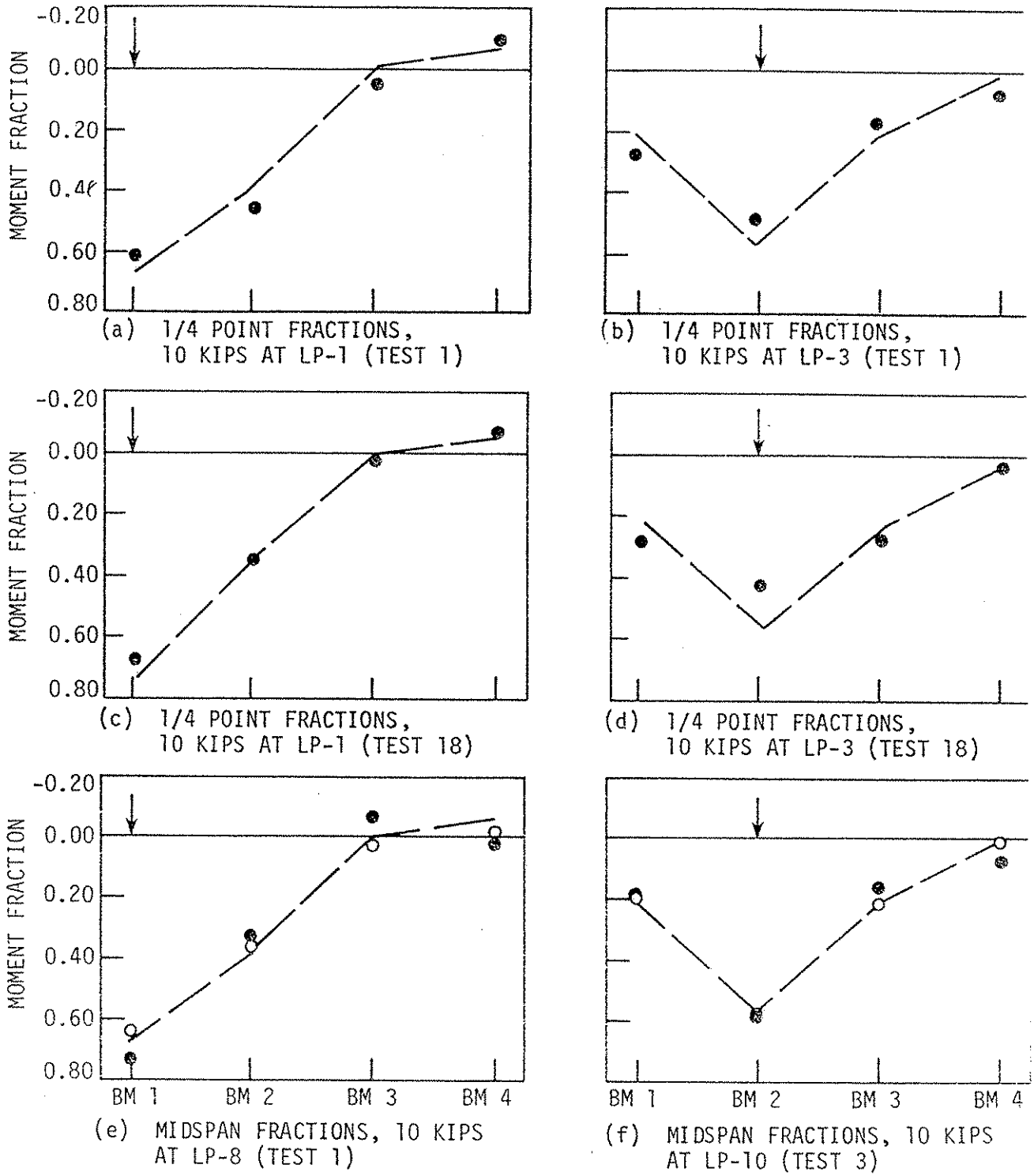Fig. 48.   Moment distribution due to vertical load.

Fig. 49. Moment distribution due to vertical load for 1/4 points and midspan.

with the theoretical fractions at midspan. As indicated earlier and as
shown in the figures, the loaded beam tends to carry a smaller fraction
of the total moment at bridge cross sections away from midspan. The
variation in moment fractions tends to decrease toward bridge supports.

A further check on moment distribution was performed by loading
at quarter points LP-8 and LP-10 and computing moment fractions from
strain and deflection data at midspan. Figures 49(e) and (f) present
two comparisons, both showing good agreement between theoretical results
for concentrated loads at midspan and experimental moment fractions for
concentrated loads at the quarter points.

For PTS-1 theoretical moment fractions and experimental moment
fractions at midspan are compared in Fig. 50(a) and at the quarter
points in Fig. 50(b). The moment fractions computed from strains at
the quarter points indicate that the post-tensioned beams carry a larger
share of the post-tensioning toward the bridge supports..

4.6. Effect of Curbs

Curbs of the type on the prototype and model bridges have a rela-
tively minor effect on distribution of moments to bridge beams. The
curbs do provide additional stiffness to exterior beams, and computa-
tions indicate that the increase in stiffness raises the moment of iner-
tia of exterior beams almost to the same value as that for the interior
beams. The change in stiffness increases moment fractions for exterior
beams. For a 10-kip vertical load at LP-1, Table 7 shows that curbs in-
crease the moment to Beam 1 0.06 (6%) of the total midspan bridge moment.

114
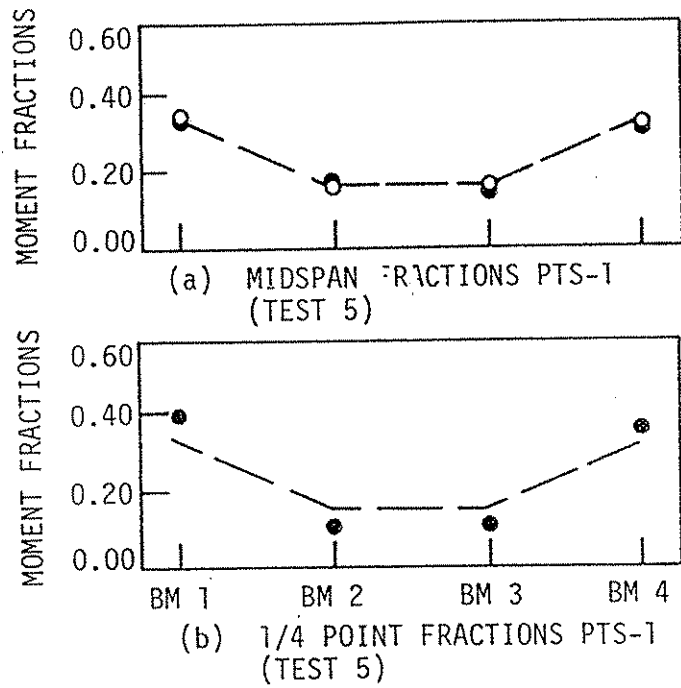
Fig. 50. Moment distribution due to post-tensioning for 1/4 points
and midspan.

Table 7. Orthotropic plate theory moment fractions for 10-kip load at
LP-1.

Model Bridge	Beam 1 M Fraction	Beam 2 M Fraction	Beam 3 M Fraction	Beam 4 M Fraction
With Curbs With Diaphragms	0.735	0.329	-0.009	-0.060
With Curbs Without Diaphragms	0.745	0.306	-0.017	-0.046
Without Curbs With Diaphragms	0.674	0.384	-0.005	-0.063
Without Curbs Without Diaphragms	0.687	0.362	-0.014	-0.049

Figures 51(a) and (b) show moment fractions for vertical load
on the model bridge. Both theoretical and experimental results indicate
little difference in beam moment fractions caused by absence or presence
of curbs. Likewise, the comparison in Figs. 51(c) and (d) for post-ten-
sioning only shows little effect of curbs. It is apparent, however,
that the exterior beams with curbs do retain a larger fraction of the
applied post-tensioning.

Qualitatively, the change in behavior of the bridge depending on
absence or presence of curbs is illustrated in Fig. 52. The figure in-
dicates a decreased deflection for both exterior beams and interior
beams. Interior beam deflections are reduced because the stiffening ef-
fect of curbs shifts some of the applied load away from interior beams.

4.7. Effect of Diaphragms

Diaphragms appear to have had even less effect than curbs on the
behavior of the model bridge. Table 7 shows a numerical change in
moment fraction of about 0.025 (2.5%) or less of the total bridge mo-
ment. This change may be inflated since the moment fractions are based
on full diaphragm stiffness. Sanders and Elleby [43] suggest that only
a fraction of diaphragm stiffness be considered because of the flexibil-
ity of diaphragm-beam connections.

Absence of diaphragms does shift more moment to loaded or post-
tensioned beams, as indicated in the comparisons in Table 7 and Fig. 53.
A detailed examination of the figures is required, however, to see any
significant change.
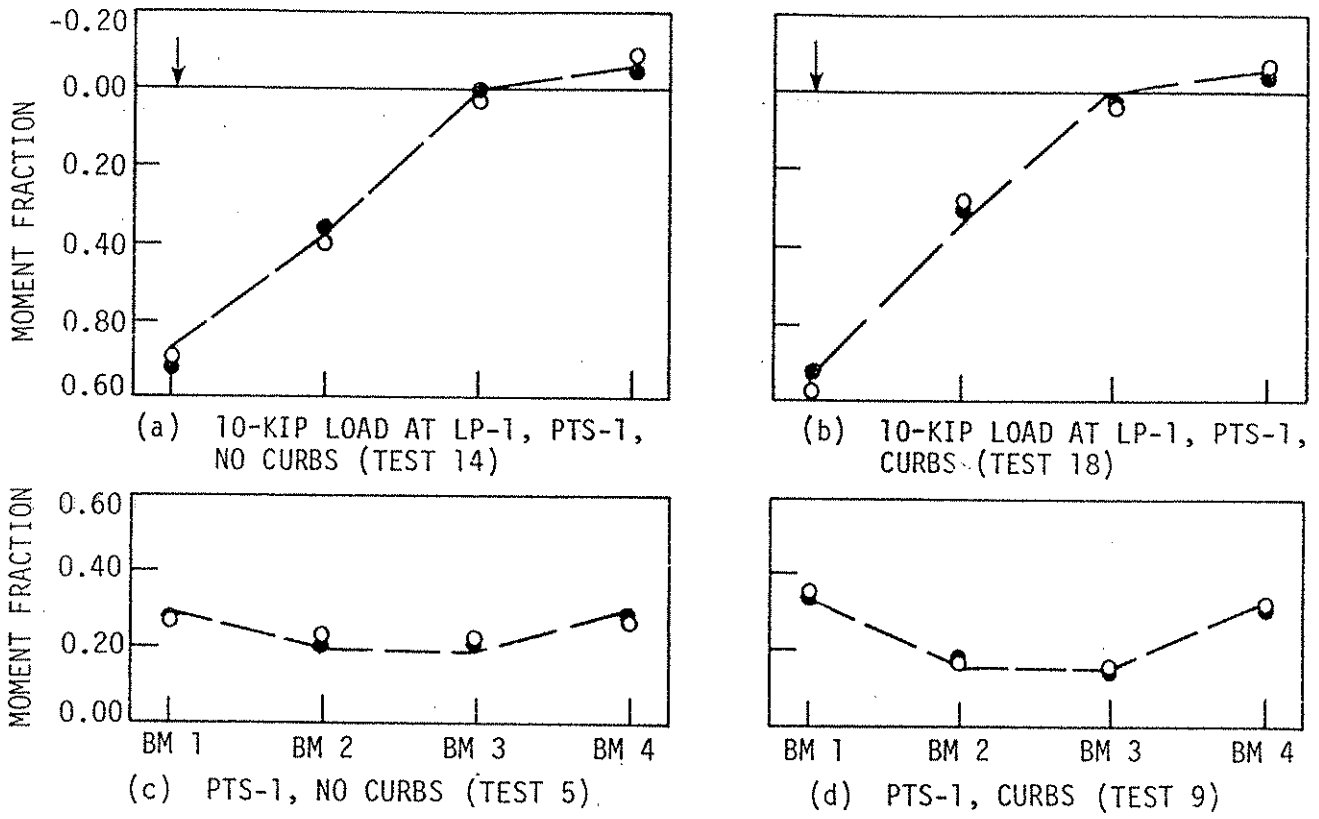
Fig. 51. Moment distribution for bridge without and with curbs.
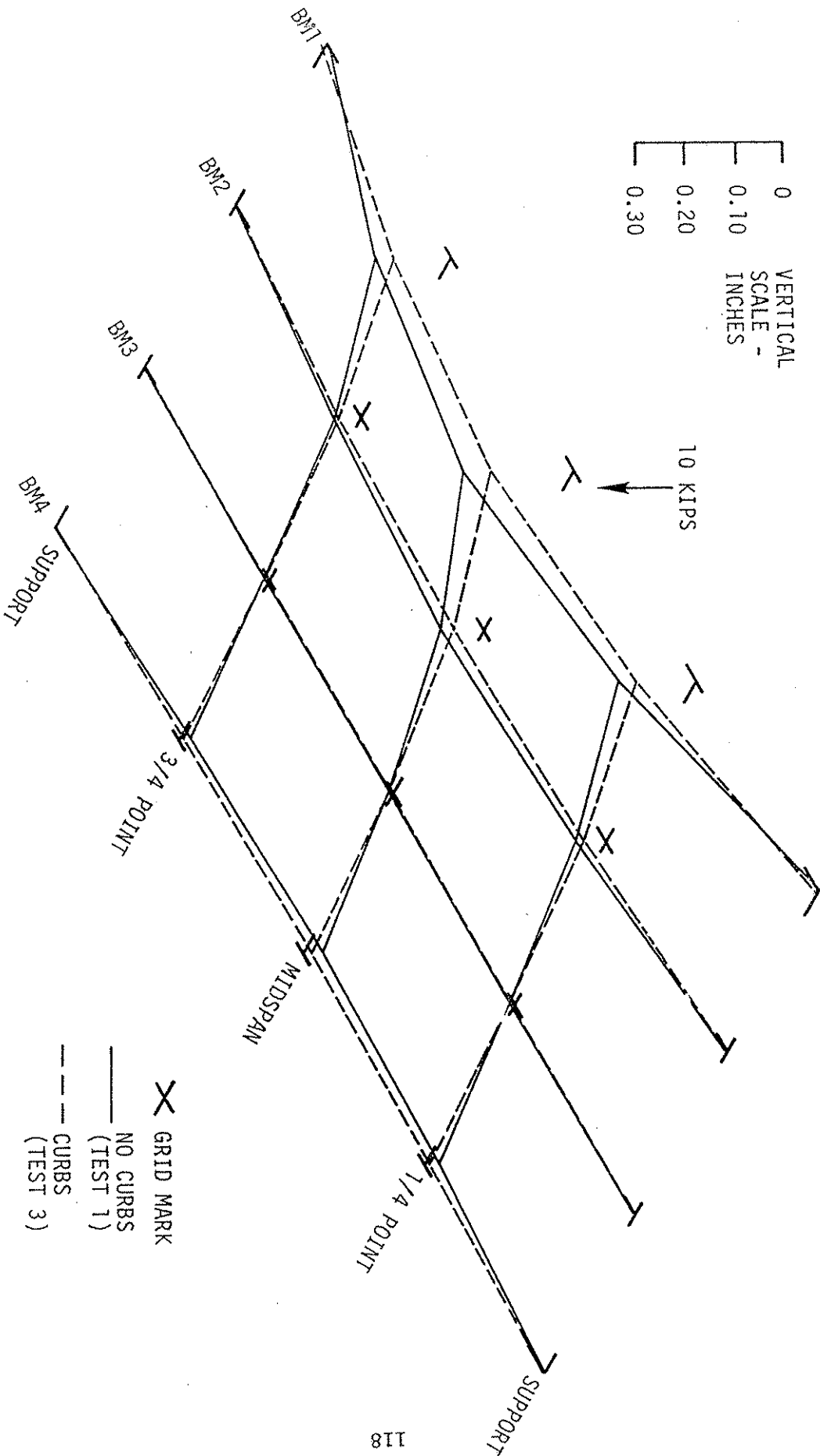
Fig. 52. Deflected shape for model bridge, 10-kip load at LP-1, without and with PTS-1.
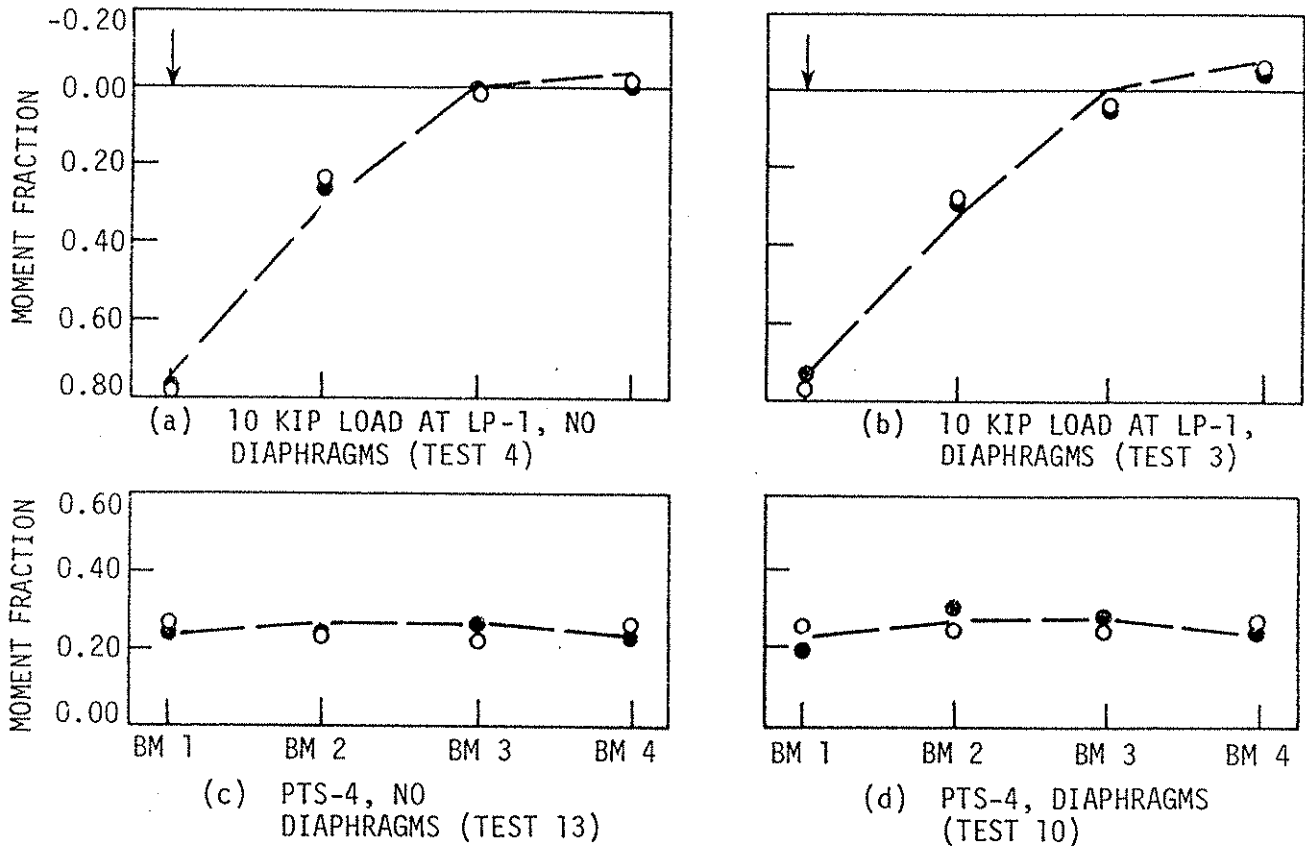
VERTICAL
SCALE -
INCHES

0
0.10
0.20
0.30

10 KIPS

GRID MARK
NO CURBS
(TEST 1)
CURBS
(TEST 3)

BM1
BM2
BM3
BM4
SUPPORT
3/4 POINT
MIDSPAN
1/4 POINT
SUPPORT

118

Fig. 53.   Moment distribution for bridge without and with diaphragms.

5. SUMMARY AND CONCLUSIONS

5.1. Summary

The literature review undertaken as one of the tasks of this project revealed considerable use of post-tensioning for the repair and strengthening of various types of structures. Although several references were found which reported on post-tensioned steel beams, none was found which dealt with post-tensioning existing composite steel beams. Thus the testing program was undertaken.

The half-scale model bridge constructed in the ISU Structures Laboratory provided an excellent means for evaluating the behavior of a composite bridge. By testing the model at various constructional stages (with and without curbs, with and without diaphragms) the authors were able to include in the testing program aspects of a variety of the Iowa bridges in need of strengthening.

Instrumentation of the model for both strain and beam deflection provided redundant results which permitted checking of experimental data. Although concrete strains were small and thus too subject to error to interpret, they did indicate the general character of slab performance. Strains measured in the flanges of beams or cover plates agreed with those predicted by theory. Both moment fractions computed from bottom flange strains and moment fractions computed from deflections correlated well with orthotropic plate theory.

Orthotropic plate theory, as used in this report, utilizes a Levy series solution for vertical loads at the midspan cross section of the plate. That solution yields results that fit the experimental data very

closely. Although the solution is not derived for cross sections or loads away from midspan or for post-tensioning, the solution does give reasonable correlation for those conditions. Although only one bridge has been analyzed and tested, on the basis of the good correlation found between theoretical and experimental results, orthotropic plate theory can be used for preliminary design of post-tensioning schemes for actual bridges.

Effective flange widths and neutral axis locations were found to vary as different loads were applied to the model bridge. Although the AASHTO effective slab widths fit the measured widths reasonably well, discrepancies are apparent. Ordinarily, the discrepancies would have minor effects on the composite beam stresses; however, in the case of post-tensioned beams, neutral axis location gains importance. The moment due to prestress is equal to the force in post-tensioning tendons times the distance to the neutral axis.

Post-tensioning had little noticeable effect on vertical load distribution within the bridge; therefore, AASHTO wheel load fractions should apply to the post-tensioned bridge, as well. Both P-Δ and Δ-T effects are small. Since the Δ-T effect is due only to load applied to the bridge after post-tensioning and since it generally increases the post-tensioning force, its effect is conservative. Post-tensioning reduces tensile strain in bottom flanges or cover plates and thus solves one of the major problems with the composite bridges toward which this study was directed. Post-tensioning did cause some cracking of the concrete deck in the model, although the first cracks were caused by negative moment on the side of the bridge opposite to an eccentric vertical load.

There are other variations, not included in this study, for applying post-tensioning to bridge beams. Since this study shows that post-tensioning applied above the bottom flanges of bridge beams is adequate, it is reasonable to expect that post-tensioning applied below flanges will also work, since in that case the post-tensioning force does not have to be as large and since uncertainty regarding neutral axis location would have less effect. Dywidag Threadbars worked well for post-tensioning; however, other systems of post-tensioning could be used with appropriate modifications of the brackets.

Because of symmetry, the concentrated loads applied to the model bridge provided mirror image results suitable for checking of data. Eccentric vertical loads, as well as the eccentric truck load, caused negative moment to develop in the opposite side of the bridge.

Curbs and diaphragms proved to have relatively minor effects on the behavior of the bridge deck. Presence of curbs did increase the fraction of moment carried by exterior beams and also reduced strains and deflections for both interior and exterior beams. Absence of diaphragms reduced vertical load and post-tensioning transfer among the bridge beams. However, in the field, portions of diaphragms found to obstruct the placing of the post-tensioning system may be removed without serious consequences since the diaphragm effect was small.

To post-tension a bridge successfully, there must be a simple method of transmitting the required force from the prestressing tendons to the bridge beam. Thus, one of the tasks undertaken during this project was the design and testing of three different brackets for transmitting the force in the tendons to the bridge beams. Because of the

uncertainty about the steel in actual bridge beams and the consequent uncertainty about weldability, all three brackets investigated utilized bolted connections.

Bracket I, designed for use on the model bridge and fabricated from structural angles, transmitted a force approximately six times its design load. On the basis of its behavior, Bracket I was used on the model bridge without any difficulty.

Bracket II, fabricated from structural tubing, exhibited no distress or distortion when its design load of 80 kips was applied. However, when load was increased to 142 kips (1.75 times the design load) large deformations of the beam flange were noted.

Two sections of structural tubing were the main components of Bracket III. Failure--large deformation of the structural tubing-- occurred when approximately 2/3 of the design load was applied. Thus, in its present configuration Bracket III is not acceptable.

5.2. Conclusions

1. On the basis of variables within the scope of this research study, post-tensioning can be used to provide strengthening for composite bridges.

2. During the actual post-tensioning of a given bridge, post-tensioning need not be applied symmetrically to the beams (i.e., exterior beams stressed simultaneously, etc.). The final result of any reasonable post-tensioning sequence is essentially the same.

3. A post-tensioning strengthening design requires check of flexural stresses at five different locations within a span: the two

post-tensioning bracket locations, the two cover plate cutoff

points, and the midspan section.

4. In a post-tensioning scheme in which only exterior beams are post-
    tensioned approximately two-thirds of the post-tensioning force
    (for a four-beam bridge) affects the exterior beams. For adequate
    post-tensioning, therefore, more force must be applied in order to
    compensate for post-tensioning distributed to the remainder of the
    bridge. Obviously the amount of post-tensioning force affecting
    the exterior beam is a function of beam spacing, beam size, span
    length, etc. and thus the 2/3 fraction will be different for vari-
    ous bridges.

5. Post-tensioning, in either of the schemes studied, did not signi-
    ficantly affect the overall load distribution characteristics of
    the bridge.

6. Orthotropic plate theory, which has been established as a means to
    predict vertical load distribution in bridge decks, may be used
    to predict approximate distribution of post-tensioning axial forces
    and moments.

7. In the bridge tested, $P-\Delta$ effects due to post-tensioning were
    secondary and thus could be neglected.

8. $\Delta-T$ effects in post-tensioning tendons are small and have a conserv-
    ative effect. Thus $\Delta-T$ effects may be neglected in most designs.

9. Post-tensioning forces generally are of sufficient magnitude to
    cause significant cracking of concrete bridge decks.

10. The stiffening effect of low curbs had minimal effects on behavior
    of post-tensioned bridges. The added stiffness of curbs increases

the vertical loading and post-tensioning force carried by exterior

beams; however, the net effect may still be a reduction in the maxi-

mum stresses in exterior beams.

11. Diaphragms have minimal effects at service loads; however, removal

of diaphragms does reduce vertical load transfer and post-tensioning

transfer among beams.

12. It is extremely important in design of brackets for transmitting

force from the bracket to the beam to consider the strength of the

bracket, the strength of the beam to which the bracket is being

attached, and the strength of the bolts. Brackets I and II per-

formed very well in transmitting load from the bracket to the beams.

Bracket I transmitted six times its design load while Bracket II

transmitted 1.75 times its design load. Bracket III, with the

modifications presented, will in the opinion of the writers transmit

more than its design load safely.

6. RECOMMENDED CONTINUED STUDIES

The present study has shown that composite concrete deck - steel I-beam single span bridges can be strengthened through use of various arrangements of post-tensioning forces. In view of this finding the following areas should be pursued:

- One or more actual bridges should be strengthened utilizing the post-tensioning techniques and preliminary design methodology developed in this study. The behavior of these bridges should be monitored for a period of several years.

- Various experiments should be continued on the bridge model now constructed in the ISU Structures Laboratory. The testing program should be determined with considerable input from the Bridge Department of the Iowa DOT. Several possibilities exist--dynamic load testing, converting the model into a skewed bridge and redoing several of the tests done in Phase I--to ascertain the skew effect, etc.

- Several of the items mentioned in Section 1 should be investigated: shear capacity, corrosion protection of post-tensioning system, effects of fatigue, etc.

7. ACKNOWLEDGMENTS

8. REFERENCES

1. Arendts, J. G., "Study of Experimental and Theoretical Load Distribution in Highway Bridges," M.S. Thesis, Iowa State University, Ames, Iowa, 1968.

2. Badaruddin, S., "Analyses of Slab and Girder Highway Bridges," Ph.D. Dissertation, University of Illinois, Urbana, Illinois, 1965.

3. Bakht, B., M. S. Chueng, and T. S. Aziz, "Application of a Simplified Method of Calculating Longitudinal Moments to the Ontario Highway Bridge Design Code," Canadian Journal of Civil Engineering, Vol. 6, 1979, pp. 36-50.

4. Bares, R., Berechnungstafeln fuer Platten und Wandscheiben/Tables for the Analysis of Plates, Slabs and Diaphragms Based on the Elastic Theory, Wiesbaden and Berlin: Bauverlag GMBH., 1971.

5. Bares, R., and C. Massonnet, Analysis of Beam Grids and Orthotrpic Plates, New York: Frederick Ungar Publishing Co., 1966.

6. Barnard, P. F., "Prestressed Steel Bridges," (unpublished manuscript), Iowa Highway Commission, Ames, 1960.

7. Barnett, R. L., "Prestressed Truss-Beams," American Society of Civil Engineers, Journal of the Structural Division, Vol. 83, No. ST2, March 1957, pp. 1191-1 - 1191-22.

8. Belenya, E. I., and D. M. Gorovskii, "The Analysis of Steel Beams Strengthened by a Tie Rod," International Civil Engineering, Vol. II, No. 9, March 1972, pp. 412-419.

9. Benthin, K., Letter and Sketch Plans for Strengthening Minnesota Bridge No. 3699, 1975.

10. Berridge, P. S. A., and D. H. Lee, "Prestressing Restores Weakened Truss Bridge," Civil Engineering, Vol. 26, No. 9, September 1956, pp. 578-579.

11. Botzler, P. W., J. Colville, and C. P. Heins, Ultimate Load Tests of Continuous, Composite Bridge Models, Report No. FHWA-MD-R-76-14, Civil Engineering Department, University of Maryland, College Park, 1976.

12. Carpenter, J. E. and D. D. Magura, "Structural Model Testing--Load Distribution in Concrete I-Beam Bridges," Journal of the Portland Cement Association Research and Development Laboratories, Vol. 7, No. 3, September 1965, pp. 32-48.

13. Cheung, M. S. and M. Y. T. Chan, "Finite Strip Evaluation of Effective Flange Width of Bridge Girders," Canadian Journal of Civil Engineering, Vol. 5, No. 2, June 1978, pp. 174-185.

14. Coff, L., "American Engineer Studies Prestressing of Structural Steel," Civil Engineering, Vol. 20, No. 11, November 1950, p. 64.

15. "Composite Prestressed Steel WF Beam Bridge Over Quittaphilla Creek" (unpublished bridge plans), Bridge Unit, Department of Highways, Commonwealth of Pennsylvania, Harrisburg, 1965.

16. Cusens, A. R., and R. P. Pama, Bridge Deck Analysis, New York: John Wiley and Sons, Inc., 1975.

17. Dischinger, F., "Stahlbruecken im Verbund mit Stahlbeton Druckplatten bei gleichzeitiger Vorspannung durch hochwertige Seile," der Bauingenieur, Vol. 24, No. 11 and 12, November and December 1949, pp. 321-332, pp. 364-376.

18. Ekberg, C. E., "Development and Use of Prestressed Steel Flexural Members, Subcommittee 3 Report on Prestressed Steel of Joint ASCE-AASHO Committee on Steel Flexural Members," American Society of Civil Engineers, Journal of the Structural Division, Vol. 94, No. ST9, September 1968, pp. 2033-2060.

19. Ferjencik, P., "Czechoslovak Contribution in the Field of Prestressed Steel Structures," International Civil Engineering, Vol. II, No. 11, May 1972, pp. 481-491.

20. Finn, E. V. and F. H. Needham, "The Use of Prestressed Steel in Elevated Roadways," The Structural Engineer, Vol. 42, No. 1, January 1964, pp. 5-18.

21. Fritz, B., "Ueber die Berechnung und Konstruktion vorgespannter, Staehlerner Fachwerkträger," der Stahlbau, Vol. 24, No. 8, August 1955, pp. 169-174.

22. Gurbuz, O., "Theories of Transverse Load Distribution on Simple Span, (Non-Skewed) Beam-and-Slab and Slab Bridges," M.S. Thesis, Iowa State University, Ames, Iowa, 1968.

23. Hadley, H. M., "Heavy Duty Composite Bridge," Civil Engineering, Vol. 30, No. 5, May 1960, pp. 44-48.

24. Hadley, H. M., "Steel Bridge Girders with Prestressed Composite Tension Flanges," Civil Engineering, Vol. 36, No. 5, May 1966, pp. 70-72.

25. Hambly, E. C., Bridge Deck Behavior, New York: John Wiley and Sons, Inc., 1976.

26. Heins, C. P., "LFD Criteria for Composite Steel I-Beam Bridges," American Society of Civil Engineers, Journal of the Structural Division, Vol. 106, No. ST11, November 1980, pp. 2297-2312.

27. Hoadley, P. G., "Behavior of Prestressed Composite Steel Beams," American Society of Civil Engineers, Journal of the Structural Division, Vol. 89, No. ST3, June 1963, pp. 21-34.

28. Hondros, G. and Marsh, J. G., "Load Distribution in Composite Girder-Slab Systems," American Society of Civil Engineers, Journal of the Structural Division, Vol. 86, No. ST11, November 1960, pp. 79-109.

29. "How to Keep that Old Bridge Up," American City and County, Vol. 96, No. 1, January 1981, pp. 29-32.

30. Joy, D. D., Senior Vice President T. Y. Lin International, letter (unpublished) to C. Pestotnik, Bridge Engineer, Iowa Department of Transportation, October 2, 1980.

31. Kandall, C., "Increasing the Load-Carrying Capacity of Existing Steel Structures," Civil Engineering, Vol. 38, No. 9, October 1968, pp. 48-51.

32. Knee, D. W., "The Prestressing of Steel Girders," The Structural Engineer, Vol. 44, No. 10, October 1966, pp. 351-353.

33. Kostem, C. N. and E. S. Decastro, "Effects of Diaphragms on Lateral Load Distribution in Beam-Slab Bridges," Transportation Research Board, Transportation Research Record 645, Bridge Tests, pp. 6-9.

34. Lee, D. H., Prestressed Concrete Bridges and Other Structures," The Structural Engineer, Vol. 30, No. 12, December 1952, p. 302-313.

35. Magnel, G. P., "Long Prestressed Steel Truss Erected for Belgian Hangar," Civil Engineering, Vol. 24, No. 10, October 1954, pp. 38-39.

36. Magnel, G., "Prestressed Steel Structures," The Structural Engineer, Vol. 28, No. 11, November 1950, pp. 285-295.

37. Manual for Maintenance Inspection of Bridges 1978, Third Edition, Washington, D.C. American Association of State Highway and Transportation Officials, 1979.

38. Miklofsky, H. A., Correlation of Theoretical and Experimental Data for Highway Bridges, Report No. FHWA-RD-75-77, Federal Highway Administration, Washington, D.C., 1975.

39. Murphy, G., Similitude in Engineering, New York: The Ronald Press Company, 1950.

40. Palmer, R. A., "Emergency Bridge Repair in Minnesota," Journal of the Prestressed Concrete Institute, Vol. 19, No. 1, January-February 1974, pp. 73-75.

41. Reagan, R. S., and N. W. Krahl, "Behavior of Prestressed Composite Beams," American Society of Civil Engineers, Journal of the Structural Division, Vol. 93, No. ST6, December 1967, pp. 87-107.

42. Rowe, R. E., Concrete Bridge Design, New York: John Wiley & Sons, Inc., 1962.

43. Sanders, W. W., Jr., and H. A. Elleby, Distribution of Wheel Loads on Highway Bridges, National Cooperative Highway Research Program Report 83, Washington, D.C., 1970.

44. Standard Specifications for Highway Bridges, Twelfth Edition, Washington, D.C.: American Association of State Highway and Transportation Officials, 1977.

45. Sterian, D. S., "Introducing Artificial Initial Forces into Steel Bridge Decks," Acier-Stahl-Steel, Vol. 34, No. 1, January 1969, pp. 31-37.

46. Stras, J. C., III, "An Experimental and Analytical Study of Prestressed Composite Beams," M.S. Thesis, Rice University, Houston, 1964.

47. Szilard, R., "Design of Prestressed Composite Steel Structures," American Society of Civil Engineers, Journal of the Structural Division, Vol. 85, No. ST9, November 1959, pp. 97-123.

48. Tamberg, K. G., The Analysis of Right, Multi-Girder Simple-Span Bridge Decks as Equivalent Torsionally-Weak Grid Systems, D. H. O. Report No. 102, Downsview, Department of Highways, Ontario, Canada, 1965.

49. Tochacek, M. and F. G. Amrhein, "Which Design Concept for Prestressed Steel," Engineering Journal, Vol. 8, No. 1, January 1971, pp. 18-30.

50. Tochacek, M., and C. L. Mehta, "Economical Design of Prestressed Plate Girder," American Society of Civil Engineers, Journal of the Structural Division, Vol. 98, No. ST6, June 1972, pp. 1273-1289.

51. Vernigora, et al., "Bridge Rehabilitation and Strengthening by Continuous Post-Tensioning," Prestressed Concrete Institute Journal, Vol. 14, No. 2, April 1969, pp. 88-104.

52. Wei, B. C. F., "Load Distribution of Diaphragms in I-Beam Bridges," American Society of Civil Engineers, Journal of the Structural Division, Vol. 85, No. ST5, May 1959, pp. 17-55.

53. Whipple, S., A Work On Bridge Building, Utica: H. H. Curtiss, 1847.

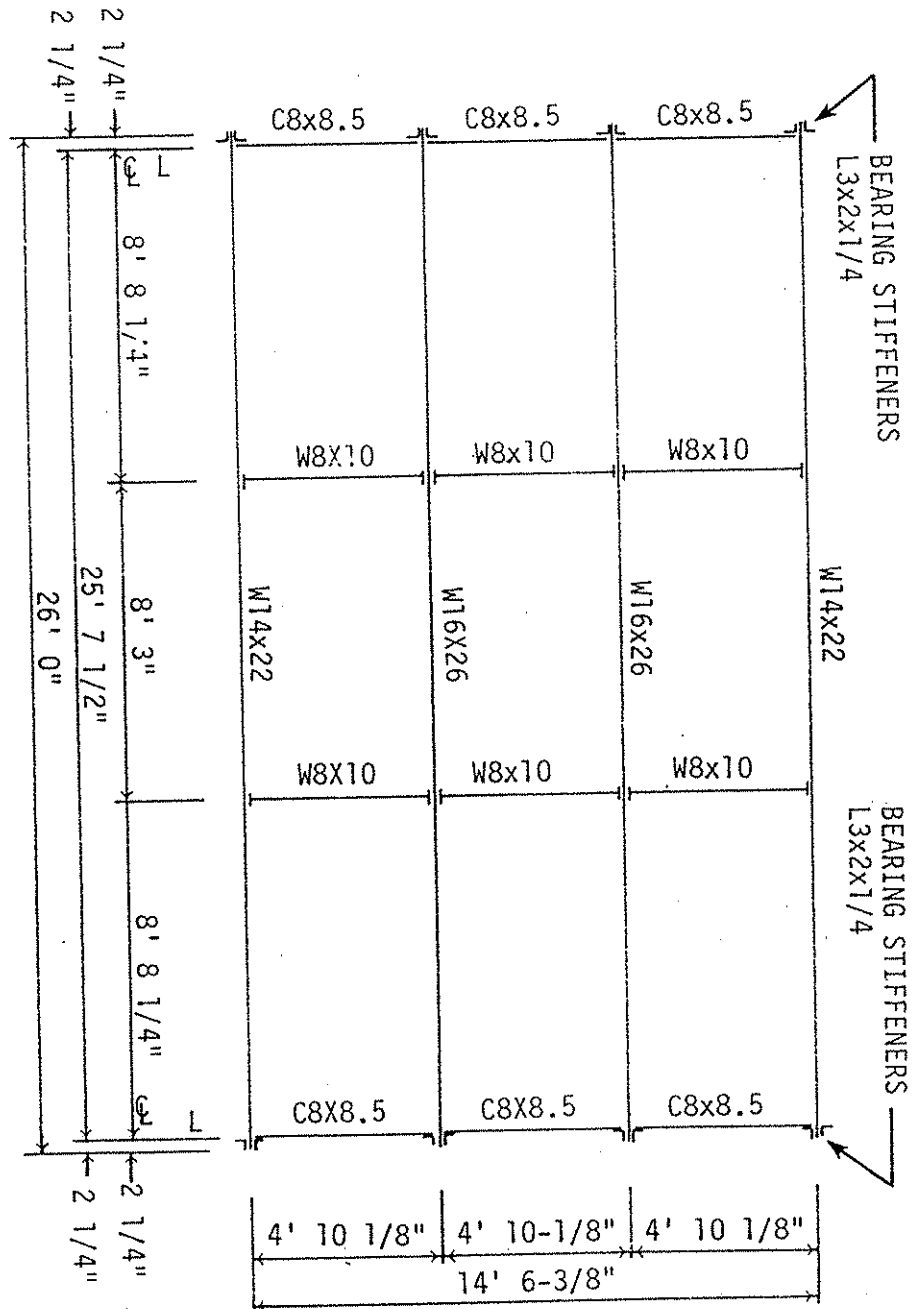9. APPENDIX

FRAMING PLAN AND STRUCTURAL STEEL DETAILS
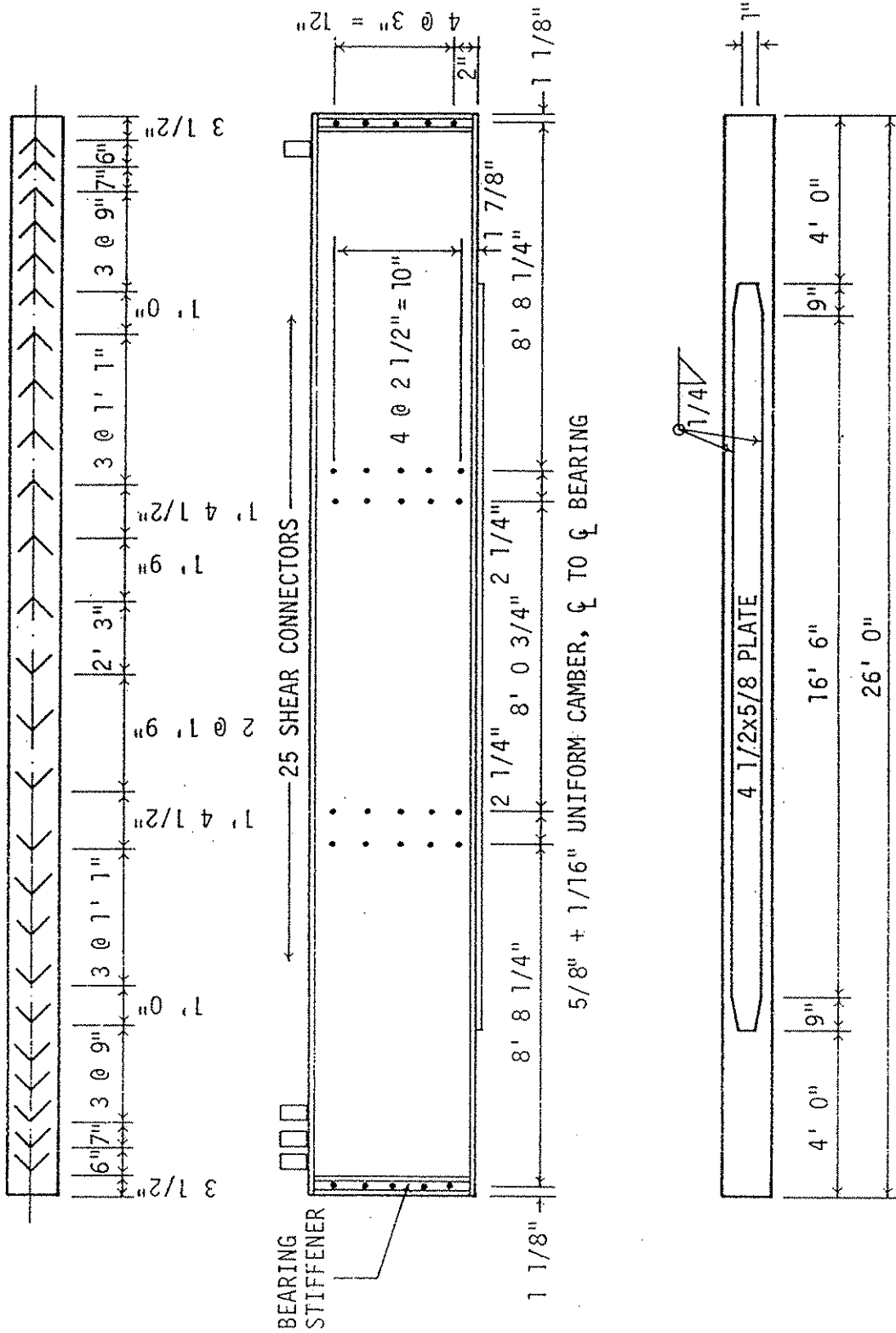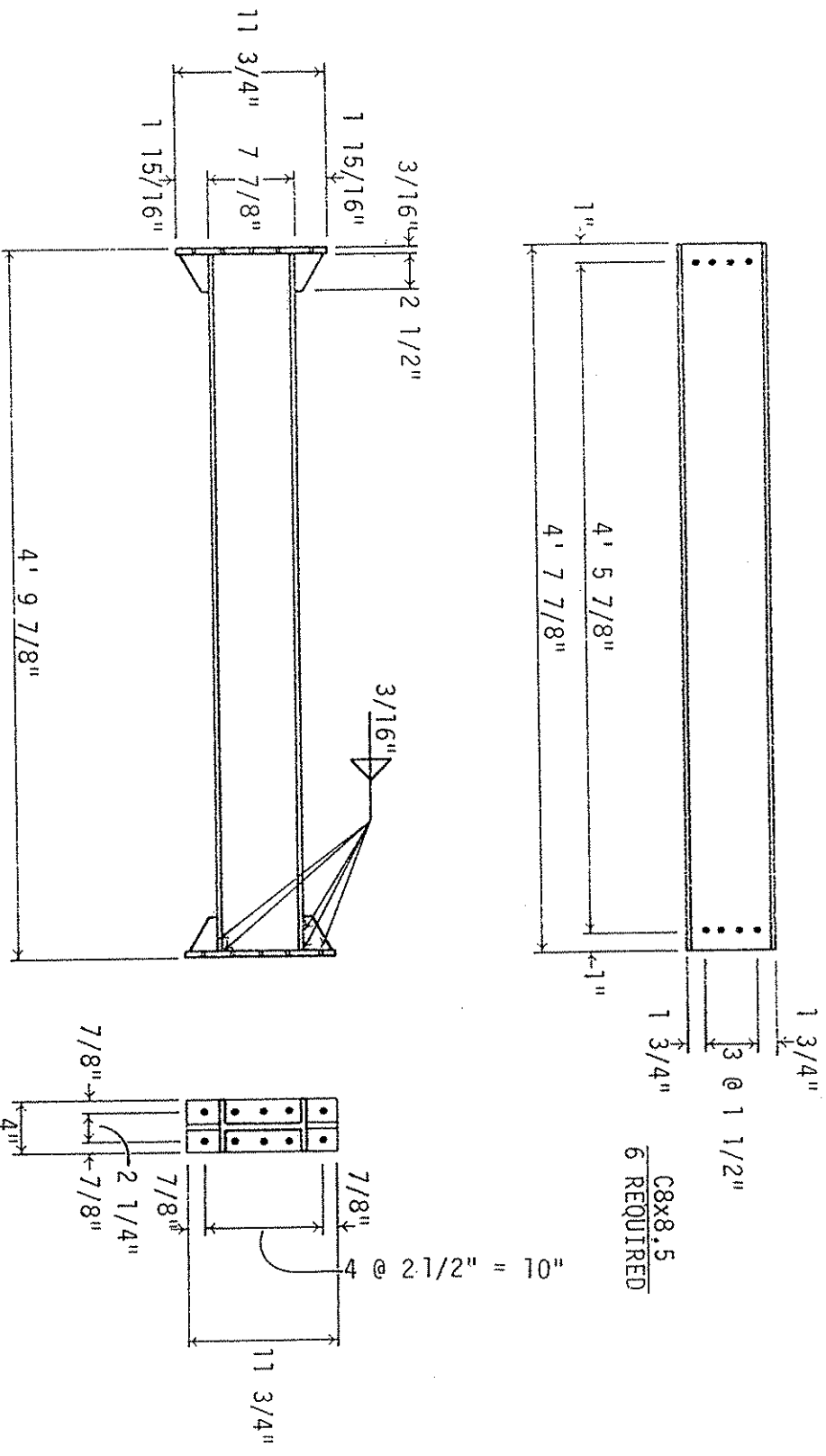
Fig. A.1. Model bridge framing plan.

C8x8.5 C8x8.5 C8x8.5

W8X10 W8x10 W8x10

W14x22 W16X26 W16x26 W14x22

W8X10 W8x10 W8x10

C8X8.5 C8X8.5 C8X8.5

BEARING STIFFENERS
L3x2x1/4

BEARING STIFFENERS
L3x2x1/4

2 1/4"
2 1/4"

₵ L

8' 8 1/4"

25' 7 1/2"

26' 0"

8' 3"

8' 8 1/4"

₵ L

2 1/4"
2 1/4"

4' 10 1/8" 4' 10-1/8" 4' 10 1/8"

14' 6-3/8"

Fig. A.2.   Exterior beam details.

W14x22
2 REQUIRED

Fig. A.3. Interior beam details.

Fig. A.4. Diaphragm details.
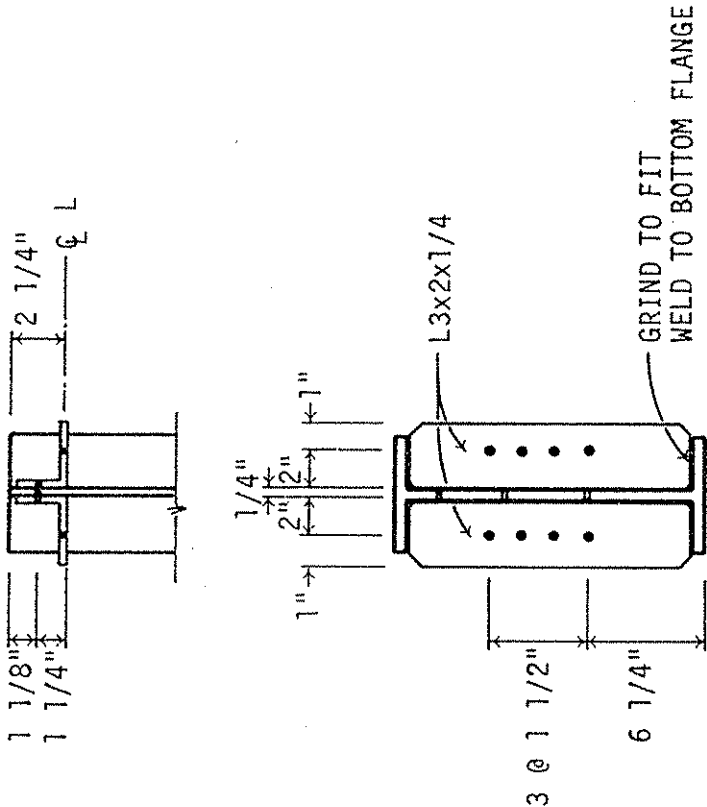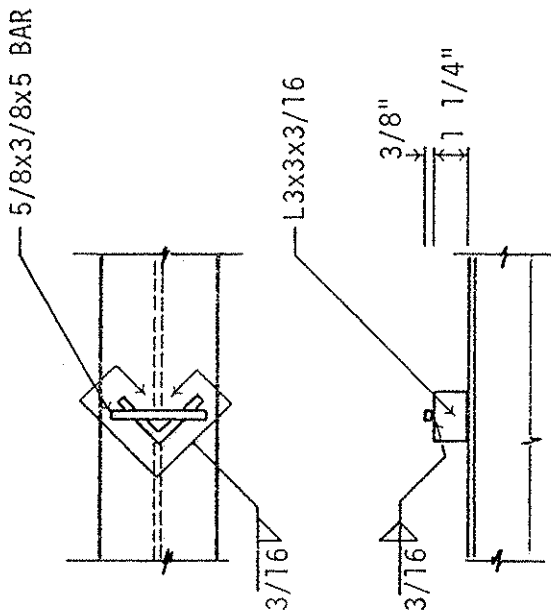
Fig. A.5. Shear connector and bearing stiffener details.